The Photoprotective Effects of Almond Polyphenols and α-Tocopherol in a Three-Dimensional Human Skin Tissue Model

A dissertation submitted by
Julie A. Evans

In partial fulfillment of the requirements for the degree of
Doctor of Philosophy in
Biochemical and Molecular Nutrition

TUFTS UNIVERSITY
September 2011

Advisor
Elizabeth J. Johnson, PhD
Friedman School of Nutrition Science and Policy, Tufts University
Carotenoids and Health Laboratory, Jean Mayer USDA HNRCA

ABSTRACT

Introduction: Almonds contain the nutrients alpha-tocopherol (AT) and almond polyphenols (AP), which have shown promise as photoprotectants in skin. Our study aims were: 1.) assess the feasibility of nutrient studies in a 3-dimensinal (3D) human skin tissue model and 2.) determine the photoprotection of AT and AP from ultraviolet-A (UVA) irradiation using this model.

Methods and Materials: AT or AP was applied to medium (25 and 5 μM, respectively) or topically (1 mg/cm^2 and 14 μg/cm^2, respectively). Optimal dose and incubation time for each treatment were selected based on maximal nutrient absorption while maintaining healthy skin tissue parameters (morphology, proliferation and apoptosis). Skin absorption of AT was quantified in dermis and epidermis by HPLC with UV detection after proteolysis and standard lipid extraction. After nutrient incubation, tissues were UVA irradiated (35 J/cm^2) and photodamage was assessed in comparison to control tissues after 96 h. Photodamage was assessed by morphological outcomes (basal layer organization, fibroblast presence, epidermal development) in hemotoxylin and eosin-stained tissue cross-sections; proliferation of basal cells by bromodeoxyuridine incorporation assay; apoptosis by TUNEL assay; differentiation by cytokeratin-10 immunohistochemistry; and protein secretion of growth factors, interleukin 1α (IL-1α) and matrix metalloprotease (MMP)-2 by ELISA. Morphology and differentiation comparisons were qualitative while semi-quantitative comparisons were made for other outcome measures.

Results: After 48 h medium incubation with AT, dermal and epidermal concentrations of AT were approximately 3 and 30 ng/mg wet weight, respectively. After 2 h incubation with topical AT, dermal and epidermal concentrations of AT were 1 and 37 μg/mg wet weight, respectively. Nutrient treatments alone did not induce changes in the percentage of apoptotic fibroblasts or morphologic parameters. Topical AP tended to increase percent proliferating basal keratinocytes. Topical AT treatment tended to stimulate hepatocyte growth factor (HGF), keratinocyte growth factor (KGF) and IL-1α. However, UVA irradiation tended to increase apoptotic fibroblasts and decrease proliferating basal keratinocytes, compared to control tissues. Negative morphologic changes were also observed at 96 h after irradiation, including disappearance of fibroblasts in the upper dermis, disorganized basal layer and less developed epithelium. UVA delayed keratinocyte differentiation and tended to suppress secretion of HGF and induce secretion of MMP-2. Tissues pretreated with all nutrient treatments tended to have increased proliferating basal keratinocytes and decreased apoptotic fibroblasts, compared to corresponding vehicle treated tissues after UVA irradiation. Morphological deterioration was partially prevented and delayed keratinocyte differentiation was attenuated by pretreatment of all nutrient applications to UVA-irradiated tissue. Pretreatment with medium and topical AT tended to stimulate HGF secretion, compared to corresponding vehicle controls after UVA irradiation. Pretreatment with medium AT, topical AT and topical AP modulated MMP-2, compared to corresponding vehicle controls after UVA irradiation.

Conclusions: Our 3D skin tissue model is a feasible tool to assess nutrient photoprotection. AT absorption into dermal and epidermal compartments of this model was time and dose-dependent with concentrations reaching those found *in vivo*. All four nutrient treatments provided some degree of photoprotection from UVA as assessed by morphology, proliferation, apoptosis, differentiation and protein secretion. These data may have positive implications for the use of

dietary and topical almond phytonutrients to prevent sun damage. This model allows for further investigation into the mechanisms by which nutrition may play a role in skin health.

AWKNOWLEDGEMENTS

I could not have completed this dissertation without the support of many individuals. First, I would like to thank my dissertation committee who provided excellent advice and mentoring. I am very fortunate to have worked with my advisor Dr. Elizabeth Johnson. She guided me through my nutrition science training and encouraged my interest in skin health and nutrition. Her unwavering support and enthusiasm were invaluable. Dr. Oliver Chen taught me to never stop analyzing and to approach a problem from many angles. Dr. Jonathan Garlick took me into his lab where I learned about skin and histology from scratch and gave me the opportunity to work independently but provided guidance whenever I needed it. Dr. Xiang-Dong Wang welcomed me into his lab meetings where I greatly enjoyed the scientific debate.

I add my sincere gratitude to the members of the laboratories in which I worked. In the Carotenoids and Health Lab, Dr. Guangwen Tang, Dr. Kyung-Jin Yeum, Dr. Rohini Vishwanathan and Tawanda Muzhingi were always willing to help and lend an ear. In the Antioxidants Research Lab, Dr. Jeff Blumberg, Dr. Diane McKay, Carly Zampariello, Kendra French, Kenneth Racicot and Desiree Kelley provided excellent guidance and training. In the Division of Cancer Biology and Tissue Engineering, a.k.a. the Garlick Lab, Dr. Addy Alt-Holland, Dr. Christophe Egles, Elana Knight, Avi Smith, Anna Maione, Yulia Shamis, Mariam Margvelashvili, Kyle Hewitt, Shumin Dong and Judith Edwards welcomed me into their lab and were generous with their time and knowledge.

Also, I would like to thank my academic advisor Dr. Sarah Booth who inspired me to apply to the Friedman School and provided great academic guidance.

Finally, I would like to thank my family and friends for their encouragement throughout my graduate career. Thank you for keeping things in perspective and pushing me through to the end.

Table of Contents

LIST OF TABLES

CHAPTER 2

CHAPTER 7

LIST OF FIGURES

CHAPTER 2

CHAPTER 4

CHAPTER 5

CHAPTER 6

LIST OF ABBREVIATIONS

almond polyphenols, AP;

α-tocopherol, AT;

basal cell carcinoma, BCC;

cyclooxygenase-2, COX-2;

dimethyl sulfoxide, DMSO;

enzyme-linked immunosorbent assay, ELISA;

epigallocatechin-3-gallate, EGCG;

extracellular-signal-regulated protein kinase ERK;

fibroblast growth factor, FGF;

green tea polyphenol, GTP;

hepatocyte growth factor, HGF;

Hematoxylin and Eosin, H&E;

Heme oxygenase, HO-1;

High Performance Liquid Chromatography, HPLC;

human dermal fibroblasts, HDF;

Jun N-terminal Kinase, JNK;

keratinocyte growth factor, KGF;

malondialdehyde, MDA;

mitogen-activated protein kinase, MAPK;

matrix metalloproteinase, MMP;

minimal erythema dose, MED;

necrosis factor κB, NFκB;

nitric oxide, NO;

normal human keratinocyte, NHK;

phorbol 12-myristate 13-acetate and calcium ionophore A23187, PMACI;

phosphate buffered solution, PBS;

prostaglandin E2, PGE2;

reactive nitrogen species, RNS;

reactive oxygen species, ROS;

squamous cell carcinoma, SCC;

superoxide dismutase, SOD;

terminal deoxynucleotidyl transferase dUTP nick end labeling, TUNEL;

tissue inhibitor metalloproteinases, TIMP;

tocopherol transfer protein, TTP;

total antioxidant capacity, TAC;

tumor necrosis factor-α, TNFα;

ultraviolet, UV;

ultraviolet-A, UVA;

vitamin C, VC;

vitamin E, VE;

3-dimensional, 3D;

8-oxo-deoxyguanosine, 8-OHdG;

CHAPTER 1: Introduction

1.1 Background

Skin is the largest organ in the human body. It is exposed to environmental insult of which ultraviolet (UV) light is thought to be the most harmful (Lippens *et al.*, 2009). UV exposure can cause oxidative stress, inflammation, erythema, breakdown of the extracellular matrix, wrinkling and skin cancer (Boelsma *et al.*, 2001; Iddamalgoda *et al.*, 2008; Mudgil *et al.*, 2003). In fact, cumulative sun exposure is one of the most important risk factors for both nonmelanoma and melanoma skin cancers (Gloster and Brodland, 1996; Miller and Mihm, 2006). Of the UV light spectrum, UVA and UVB rays reach the earth's surface, of which, UVA is 95% (http://www.skincancer.org/understanding-uva-and-uvb.html). UVA has a longer wave length which allows it to penetrate deeper into the skin, causing unique damage in the dermal compartment. Tanning of the skin is induced by UVA and for this reason, it is the primary wavelength used in tanning beds. Recent FDA regulations for sunscreen labeling highlight the importance of UVA (FDA, 2011). For any sunscreen labeled as broadspectrum, the SPF value will refer equally to UVA and UVB protection whereas UVA protection was previously unquantified. While UVA has been historically understudied in comparison to UVB, UVA-focused research is growing as the implications of exposure are revealed.

There are many ways to protect oneself from UV exposure including avoidance of the sun, wearing protective clothing (hats, long-sleeved shirts, treated fabrics, etc), and topical sunscreen. However, the potential for dietary UV protection is a relatively recent concept. Compared to topical sunscreens which require reapplication and have localized effects, dietary methods are thought to provide continual whole body protection. This promise has led to an explosion in nutrient containing products which are marketed for skin health improvement (e.g.

Glowelle®, Crystal Light Skin Essentials, Borba Skin Balance Water). Common ingredients of these products, both cosmetic and consumable, are antioxidant nutrients. However, the market is ahead of the science in this case as there is a lack of published evidence to support skin improvements of these formulated products. Some of these antioxidant nutrients (alpha-tocopherol (AT) and polyphenols found in the skin of almonds (AP)), which have strong scientific evidence of their role in photoprotection, were selected for this research.

Almonds are among the richest sources of AT and contain an array of polyphenols. AT is well known for its role as a chain-breaking antioxidant during lipid peroxidation and it protects polyunsaturated fatty acids in cell membranes from oxidation. AT concentrations in skin can be increased with oral (5 fold increase of deuterated AT in skin surface lipid) or topical delivery (>20 fold increase) (Lopez-Torres *et al.*, 1998; Thiele and Ekanayake-Mudiyanselage, 2007) and are decreased by 50% in the stratum corneum with UV exposure (Rijnkels *et al.*, 2003). Individual AP compounds have been reported to be radical scavengers, UVA absorbent, cytoprotective, anti-inflammatory, anti-apoptotic, and to inhibit DNA damage and to affect cellular signaling pathways (Fahlman and Krol, 2009; Kang *et al.*, 2008; Selmi *et al.*, 2006). Collectively, APs act *in vitro* as antioxidants and induce quinine reductase activity, a marker of chemoprevention (Chen and Blumberg, 2008). Addition of almonds to human diet has reduced biomarkers of oxidative stress in male smokers (Li *et al.*, 2007).

These nutrients have shown promise as photoprotectants in clinical, animal and monolayer cell culture studies. In humans, dietary AT was found protective of UV-induced erythema and lipid peroxidation (McArdle *et al.*, 2004; Mireles-Rocha *et al.*, 2002) but combinations with supplemental vitamin C show greater protection. Epidemiological data indicates a weak protective effect of dietary vitamin E (including AT) in nonmelanoma skin

cancer (McNaughton *et al.*, 2005). Animal studies have demonstrated protection of topically applied AT against wrinkling, sunburn cell formation and skin tumor incidence from (Bissett *et al.*, 1990, 1992; Bissett *et al.*, 1989). Because most of these studies have focused on UVB, our knowledge of AT and UVA photoprotection is limited.

Polyphenol rich foods or extracts have been found to have photoprotective activity in clinical, epidemiological and *in vitro* research. In a clinical trial, long-term, daily ingestion of a cocoa beverage rich in catechin and epicatechin decreased UV-induced erythema by 25% after 12 wks (Heinrich *et al.*, 2006) while topical application of a plant extract containing isorhamnetin, quercetin and kaempferol significantly decreased erythema when applied after UVB irradiation (Aquino *et al.*, 2002). Epidemiologic evidence suggests a negative association between flavonoid-rich dietary factors, including daily tea drinking, high consumption of vegetables, particularly carrots, cruciferous and leafy vegetables, and fruits, especially citrus and melanoma incidence (Fortes *et al.*, 2008). In the "Food Habits in Later Life" study, tea consumption was negatively correlated with actinic skin damage in (Purba *et al.*, 2001). Topical quercetin treatment was found protective of UVB-induced oxidative stress in mouse skin as well (Casagrande *et al.*, 2006).

To our knowledge, there are currently no studies to evaluate the potential photoprotective effects of AT or AP in a 3D human skin model.

1.2 Significance

UV exposure is a public health concern for many reasons. Photosensitivity is a common side-effect of many medications. Both the US Department of Health and Human Services and the World Health organizations have identified UV as a carcinogen. The Healthy People 2020 goals

include reducing sun exposure as part of the skin cancer reduction goals (http://www.healthypeople.gov/2020/default.aspx). Over 1 million skin cancers in the US are attributed to UV exposure per year (Greenlee *et al.*, 2001). Skin cancer can be categorized as nonmelanoma and melanoma. Nonmelanoma cancer includes basal cell carcinoma (BCC) and squamous cell carcinoma (SCC). Nonmelanoma skin cancer has an estimated incidence of over 600,000 cases per year in the US. Approximately 500,000 are BCCs and 100,000–150,000 are SCCs (Silverberg *et al.*, 1990). Melanoma has an estimated incidence of between 11 and 14 per 100,000 cases per year in the US among white populations (National Cancer Institute, 1993).

There are many ways to protect ourselves from UV exposure and thereby reduce the risk of UV damage. Despite this, skin cancer incidence rates are not decreasing. Nutrition has only recently been considered to have a role in UV protection and certain nutrients are now hypothesized to provide low levels of continual, whole body UV protection. Aside from sun avoidance, no other method currently in use can do this. However, the research tools currently used to evaluate the effectiveness of nutrients in photoprotection have limitations. Given this, the 3D human skin model holds much promise. 3D human skin models have been used to study cancer development, wound healing processes and to screen pharmacologic agents (Garlick, 2007) but have not been previously used for nutrient studies. This is a dynamic model that mimics *in vivo* conditions better than monolayer cell models in terms of morphology, stratification, differentiation and signaling pathways. This model can be used as an alternative to animal testing. This is particularly important given that nutrient bioavailability and metabolism as well as skin structure differs between animal models and humans. Furthermore, *in vivo* nutrient photoprotection studies in human skin are difficult because they require scar-inducing skin biopsies and can be costly. When used as a screening tool, this model can rapidly assess

many variables for safety and efficacy. Therefore, the 3D model provides a unique opportunity to efficiently, effectively, and economically assess histological, biochemical and molecular outcomes under conditions similar to those found *in vivo.*

Our investigation of AT and AP in a novel 3D human skin model will generate more insight into their skin health effects, photoprotective potential as well as the feasibility of using this model for future nutrient photoprotection studies. Our results may provide experimental evidence for future dietary and/or topical nutrient application to target and prevent photodamage in humans. This is crucial given the very limited data to support a mechanistic role for nutrients in skin health and disease prevention.

1.3 Hypothesis

The purpose of this study is to investigate the potential effects of alpha-tocopherol (AT) and almond polyphenols (AP) on skin health and photoprotection in a 3D skin model.

Central Hypothesis: Almond phytonutrients (AT and AP) will provide protection from UVA-induced damage and will be absorbed into 3D human skin models.

1.4 Specific Aims

Specific Aim #1: To optimize nutrient treatment parameters for application to 3D skin models.

Sub Aim 1a. Safety: To determine safe doses of almond phytonutrients, AT and AP, for medium and topical application to a 3D skin tissue model. A range of doses from physiologic to pharmacologic will be tested. Based on morphologic and apoptotic response observed in the skin model, one medium (from the physiologic range) and one topical dose will be chosen for subsequent photoprotection and nutrient absorption studies. Doses will be

considered safe when skin tissue architecture is not severely altered and apoptosis is not stimulated when compared to vehicle control skin tissue.

Sub Aim 1b. Absorption: To determine if AT is absorbed into skin tissue from topical or medium application to a 3D human skin models. The working hypothesis of this aim is that AT will be absorbed into the skin tissue based on previous findings of these nutrients in human and murine skin (Lee *et al.*, 2004; Peng *et al.*, 1995; Richelle *et al.*, 2006). To test this hypothesis, the concentration of phytonutrients in the skin cells of the epidermal and dermal compartments as well as medium will be measured (Peng *et al.*, 1993).

Specific Aim #2. Photoprotection: To determine photoprotective effects of topical and medium application (mimicking oral consumption and deposition to skin via the circulation) of phytonutrients to a 3D skin model. Our working hypothesis is that skin tissue from 3D skin models will have less UVA-induced photodamage when pretreated with medium or topical AT or AP as compared to vehicle controls. To test this hypothesis, morphology, apoptosis, proliferation, protein secretion (hepatocyte growth factor (HGF), interleukin 1-alpha (IL1-α), keratinocyte growth factor (KGF) and matrix metalloproteinase-2 (MMP-2), and antioxidant status (measured by total antioxidant capacity assay), will be assessed (Bernerd and Asselineau, 2008; Lejeune *et al.*, 2008; Mudgil *et al.*, 2003; Murray *et al.*, 2007). In nutrient treated skin models, we expect to see better morphology, significantly less apoptosis, more proliferation, less expression of MMP-2 and IL-1α, increased total antioxidant capacity, and reduced loss of dermal fibroblasts from UVA exposure when compared to vehicle controls. These studies will provide information to support the photoprotection in skin provided by phytonutrients as well as their differential efficacy with topical and medium exposure *in vitro*.

References

Aquino R, Morelli S, Tomaino A, Pellegrino M, Saija A, Grumetto L*, et al.* (2002) Antioxidant and photoprotective activity of a crude extract of Culcitium reflexum H.B.K. leaves and their major flavonoids. *J Ethnopharmacol* 79:183-91.

Bernerd F, Asselineau D (2008) An organotypic model of skin to study photodamage and photoprotection in vitro. *J Am Acad Dermatol* 58:S155-9.

Bissett DL, Chatterjee R, Hannon DP (1990) Photoprotective effect of superoxide-scavenging antioxidants against ultraviolet radiation-induced chronic skin damage in the hairless mouse. *Photodermatol Photoimmunol Photomed* 7:56-62.

Bissett DL, Chatterjee R, Hannon DP (1992) Protective effect of a topically applied anti-oxidant plus an anti-inflammatory agent against ultraviolet radiation-induced chronic skin damage in the hairless mouse. *J Soc Cosmet Chem* 43:85-92.

Bissett DL, Hillebrand GG, Hannon DP (1989) The hairless mouse as a model of skin photoaging: its use to evaluate photoprotective materials. *Photodermatol* 6:228-33.

Boelsma E, Hendriks HF, Roza L (2001) Nutritional skin care: health effects of micronutrients and fatty acids. *Am J Clin Nutr* 73:853-64.

Casagrande R, Georgetti SR, Verri WA, Jr., Dorta DJ, dos Santos AC, Fonseca MJ (2006) Protective effect of topical formulations containing quercetin against UVB-induced oxidative stress in hairless mice. *J Photochem Photobiol B* 84:21-7.

Chen CY, Blumberg JB (2008) In vitro activity of almond skin polyphenols for scavenging free radicals and inducing quinone reductase. *J Agric Food Chem* 56:4427-34.

Fahlman BM, Krol ES (2009) Inhibition of UVA and UVB radiation-induced lipid oxidation by quercetin. *J Agric Food Chem* 57:5301-5.

FDA (2011) Labeling and Effectiveness Testing; Sunscreen Drug Products for Over-the-Counter Human Use. In: *21 CFR Parts 201 and 310* (35620-65).

Fortes C, Mastroeni S, Melchi F, Pilla MA, Antonelli G, Camaioni D*, et al.* (2008) A protective effect of the Mediterranean diet for cutaneous melanoma. *Int J Epidemiol* 37:1018-29.

Garlick JA (2007) Engineering skin to study human disease--tissue models for cancer biology and wound repair. *Adv Biochem Eng Biotechnol* 103:207-39.

Gloster HM, Jr., Brodland DG (1996) The epidemiology of skin cancer. *Dermatol Surg* 22:217-26.

Greenlee RT, Hill-Harmon MB, Murray T, Thun M (2001) Cancer statistics, 2001. *CA Cancer J Clin* 51:15-36.

Heinrich U, Neukam K, Tronnier H, Sies H, Stahl W (2006) Long-term ingestion of high flavanol cocoa provides photoprotection against UV-induced erythema and improves skin condition in women. *J Nutr* 136:1565-9.

Iddamalgoda A, Le QT, Ito K, Tanaka K, Kojima H, Kido H (2008) Mast cell tryptase and photoaging: possible involvement in the degradation of extra cellular matrix and basement membrane proteins. *Arch Dermatol Res* 300 Suppl 1:S69-76.

Kang BY, Kim S, Lee KH, Lee YS, Hong I, Lee MO*, et al.* (2008) Transcriptional profiling in human HaCaT keratinocytes in response to kaempferol and identification of potential transcription factors for regulating differential gene expression. *Exp Mol Med* 40:208-19.

Lee EH, Faulhaber D, Hanson KM, Ding W, Peters S, Kodali S*, et al.* (2004) Dietary lutein reduces ultraviolet radiation-induced inflammation and immunosuppression. *J Invest Dermatol* 122:510-7.

Lejeune F, Christiaens F, Bernerd F (2008) Evaluation of sunscreen products using a reconstructed skin model exposed to simulated daily ultraviolet radiation: relevance of filtration profile and SPF value for daily photoprotection. *Photodermatol Photoimmunol Photomed* 24:249-55.

Li N, Jia X, Chen CY, Blumberg JB, Song Y, Zhang W*, et al.* (2007) Almond consumption reduces oxidative DNA damage and lipid peroxidation in male smokers. *J Nutr* 137:2717-22.

Lippens S, Hoste E, Vandenabeele P, Agostinis P, Declercq W (2009) Cell death in the skin. *Apoptosis* 14:549-69.

Lopez-Torres M, Thiele JJ, Shindo Y, Han D, Packer L (1998) Topical application of alpha-tocopherol modulates the antioxidant network and diminishes ultraviolet-induced oxidative damage in murine skin. *Br J Dermatol* 138:207-15.

McArdle F, Rhodes LE, Parslew RA, Close GL, Jack CI, Friedmann PS*, et al.* (2004) Effects of oral vitamin E and beta-carotene supplementation on ultraviolet radiation-induced oxidative stress in human skin. *Am J Clin Nutr* 80:1270-5.

McNaughton SA, Marks GC, Green AC (2005) Role of dietary factors in the development of basal cell cancer and squamous cell cancer of the skin. *Cancer Epidemiol Biomarkers Prev* 14:1596-607.

Miller AJ, Mihm MC, Jr. (2006) Melanoma. *N Engl J Med* 355:51-65.

Mireles-Rocha H, Galindo I, Huerta M, Trujillo-Hernandez B, Elizalde A, Cortes-Franco R (2002) UVB photoprotection with antioxidants: effects of oral therapy with d-alpha-tocopherol and ascorbic acid on the minimal erythema dose. *Acta Derm Venereol* 82:21-4.

Mudgil AV, Segal N, Andriani F, Wang Y, Fusenig NE, Garlick JA (2003) Ultraviolet B irradiation induces expansion of intraepithelial tumor cells in a tissue model of early cancer progression. *J Invest Dermatol* 121:191-7.

Murray AR, Kisin ER, Kommineni C, Vallyathan V, Castranova V, Shvedova AA (2007) Pro/antioxidant status and AP-1 transcription factor in murine skin following topical exposure to cumene hydroperoxide. *Carcinogenesis* 28:1582-8.

National Cancer Institute (1993) SEER Program Cancer Facts and Figures. (National Institute of Health ed) NIH Publications: Washington, 93-2789.

Peng YM, Peng YS, Lin Y (1993) A nonsaponification method for the determination of carotenoids, retinoids, and tocopherols in solid human tissues. *Cancer Epidemiol Biomarkers Prev* 2:139-44.

Peng YM, Peng YS, Lin Y, Moon T, Roe DJ, Ritenbaugh C (1995) Concentrations and plasma-tissue-diet relationships of carotenoids, retinoids, and tocopherols in humans. *Nutr Cancer* 23:233-46.

Purba MB, Kouris-Blazos A, Wattanapenpaiboon N, Lukito W, Rothenberg EM, Steen BC*, et al.* (2001) Skin wrinkling: can food make a difference? *J Am Coll Nutr* 20:71-80.

Richelle M, Sabatier M, Steiling H, Williamson G (2006) Skin bioavailability of dietary vitamin E, carotenoids, polyphenols, vitamin C, zinc and selenium. *Br J Nutr* 96:227-38.

Rijnkels JM, Moison RM, Podda E, van Henegouwen GM (2003) Photoprotection by antioxidants against UVB-radiation-induced damage in pig skin organ culture. *Radiat Res* 159:210-7.

Selmi C, Mao TK, Keen CL, Schmitz HH, Eric Gershwin M (2006) The anti-inflammatory properties of cocoa flavanols. *J Cardiovasc Pharmacol* 47 Suppl 2:S163-71; discussion S72-6.

Silverberg E, Boring CC, Squires TS (1990) Cancer statistics, 1990. *CA Cancer J Clin* 40:9-26.

Thiele JJ, Ekanayake-Mudiyanselage S (2007) Vitamin E in human skin: organ-specific physiology and considerations for its use in dermatology. *Mol Aspects Med* 28:646-67.

CHAPTER 2: Literature Review

2.1 Skin

Human skin is made up of two main layers, including the outer cellular epidermis and the inner largely extracellular dermis (**Figure 1**). The main epidermal cell type is the keratinocyte which differentiates until death and generates the outermost layer called the stratum corneum which serves an important barrier function. These cells are replaced by cell division of basal keratinocytes. Pigment-producing melanocytes and immuno-responsive Langerhans cells are also found in this skin layer. The dermal extracellular matrix is mostly collagen synthesized by fibroblasts (Young, 2006).

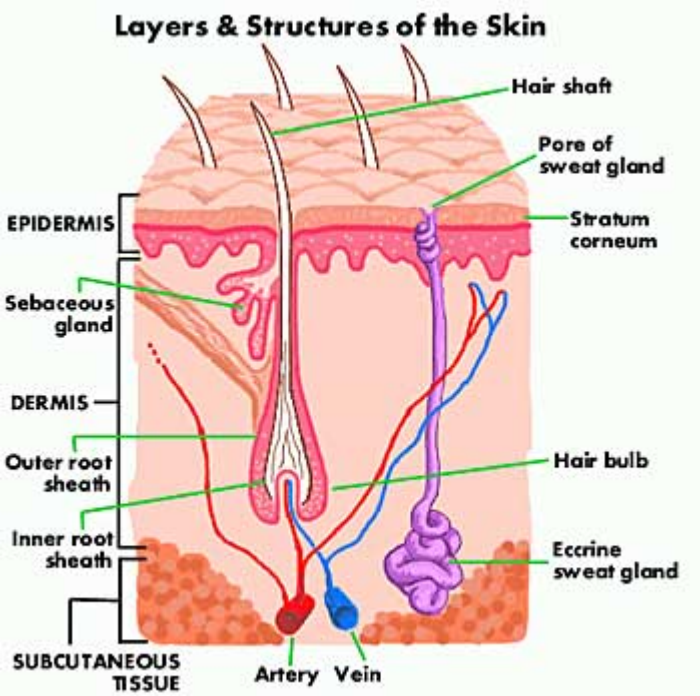

Figure 1. Anatomy of human skin (healthy-skin-guide.com)

2.2 UVA damage

UV light is grouped as UVA (315-400 nm), UVB (280-315 nm) and UVC (220-280 nm), from lowest to highest energy. The Earth's atmosphere filters out UVC light and of the

remaining UV light to which we are exposed, approximately 95% is UVA. While UVB photons are on average 1000 times more energetic than UVA photons, UVA is at least 10 fold more abundant and has greater year-round and day-long average irradiance (Yaar and Gilchrest, 2007). The primary focus of UV research has historically been on UVB wavelengths but interest is shifting toward UVA light. This is reflected in the revised Food and Drug Administration regulations for sunscreen, in which "Broad Spectrum SPF" values are mandated to reflect both UVA and UVB protection equally beginning in the summer of 2012 (FDA, 2011). Because UVA is of higher wavelength than UVB, it penetrates deeper into the skin (Bruls *et al.*, 1984). UVB is mostly absorbed by the epidermal layer, but UVA affects the dermal layer as well.

UV damage can be direct or indirect. UVB damage is thought to be predominantly direct. UVA is thought to damage the skin primarily by indirect means via generating reactive chemical species upon absorption of photons by riboflavin, porphyrins and heme-containing proteins (McMillan *et al.*, 2008). Reactive oxygen species (ROS), reactive nitrogen species (RNS) as well as further enzymatic production of ROS have been implicated. UVA more effectively induces oxidative damage than UVB (Halliday, 2005). Reactive species can damage major biomolecules including DNA, proteins and lipids in various skin strata leading to cytotoxicity, mutations and alterations in cell signaling pathways. The epidermis contains antioxidant defenses including the enzymes, superoxide dismutase (SOD), glutathione peroxidase and catalase, which remove ROS from the skin. SOD converts superoxide anions to hydrogen peroxide, which is degraded by catalase or glutathione peroxidase to water. UVA suppresses catalase activity but not SOD in human stratum corneum (Hellemans *et al.*, 2003). Free radical scavengers, such as vitamins C and E, carotenoids and glutathione are also present in the skin to reduce the damaging effects of ROS. UV irradiation can deplete these antioxidant

molecules and ROS can accumulate. In a 3D human skin model, glutathione gene expression was upregulated 2 h after 2, 6 or 12 J/cm^2 UVA (Meloni *et al.*). Antixoidant enzymes such as catalase and SOD-1 and -2 are found in lower concentration in the dermis (Sander *et al.*, 2002), therefore this compartment may be more susceptible to oxidative damage than the epidermis.

UVA can cause DNA damage, which is thought to occur indirectly via ROS. While pyrimidine dimers are more commonly associated with UVB, UVA of 3 to 6 times the energy at 365 nm can produce such dimmers (Marrot and Meunier, 2008). 8-Oxo-deoxyguanosine (8-OHdG) is a DNA lesion resulting from oxidation of guanine bases that can be induced by UVA. Mechanisms to prevent DNA damage in skin cells include growth arrest followed by DNA repair and cell death by apoptosis, both of which prevent transmission of mutations to daughter cells (Sander *et al.*, 2004). UV-induced apoptosis has been shown to be regulated via various mechanisms involving ROS, DNA damage, activation of the tumor supressor gene p53, triggering of cell death receptors either directly by UV or by autocrine release of death ligands, mitochondrial damage and cytochrome C release.

At least 21 matrix metalloproteases (MMPs) are known, forming a family of human structurally and functionally related zinc endoproteases (Hantke *et al.*, 2002). They can be divided into subgroups of collagenases, gelatinases, stromelysins, and membrane-type MMPs according to their substrate specificity and domain structure. MMP-1 (collagenase-1) cleaves collagen type I, II and III, while MMP-2 (gelatinase A) is able to degrade elastin and basement membrane components including collagen type IV and type VII. It has recently been shown that fibrillin can also be degraded by various MMPs. UVA irradiation is reported to induce expression of MMP-1, -2, and -3 in human dermal fibroblasts (HDF) in culture and *in vivo* (Oh *et al.*, 2004). Indirect evidence has shown that singlet oxygen and H_2O_2 are the major ROS

involved in the UVA-induced MMP-1, -2 and -3 on mRNA and protein levels. In cultured human fibroblasts from foreskin biopsies, UVA induced activity in p38 and c-Jun-N-terminal kinase (JNK) of the mitogen-activated protein kinase (MAPK) family, but not extracellular signal-regulated kinases (ERK) (Klotz *et al.*, 1999). This activation was attributed to singlet oxygen ($^1O_2$) because of subsequent inhibition by $^1O_2$ quenchers. This activation can lead to downstream activation of transcription factors that activate stress-inducible genes, specifically MMP-1. MMPs are responsible for the degradation of the extracellular matrix in skin. However in normal human epidermal keratinocytes, a single UVA dose suppressed MMP-2 activity (Steinbrenner *et al.*, 2003). MMP activity is regulated at three levels: synthesis (primarily transcription), activation by cleavage of the proenzymes, and inhibition of proteolytic activity, by specific endogenous protein inhibitors called tissue inhibitors of metalloproteinases (TIMPs) (Rittie and Fisher, 2002).

Hepatocyte growth factor (HGF, also identified as scatter factor) is secreted by fibroblasts in the skin and activated by proteolytic cleavage. It signals via transmembrane tyrosine kinase receptor c-MET. Sensitive to Ca^{2+}, HGF markedly enhances the migration of keratinocytes, but suppresses cell growth and DNA synthesis at low Ca^{2+} concentrations. In contrast, HGF enhances cell migration and growth, and DNA synthesis, in keratinocytes cultured in physiological Ca^{2+} concentrations. Both HGF and keratinicyte growth factor (KGF) promote the migration of keratinocytes in low-calcium medium. HGF activates a signal transducer and activator of transcription-3, coincident with its induction of keratinocyte migration, suggesting this pathway is involved in KGF's effect on keratinocyte migration (Shirakata). In an *in vitro* experiment, supernatants of UVB-irradiated keratinocytes induced HGF production in human dermal fibroblasts, which was linked with interleukin 1α (IL-1α) (Mildner *et al.*, 2007). Direct

irradiation of fibroblasts with UVB had no effect on HGF expression, while irradiation with UVA upregulated HGF mRNA production and protein secretion. Addition of neutralizing anti-HGF antibodies after UVA irradiation, as well as transfection of fibroblasts with HGF small-interfering RNA (which completely inhibited HGF secretion), led to a rise of fibroblast apoptosis demonstrating that autocrine HGF protected fibroblasts from UVA-induced apoptosis.

Keratinocyte growth factor (KGF, also identified as FGF7) is a member of the fibroblast growth factor (FGF) family and an important mitogen to keratinocytes. In the skin, it is secreted by dermal fibroblasts and acts on epidermal keratinocytes in a paracrine fashion, recognized by transmembrane protein tyrosine kinase FGF receptor 2b (Shirakata). In HaCaT cells, KGF treatment increased cell survival after intermediate doses of UVA and UVB. It was also protective of UVB-induced apoptosis in the skin of mice (Braun *et al.*, 2006).

IL-1α gene expression was not stimulated by low dose UVA (2, 6 or 12 J/cm^2) in a 3D human skin model 2, 6, 24 or 168 h post-irradiation (Meloni *et al.*).

UV irradiation augments the presence of leukocytes, including macrophages and neutrophils, to the skin which is referred to clinically as inflammation (Halliday, 2005). These migrations may be attributed to increased nitric oxide (NO) and prostaglandins. Both UVA and UVB can activate NO synthase in the skin causing an increase in NO. NO can react with UV-induced superoxide to form highly toxic peroxynitrite. Prostaglandin increases are perhaps due to UV-induced phospholipase activity which frees arachidonic acid for conversion to prostaglandin E2 (PGE2) by cyclooxygenase-2 (COX-2). Recruited leukocytes also produce ROS which can damage biomolecules.

Both UVA and UVB are immunosuppressive in humans. However, in an experiment using a range of UV doses to assess immune protection provided by six sunscreens, the level of

protection to skin immunity in humans were found to be directly related to the level of UVA protection (Poon *et al.*, 2003).

In a 3D skin model, UVA induced keratinocyte and fibroblast vacuolation and nuclear pyknosis, intense terminal deoxynucleotidyl transferase dUTP nick end labeling (TUNEL) staining of fibroblasts and increased staining of cells and nuclei for 8-OHdG, but smaller increased intensity staining for heme oxygenase (HO-1) and IL-lα (confirmed by ELISA assays of the medium supernatants). Quercetin-3-glucoside reduced changes in morphology, 8-OHdG, TUNEL and IL-lα (Dekker *et al.*, 2005). Bernard et al have demonstrated UVA damage in 3D skin tissue models, including disappearance of superficial fibroblasts in the dermis via apoptosis (Bernerd and Asselineau, 2008).

UVA has demonstrated carcinogenicity in animal models (McMillan *et al.*, 2008), emphasizing the need to understand and prevent the processes by which UVA exerts its biological effects. Clinical changes seen with photoaging, such as roughness, fine wrinkles, spotty hyperpigmentation, vasodilation, and loss of elasticity, are attributed primarily to UVA as well (Touitou and Godin, 2008).

2.3 Nutrients

Based on the accumulating data from human intervention trials, epidemiology, animal studies and cell culture, nutrients of interest in the study of photoprotection in skin include α-tocopherol (AT) and almond polyphenols (AP).

2.3.1 α-Tocopherol Vitamin E (VE) refers to a family of eight nutrients of which AT is the most abundant and biologically active form in the human body (**Figure 1**). Based on epidermal content from the trunk (abdominal or back) of 16 subjects, VE content by isoform is 1% α-

tocotrienol, 3% γ-tocotrienol, 87% α-tocopherol, and 9% γ-tocopherol (Fuchs *et al.*, 2003). Another group found γ-tocopherol in greater abundance than α-tocopherol in human skin (unknown source location) in 2 of 6 samples (Burton *et al.*, 1998). γ-tocopherol was not detected in the 4 other samples. A different extraction method was used (saponification but not homogenization) in the later group. The conflicting results leave room for uncertainty of the predominant form of VE in human skin. Skin content of VE may vary by body region, which has been found for carotenoids (Richelle *et al.*, 2006), and may explain some of the conflicting results. VE content analysis of skin as it relates to diet and plasma is needed. The AT form has 3 methyl groups on its chromanol ring and is recognized by the tocopherol transfer protein (TTP) which is responsible for its intracellular transport. This essential lipophilic nutrient is well known for its role as a chain-breaking antioxidant during lipid peroxidation and it protects polyunsaturated fatty acids in cell membranes from oxidation. One molecule of AT has been shown to protect up to 220 polyunsaturated fatty acid molecules from oxidation in this manner before itself being degraded (Fukuzawa *et al.*, 1982). VE also has the ability to affect signal transduction and gene expression (Zingg, 2007). Food sources include vegetables, vegetable oils, cereals and nuts (Thiele and Ekanayake-Mudiyanselage, 2007). Almonds are a particularly good source of AT, containing approximately 26 mg per 100 g which is greater than the recommended dietary allowance of 15 mg/day for women and men over the age of 13 (U.S. Department of Agriculture, 2007).

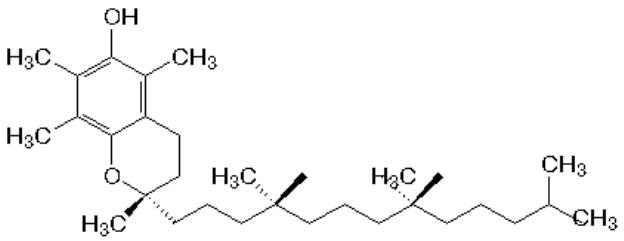

Figure 2. Chemical structure of α-Tocopherol (AT).

AT concentrations in skin can be increased with oral or topical delivery (Thiele and Ekanayake-Mudiyanselage, 2007) and are decreased with UV exposure (Rijnkels *et al.*, 2003). Distribution among the layers of human skin has been determined (**Table 1**). Within human upper arm stratum corneum, a gradient of highest to lowest AT concentration was found from inner to outer layers (Thiele *et al.*, 1998). AT content of aged skin was found to be lower in the epidermis but not the dermis (Rhie *et al.*, 2001). AT's activity as an antioxidant, combined with its presence in human skin, provide biologic plausibility for its role as a photoprotectant in skin.

Table 1. Distribution of α-tocopherol (AT) in human skin compartments.

Skin Layer	**Concentration**	**Reference**
Epidermis	31 $\pm$ 3.8 nmol /g tissue	(Shindo *et al.*, 1994)
Dermis	16.2 $\pm$ 1.1 nmol/g tissue	(Shindo *et al.*, 1994)
Stratum corneum	33 $\pm$ 4 nmol/g tissue	(Thiele *et al.*, 1998)
Sebum	76.5 $\pm$ 1.5 nmol/g sebum	(Thiele *et al.*, 1999)

2.3.1.1 Clinical Trials

Clinical trials suggest that dietary VE may act as a photoprotectant with the aid of other antioxidants and topical VE may provide protection as well, although reports have not been entirely consistent.

One study showed subjects treated with 400 IU/d AT for eight weeks had reduced skin malondialdehyde (MDA) after UV exposure but this intervention provided no protection from erythema, the reddening of the skin commonly referred to as sunburn (McArdle *et al.*, 2004). Wernignaus et al (Werninghaus *et al.*, 1994) showed no photoprotective effect after 6 months of daily dietary supplementation of AT acetate (400 IU) in 12 subjects of skin types II-IV. Both clinical measure of minimal erythema dose (MED), the minimum dose of UV necessary to induce erythema in a subject, and histologic measure of sunburn cells were compared. No difference was seen in skin AT concentrations between treatment and placebo groups. Plasma AT concentrations increased by 65% in the treatment group and 18% in the placebo group, so there was no question of bioavailability. Although a very modest increase in MED was observed in the treatment group after 6 months, the sample size of this study may have been too small to observe significant changes. It is possible that AT will provide the most benefit in subjects with a limited range in skin types of increased risk for photodamage (very light to light). Additionally, repetitive UV doses lower than necessary to produce erythema are enough to cause local immunosuppression and skin carcinogenesis (Touitou and Godin, 2008), suggesting that other markers of damage may be important such as DNA damage.

Other dietary studies have shown VE as a photoprotectant when combined with other antioxidants. Fuchs et al (Fuchs and Kern, 1998) reported no protection when vitamin C (VC, 3 g) and AT (2 g or 3000 IU) were supplemented individually, but in combination these nutrients provided protection as assessed by increased MED after 50 days of daily supplementation. Eberlein-Konig et al (Eberlein-Konig *et al.*, 1998b) also showed increased MED in subjects supplemented daily with a combination of VC (2 g) and AT (1000 IU) after only 8 days. A similar study showed increased MED in subjects supplemented daily with AT (1200 IU) for 7

days, but when combined with VC (2 g) a greater increase in MED was observed (Mireles-Rocha *et al.*, 2002). Placzek et al (Placzek *et al.*, 2005) demonstrated a photoprotective effect after 3 months of daily dietary supplementation with VC (1 g) and AT (500 IU). Participants showed increased resistance to UVB-induced sunburn, as assessed by MED, and protection from DNA damage. This study provides evidence of long-term photoprotection of lower doses than previously tested. Stahl et al. found that 12-week oral supplementation with a combination of carotenoids (25 mg total/day, including 13.0 mg *all-trans*-β-carotene, 10.5 mg 9-*cis* β-carotene, 0.3 mg other *cis* isomers of β-carotene, 0.75 mg α-carotene, 0.18 mg cryptoxanthin, 0.15 mg zeaxanthin, and 0.12 mg lutein) and AT (500 IU/day) provided greater protection from UVR-induced erythema than carotenoids alone (Stahl *et al.*, 2000), but the difference was not statistically significant. This suggests that AT may provide additional benefit beyond carotenoids.

Clinical trials suggest that VE applied topically also provides photoprotection. Chung et al demonstrated topical application of 5% VE (24 hours prior to UV exposure) inhibited UV-induced MMP-12 mRNA by 47% (Chung *et al.*, 2002). Other groups have reached opposing conclusions on the protection that VE can provide from erythema. One group demonstrated reduced erythema when VE was applied prior to UV exposure but not after (Dreher *et al.*, 1999). Another group found VE application after UV exposure protective, but not pretreatment (Montenegro *et al.*, 1995).

2.3.1.2 Epidemiology

In a review of epidemiologic literature, McNaughton et al found evidence of a weak protective effect of VE in nonmelanoma carcinoma (BCC and SCC) (McNaughton *et al.*, 2005). Of the 12 studies examined, two identified an inverse relationship between intake and BCC risk

while one demonstrated a positive relationship. Six found no relationship between plasma or intake of VE and BCC risk. Four studies found no association between VE and SCC. More recently, two studies in an Australian population reported no association between serum AT and nonmelanoma carcinoma but a positive association between dietary AT including supplements, and BCC (Heinen *et al.*, 2007; van der Pols *et al.*, 2009). However, in these two studies a single baseline serum measurement or dietary assessment was compared to cancer incidence during an eight year period. These unexpected findings may reflect the possible inability of a single measure of VE to accurately reflect VE status and a change in eating habit cannot be ruled out over the 8 year period. Furthermore, these studies analyzed the association between cancer, which is a long-term outcome, and short-term markers of VE intake or status such as dietary assessment and serum concentration. Cancer may be closer related to skin concentrations which were not compared in any of these studies.

There are no epidemiological studies assessing the relationship between topically applied AT and skin cancer.

2.3.1.3 Animal Studies

UVB irradiated mice fed α-tocopheryl acetate had less cancer incidence in a dose-dependent manner (Gerrish and Gensler, 1993). However, the doses used were considered toxic given that more treated mice died compared to control mice. Dietary AT esters are readily cleaved and free AT is absorbed into the circulatory system. A more recent experiment tested an oral combination of VC, VE, pycnogenol (a pine bark extract rich in polyphenols and procyanidins), and evening primrose oil in mice (Cho *et al.*, 2007). The nutrient cocktail treatment significantly inhibited UVB-induced wrinkling and many associated events, including expressions of MMPs, MAPK and activation of activator protein (AP)-1 transcriptional factor.

While these results support a role for nutrient effects in photoprotection, specific effects of VE could not be determined.

Studies in mice treated topically with AT provide strong evidence of photoprotection (Thiele and Ekanayake-Mudiyanselage, 2007). Mice treated topically with 25 mg AT three times per week for three weeks before and during twelve weeks of UVB irradiation had significantly less incidence of skin cancer compared to untreated mice (Gensler and Magdaleno, 1991). Four additional murine studies demonstrated photoprotection, assessed as skin tumor incidence, from topical AT treatment (Bissett *et al.*, 1990, 1992; Bissett *et al.*, 1989; Burke *et al.*, 2000). A follow-up study using this AT treatment reduced induction of DNA damage by UVB (Chen *et al.*, 1997). Later studies by this group found acetate and succinate esterified forms of AT applied in the same manner do not provide the same chemoprevention (Gensler *et al.*, 1996a). This difference may be due to the limited capacity to cleave acetate or succinate when applied topically. This limitation may compromise the antioxidant activity given that ester forms do not have a free hydroxyl group on the aromatic ring necessary for scavenging free radicals. However, topical application of 8 mg/cm^2 AT acetate on the backs of guinea pig for 3 weeks before a single UVB exposure was protective of skin SOD decrease and lipid peroxidation (Saral *et al.*, 2002). Sufficient cleavage of AT may have occurred to provide protection from a single UVB dose whereas the mice studies used chronic UVB exposure.

Summarized in **Table 2** are animal studies consistently showing topical pretreatment with VE is photoprotective using a variety of outcome measures, including erythema, lipid peroxidation, wrinkling, epidermal thickness and sunburn cell formation (Beijersbergen van Henegouwen *et al.*, 1995; Darr *et al.*, 1996; Evelson *et al.*, 1997; Jurkiewicz *et al.*, 1995; Khettab *et al.*, 1988; Lin *et al.*, 2003; Lopez-Torres *et al.*, 1998; McVean and Liebler, 1997, 1999;

Potapenko *et al.*, 1984; Record *et al.*, 1991; Ritter *et al.*, 1997; Roshchupkin *et al.*, 1979; Schoonderwoerd *et al.*, 1991; Yuen and Halliday, 1997).

Table 2. Summary Vitamin E photoprotection studies in animals (Thiele and Ekanayake-Mudiyanselage, 2007)

	Species	**Outcome measure(s)**	**Efficacy**	**Reference**
1	Rabbit	Erythema (MED)	Vitamin E protective; vitamin E acetate not protective	Roshchupkin et al. (1979)
2	Human, rabbit	PUVA-induced erythema and changes in mechanoelectrical properties of skin	Vitamin E and derivatives with shorter hydrocarbon chain protective; vitamin E acetate not protective	Potapenko et al. (1984)
3	Mouse	Lipid peroxidation	Protective	Khettab et al. (1988)
4	Mouse	Skin wrinkling, skin tumor incidence, and histology	Protective	Bissett et al. (1989)
5	Mouse	Skin wrinkling and sagging, skin tumor incidence, and histology	Vitamin E esters not as protective as vitamin E or vitamin E analog Trolox ; no protection against UVA-induced skin sagging	Bissett et al. (1990)
6	Mouse	Skin tumor incidence and immunosuppression	Protective	Gensler and Magdaleno (1991)
7	Rat	UVA-induced binding of 8-MOP and CPZ to epidermal biomacromolecules	Vitamin E protective after single application; vitamin E acetate only protective after prolonged application	Schoonderwoerd et al. (1991)
8	Mouse	Lipid peroxidation and DNA-synthesis rate	Protective	Record et al. (1991)

9	Mouse	Skin wrinkling, skin tumor incidence, and histology	Protective	Bissett et al. (1992)
10	Mouse	Erythema, edema, and skin sensitivity	Protective	Trevithick et al. (1992)
11	Mouse	Edema and histology	Protective	Trevithick et al. (1993)
12	Mouse	Skin wrinkling	Vitamin E and sorbate ester protective; vitamin E acetate ester only modestly protective	Jurkiewicz et al. (1995)
13	Rat	UVA-induced binding of 8-MOP to epidermal biomacromolecules	Vitamin E protective; vitamin E acetate only protective after prolonged application	Beijersbergen van Henegouwen et al. (1995)
14	Mouse	Skin tumor incidence and immunosuppression	No protection	Gensler et al. (1996)
15	Yorkshire pig	Sunburn cell formation	Protection against UVRinduced damage	Darr et al. (1996)
16	Mouse	Immunosuppression and lipid peroxidation	Protective	Yuen and Halliday (1997)
17	Mouse	Histology (sunburn cell formation and skin thickness)	Protective	Ritter et al. (1997)
18	Mouse	Formation of DNA photoadducts	Vitamin E derivatives less protective than vitamin E	McVean and Liebler (1997)
19	Mouse	Chemiluminescence after UVA-exposure	Protective	Evelson et al. (1997)
20	Mouse	Formation of DNA photoadducts in epidermal p53 gene	Protective	Chen et al. (1996)
21	Mouse	Lipid peroxidation	Protective	Lopez-Torres et al. (1998)
22	Mouse	Formation of DNA photoadducts	Vitamin E, a-tocopherol and c-tocopherol protective; vitamin E acetate and vitamin E methyl ether not	McVean and Liebler (1999)

			protective	
23	Mouse	Erythema, pigmentation, skin tumor incidence	Protective after prolonged application	Burke et al. (2000)
24	Yorkshire pig	Antioxidant protection factor, erythema, sunburn cells, thymine dimers	1% Vitamin E protective, but stronger protective in combination with 15% vitamin C	Lin et al. (2003)

2.3.1.4 *In vitro* Studies

Absorption of topical δ-tocopherol-glucoside, δ-tocopherol and AT acetate into epidermal and dermal compartments of viable human skin explants has been measured (Mavon *et al.*, 2004), but AT was not included in this study. Pig skin biopsies have been cultured showing pretreatment with topical VE reduced UVB-induced cytotoxicity, apoptosis and lipid peroxidation (Rijnkels *et al.*, 2003). In cultured mouse skin, medium pretreatment of 9 μM α-tocopherol-6-O-phosphate, a water-soluble form of AT, reduced UVB-induced apoptosis and lipid peroxidation (Nakayama *et al.*, 2003). Medium pretreatment of AT in human melanocytes prevented UVA- and UVB-induced glutathione loss and diminished apoptosis (Larsson *et al.*, 2006). In a dose dependent manner, AT reduced UVA induced IL-8 mRNA expression and protein secretion as well as AP-1 DNA binding activity and inhibited the NADPH oxidase activity and the formation of malondialdehyde-thiobarbituric acid in human keratinocytes (Wu *et al.*, 2008). Others have found pretreatment with AT to SCL II keratinocytes (derived from a human squamous cell carcinoma) suppressed UVB-induced IL1-α and IL-6 secretion (Eberlein-Konig *et al.*, 1998a). In 3D cultures of normal human keratinocytes, IL-1α was induced by UVA irradiation and pretreatment with topical, but not medium, AT reduced cell death (Noel-Hudson

et al., 1997). Finally, AT pretreatment partially inhibited UVA-induced MMP-2 activity in human dermal fibroblasts (both monolayer and in collagen gel) (Hantke *et al.*, 2002).

2.3.2 Almond polyphenols Predominant AP include the flavonoids isorhamnetin, catechin, kaempferol, epicatechin and quercetin (**Figure 2**) (Milbury *et al.*, 2006). Flavonoids are a family of over 5000 compounds found in plants. Flavonoid structure is based on a flavane nucleus, which contains two benzene rings separated by an oxygen containing pyrane ring. Individual AP compounds have been reported to be radical scavengers, UVA absorbent, cytoprotective, anti-inflammatory anti-apoptotic, and to inhibit DNA damage and to affect cellular signaling pathways (Fahlman and Krol, 2009; Kang *et al.*, 2008; Selmi *et al.*, 2006). Collectively, APs act *in vitro* as antioxidants and induce quinine reductase activity, a marker of chemopreventive activity (Chen and Blumberg, 2008). Addition of almonds to human diet has reduced biomarkers of oxidative stress (Li *et al.*, 2007). In addition to almonds, foods rich in these flavonoids include tea, cocoa, onion, kale and other fruits and vegetables (Shils *et al.*, 2006).

Absorption of AP to human skin has not been tested. However, radioactivity was detected in the skin of mice fed ^{3}H-labeled epigallocatechin-3-gallate (EGCG), a closely related flavanol found in green tea (Suganuma *et al.*, 1998). From a single topical dose of EGCG, maximal concentrations of 1366 and 411 ng/mL were measured in mouse epidermis and dermis, respectively (Lambert *et al.*, 2006).

Quercetin absorbs UV radiation at 255 and 365 nm and is synthesized in some plants in response to UV exposure, suggesting a photoprotective role (Fahlman and Krol, 2009). Sun protection factor and protection factor-UVA of a 10% (w/w) quercetin emulsion are approximately 12 and 15, respectively, which is greater than some UV filters authorized by the

European Union. In combination with titanium dioxide, the sun protection factor and protection factor-UVA are approximately 30 and 16, respectively (Choquenet *et al.*, 2008).

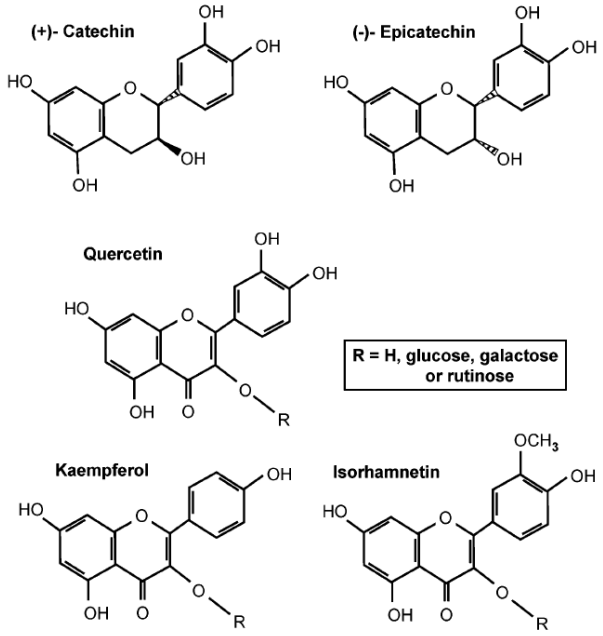

Figure 3. Chemical structures of predominant almond polyphenols (AP). (Milbury *et al.*, 2006)

2.3.2.1 Clinical Trials

The acute and long-term photoprotective effects of consumption of a flavanol-rich cocoa beverage was studied in double-blind, placebo controlled clinical trials. Epicatechin and its stereoisomer catechin are the major flavanols found in this beverage, contributing 61 and 20 mg/serving, respectively to a total of 329 mg cocoa flavanols. Two hours after a single dose of the flavanol-rich cocoa, dermal blood flow and oxygen saturation of hemoglobin significantly increased by 1.7 and 1.8-fold, respectively (Neukam *et al.*, 2007). Long-term, daily ingestion of the same flavanol-rich cocoa beverage decreased UV-induced erythema by 15% after only six weeks (Heinrich *et al.*, 2006). After twelve weeks, additional protection was evident as erythema was decreased by 25%. Blood flow of cutaneous and subcutaneous tissues, skin

density and skin hydration were also increased while skin roughness and scaling were significantly decreased. None of these skin improvements was observed in the control group.

Green tea contains the major almond skin flavanols catechin and epicatechin. An eight week clinical trial evaluating the clinical and histological effects of combined topical and oral green tea supplementation (300 mg twice daily) found improvements in elastic tissue content (Chiu *et al.*, 2005). However no significant differences in clinical grading of appearance were found. All subjects were asked to apply sunscreen daily which may have attenuated differences between groups. When applied 30 minutes beforehand, 0.4 mg/cm^2 topical green tea polyphenols (GTP) provided protection from UVR-induced erythema, sunburn cell formation, DNA damage and Langerhan cell depletion but epicatechin appeared to be the least protective component when tested alone (Elmets *et al.*, 2001).

Immunosuppression was inhibited by participants after a single topical application of either green or white tea treatment (2.5 mg/cm^2) as evaluated by hypersensitivity to dinitrochlorobenzene (Camouse *et al.*, 2009). The same topical treatments prevented DNA damage. Another study found a single topical dose of green tea treatment (1-4 mg/2.5 cm^2) protective of DNA damage, in a dose-dependent manner (Katiyar *et al.*, 2000). Long-term topical application of green tea treatment significantly reduced UV-induced p53 expression and apoptosis in keratinocytes, but not erythema (Mnich *et al.*, 2009).

Topical application of an extract of *Culcitium reflexum* H.B.K. leaves which contain other major almond skin flavonols (isorhamnetin, quercetin and kaempferol) significantly decreased erythema when applied after UVB irradiation (Aquino *et al.*, 2002).

2.3.2.2 Epidemiology

Epidemiologic evidence suggests an association between flavonoid-rich foods and skin cancer incidence. A case-control study in an Italian population found a negative correlation between cutaneous melanoma and daily tea drinking, high consumption of vegetables, particularly carrots, cruciferous and leafy vegetables, and fruits, especially citrus (Fortes *et al.*, 2008). In the "Food Habits in Later Life" study, tea consumption was negatively correlated with actinic skin damage in Anglo-Celtic Australians (Purba *et al.*, 2001).

2.3.2.3 Animal Studies

Investigations of foods rich in flavanoid nutrients, such as those found in almonds, demonstrate their efficacy as photoprotectants against UV carcinogenesis in animal models. Grape seed proanthocyanidins are polymers of flavanol monomers such as catechin and epicatechin (Katiyar, 2008). In SKH-1 hairless mice, dietary supplementation with these compounds resulted in a dose-dependent reduction in photocarcinogenesis. Green tea as well as black tea consumption also resulted in significantly fewer UV-induced tumors in mice (Record and Dreosti, 1998). The administration of GTPs in drinking water or the topical application of EGCG, a major tea flavanol, also induced partial regression or inhibition of tumor growth of established skin papillomas in mice (Wang *et al.*, 1992). Gensler et al also investigated EGCG in BALB/cAnNHsd mice and found induction of skin tumors by UV irradiation was significantly reduced by topical but not by oral treatment of EGCG (Gensler *et al.*, 1996b).

Other research has focused on acute photoprotection of EGCG. In Wistar rats, topical EGCG treatment for 30 minutes prior to UVA irradiation significantly decreased sunburn cell occurrence and dermo-epidermal activation compared to untreated rats (Sevin *et al.*, 2007). The same protection was not observed with topical EGCG application 30 minutes after UVA

exposure. UVA-induced oxidative stress was significantly attenuated in Sprague-Dawley rats by intraperitoneal injections of quercetin prior to UV exposure (Kahraman and Inal, 2002). Markers of oxidative stress included increased plasma MDA (a product of lipid peroxidation), decreased erythrocyte glutathione peroxidase and reductase activities, and decreased catalase and superoxide dismutase activities. Topical quercetin treatment was found protective of UVB-induced oxidative stress in mouse skin as well (Casagrande *et al.*, 2006).

Positive photoprotective results from the above animal studies lead some researchers to investigate the mechanism of protection. Dietary supplementation of GTPs in mice, during 8 weeks of UVB irradiation, inhibited UV-induced expression of MMPs, including MMP-2, -3, -7, and -9 (Vayalil *et al.*, 2004). All of these MMPs have been shown to be involved in the degradation of types-I and –III collagen fragments generated by collagenases and type IV collagen of the basement membrane. Topical application of plant extracts (cacao bean and cola nut, both are rich in catechin and epicatechin) to hairless mice prior to UVA irradiation 5 days/week for 15 weeks prevented wrinkling, dermal connective alteration, and collagen accumulation (Mitani *et al.*, 2007). Topical quercetin prevented some UVB-induced extracellular matrix damage and glutathione depletion in hairless mice (Vicentini *et al.*; Vicentini *et al.*, 2008). Rats treated with quercetin demonstrated less MDA, no difference in glutathione but greater glutathione peroxidase, glutathione reductase, catalase and superoxide dismutase in liver and skin tissue after UVA exposure (Erden Inal and Kahraman, 2000). Pretreatment of SENCAR mice skin with GTP or individual polyphenol components, 30 min before 12-O-tetradecanoylphorbol-13-acetate (a tumor promoter), resulted in a significant inhibition of enhanced expression of epidermal IL-lα mRNA (Katiyar *et al.*, 1995). Mice fed diets

supplement with catechin for 2 or 4 weeks prior to UVB irradiation demonstrated protection from decreased activity of catalase, SOD and glutathione peroxidase (Jeon *et al.*, 2003).

2.3.2.4 *In vitro* Studies

3D human skin models and skin explants

Ex vivo cultured human skin experiments demonstrated pretreatment with topical green and white tea (2 mg/cm^2) provided protection from UV induced immunosuppression, measured by depletion of Langerhans cells (Camouse *et al.*, 2009). Another *ex vivo* human skin experiment found topical cocoa polyphenol extract (containing catechin and epicatechin) improved skin structure after five days of application (Gasser *et al.*, 2008). Glycosaminoglycans increased as well as collagen I, II and IV expression, indicating improved elasticity and skin tonus, respectively. In UVA exposed artificial skin models, composed of differentiated epidermis on a dermal substitute, pretreatment with topical EGCG decreased expression of MMP-1 and -3 and activity of MMP-2 and -9 (Lee *et al.*, 2005). Tissue inhibitor of metalloproteinase-1 (TIMP-1) expression increased simultaneously. In a separate 3D skin model experiment, UVA induced keratinocyte and fibroblast vacuolation and nuclear pyknosis, intense TUNEL staining of fibroblasts and increased staining of cells and nuclei for 8-OHdG and lesser increases in intensity followed staining for HO-1 and IL-1α. Quercetin-3-glucoside reduced these changes (Dekker *et al.*, 2005).

Monolayer skin cell culture

MMPs appear to be responsive to polyphenols. Treatment of MMP-2 and -9 with quercetin, partially inhibited gelatinase activity in a cell-free system (Liuzzi *et al.*). The expression of active MMP-2 and MMP-9 proteins were significantly decreased in quercetin treated prostate cancer cells in a dose-dependent manner (Vijayababu *et al.*, 2006). Isorhamnetin

3-O-β-D-glucoside and quercetin 3-O-β-D-glucoside, have significant inhibitory effects on MMP-2 and -9 expression and activity in human fibrosarcoma cell line (HT1080) (Kong *et al.*, 2008). A related polyphenol, EGCG, inhibited MMP-2 and -9 activities (gelatinases) (Garbisa *et al.*, 2001). In human dermal fibroblasts, both quercetin and kaempferol inhibited MMP-1 (collagenase) activity and expression induced by UVA (Sim *et al.*, 2007).

Significant amount of research has focused on inflammatory pathways. Quercetin decreased UVR-induced necrosis factor κB (NF-κB) DNA-binding by 80% in normal human keratinocytes (NHKs). Consequently, quercetin suppressed UV irradiation-induced expression of inflammatory cytokines IL-1β, IL-6, IL-8 and tumor necrosis factor-α (TNF-α). In contrast, quercetin had no effect on UVR irradiation activation of three MAP kinases, ERK, JNK, or p38 (Vicentini *et al.*). Quercetin and its methylated derivative isorhamnetin attenuate proinflammatory gene expression (IL-1β, IL-6, macrophage inflammatory protein 1α and inducible NO synthase) in lipopolysacharide (LPS)-activated murine macrophages (Boesch-Saadatmandi *et al.*). Quercetin reduced the gene expression of two proinflammatory genes, IL-1α and TNFα, in N9 microglial cells (Bureau *et al.*, 2008). Quercetin decreased the gene expression and production of TNFα, IL-1β, IL-6, and IL-8 in phorbol 12-myristate 13-acetate and calcium ionophore A23187 (PMACI)-stimulated human mast cells. Quercetin attenuated PMACI-induced activation of NF-κB and p38 mitogen-activated protein kinase (Min *et al.*, 2007). A portion of protection in the UVA range is attributed to direct absorption at 365 nm by quercetin (Fahlman and Krol, 2009). Quercetin showed an inhibitory effect on MAPK activation, IL-1β, and COX-2 expression, and PGE2 synthesis (Gutierrez-Venegas *et al.*, 2007). Kaempferol significantly decreased the number of TNF-α and IL-1β mRNA copies in LPS-

activated J774.2 macrophages (Kowalski *et al.*, 2005). Epicatechin downregulated IL-1β induced NFκB activation in β-cells (Kim *et al.*, 2004).

Biomolecule protection has also been investigated. Quercetin protected from UVA and UVB-induced lipid peroxidation in liposomes. Human skin 68 fibroblasts incubated with either quercetin or catechin prior to UVA exposure had reduced lipid peroxidation compared to untreated cells (Filipe *et al.*, 2005). Adult human skin fibroblasts and normal human epidermal keratinocytes, cultured separately, had significantly less DNA damage from UVA irradiation when treated with EGCG (Morley *et al.*, 2005).

Quercetin pretreatment strongly suppressed UVA-induced apoptosis in human keratinocyte HaCaT cells, markedly increased protein levels of the transcription factor Nrf2, induced the expression of antioxidative genes, and dramatically reduced the production of reactive oxygen species following UVA irradiation. Importantly, these beneficial effects were greatly attenuated by downregulating Nrf2 expression (Kimura *et al.*, 2009). Epicatechin treatment protected human fibroblasts from UVA-induced cell death (Basu-Modak *et al.*, 2003).

While many *in vitro* studies have evaluated photoprotective effects of polyphenols, there are no studies investigating the metabolite forms which are found in circulation after consumption of polyphenols (e.g. glucuronides, sulfides).

2.4 Conclusions and Summary

Skin cancer is a significant public health concern. The skin is vulnerable to UV damage, which can lead to cancer. Possible mechanism by which this occurs include oxidative damage, inflammation, immunosuppression and cell signaling alterations. A diet rich in almond phytonutrients, including AT and AP, may produce continual whole body protection from such damage. Epidemiological studies support a role for diets high in these food components and

decreased risk of wrinkling and cancer. However, the data are not entirely consistent. Stronger evidence comes from intervention studies which find supplementation with AT and AP and various nutrient combinations can protect from shorter-term markers of UV damage including lipid peroxidation, erythema, MMP expression, DNA damage, and apoptosis. Similar results are observed from topical treatments of these nutrients. Further investigation of optimal doses and mechanism of protection are needed to better target and prevent photodamage with dietary and/or topical treatments.

References

Aquino R, Morelli S, Tomaino A, Pellegrino M, Saija A, Grumetto L*, et al.* (2002) Antioxidant and photoprotective activity of a crude extract of Culcitium reflexum H.B.K. leaves and their major flavonoids. *J Ethnopharmacol* 79:183-91.

Basu-Modak S, Gordon MJ, Dobson LH, Spencer JP, Rice-Evans C, Tyrrell RM (2003) Epicatechin and its methylated metabolite attenuate UVA-induced oxidative damage to human skin fibroblasts. *Free Radic Biol Med* 35:910-21.

Beijersbergen van Henegouwen GM, Junginger HE, de Vries H (1995) Hydrolysis of RRR-alpha-tocopheryl acetate (vitamin E acetate) in the skin and its UV protecting activity (an in vivo study with the rat). *J Photochem Photobiol B* 29:45-51.

Bernerd F, Asselineau D (2008) An organotypic model of skin to study photodamage and photoprotection in vitro. *J Am Acad Dermatol* 58:S155-9.

Bissett DL, Chatterjee R, Hannon DP (1990) Photoprotective effect of superoxide-scavenging antioxidants against ultraviolet radiation-induced chronic skin damage in the hairless mouse. *Photodermatol Photoimmunol Photomed* 7:56-62.

Bissett DL, Chatterjee R, Hannon DP (1992) Protective effect of a topically applied anti-oxidant plus an anti-inflammatory agent against ultraviolet radiation-induced chronic skin damage in the hairless mouse. *J Soc Cosmet Chem* 43:85-92.

Bissett DL, Hillebrand GG, Hannon DP (1989) The hairless mouse as a model of skin photoaging: its use to evaluate photoprotective materials. *Photodermatol* 6:228-33.

Boesch-Saadatmandi C, Loboda A, Wagner AE, Stachurska A, Jozkowicz A, Dulak J*, et al.* Effect of quercetin and its metabolites isorhamnetin and quercetin-3-glucuronide on inflammatory gene expression: role of miR-155. *J Nutr Biochem* 22:293-9.

Braun S, Krampert M, Bodo E, Kumin A, Born-Berclaz C, Paus R*, et al.* (2006) Keratinocyte growth factor protects epidermis and hair follicles from cell death induced by UV irradiation, chemotherapeutic or cytotoxic agents. *J Cell Sci* 119:4841-9.

Bruls WA, Slaper H, van der Leun JC, Berrens L (1984) Transmission of human epidermis and stratum corneum as a function of thickness in the ultraviolet and visible wavelengths. *Photochem Photobiol* 40:485-94.

Bureau G, Longpre F, Martinoli MG (2008) Resveratrol and quercetin, two natural polyphenols, reduce apoptotic neuronal cell death induced by neuroinflammation. *J Neurosci Res* 86:403-10.

Burke KE, Clive J, Combs GF, Jr., Commisso J, Keen CL, Nakamura RM (2000) Effects of topical and oral vitamin E on pigmentation and skin cancer induced by ultraviolet irradiation in Skh:2 hairless mice. *Nutr Cancer* 38:87-97.

Burton GW, Traber MG, Acuff RV, Walters DN, Kayden H, Hughes L*, et al.* (1998) Human plasma and tissue alpha-tocopherol concentrations in response to supplementation with deuterated natural and synthetic vitamin E. *Am J Clin Nutr* 67:669-84.

Camouse MM, Domingo DS, Swain FR, Conrad EP, Matsui MS, Maes D*, et al.* (2009) Topical application of green and white tea extracts provides protection from solar-simulated ultraviolet light in human skin. *Exp Dermatol* 18:522-6.

Casagrande R, Georgetti SR, Verri WA, Jr., Dorta DJ, dos Santos AC, Fonseca MJ (2006) Protective effect of topical formulations containing quercetin against UVB-induced oxidative stress in hairless mice. *J Photochem Photobiol B* 84:21-7.

Chen CY, Blumberg JB (2008) In vitro activity of almond skin polyphenols for scavenging free radicals and inducing quinone reductase. *J Agric Food Chem* 56:4427-34.

Chen W, Barthelman M, Martinez J, Alberts D, Gensler HL (1997) Inhibition of cyclobutane pyrimidine dimer formation in epidermal p53 gene of UV-irradiated mice by alpha-tocopherol. *Nutr Cancer* 29:205-11.

Chiu AE, Chan JL, Kern DG, Kohler S, Rehmus WE, Kimball AB (2005) Double-blinded, placebo-controlled trial of green tea extracts in the clinical and histologic appearance of photoaging skin. *Dermatol Surg* 31:855-60; discussion 60.

Cho HS, Lee MH, Lee JW, No KO, Park SK, Lee HS*, et al.* (2007) Anti-wrinkling effects of the mixture of vitamin C, vitamin E, pycnogenol and evening primrose oil, and molecular mechanisms on hairless mouse skin caused by chronic ultraviolet B irradiation. *Photodermatol Photoimmunol Photomed* 23:155-62.

Choquenet B, Couteau C, Paparis E, Coiffard LJ (2008) Quercetin and rutin as potential sunscreen agents: determination of efficacy by an in vitro method. *J Nat Prod* 71:1117-8.

Chung JH, Seo JY, Lee MK, Eun HC, Lee JH, Kang S*, et al.* (2002) Ultraviolet modulation of human macrophage metalloelastase in human skin in vivo. *J Invest Dermatol* 119:507-12.

Darr D, Dunston S, Faust H, Pinnell S (1996) Effectiveness of antioxidants (vitamin C and E) with and without sunscreens as topical photoprotectants. *Acta Derm Venereol* 76:264-8.

Dekker P, Parish WE, Green MR (2005) Protection by food-derived antioxidants from UV-A1-induced photodamage, measured using living skin equivalents. *Photochem Photobiol* 81:837-42.

Dreher F, Denig N, Gabard B, Schwindt DA, Maibach HI (1999) Effect of topical antioxidants on UV-induced erythema formation when administered after exposure. *Dermatology* 198:52-5.

Eberlein-Konig B, Jager C, Przybilla B (1998a) Ultraviolet B radiation-induced production of interleukin 1alpha and interleukin 6 in a human squamous carcinoma cell line is wavelength-dependent and can be inhibited by pharmacological agents. *Br J Dermatol* 139:415-21.

Eberlein-Konig B, Placzek M, Przybilla B (1998b) Protective effect against sunburn of combined systemic ascorbic acid (vitamin C) and d-alpha-tocopherol (vitamin E). *J Am Acad Dermatol* 38:45-8.

Elmets CA, Singh D, Tubesing K, Matsui M, Katiyar S, Mukhtar H (2001) Cutaneous photoprotection from ultraviolet injury by green tea polyphenols. *J Am Acad Dermatol* 44:425-32.

Erden Inal M, Kahraman A (2000) The protective effect of flavonol quercetin against ultraviolet a induced oxidative stress in rats. *Toxicology* 154:21-9.

Evelson P, Ordonez CP, Llesuy S, Boveris A (1997) Oxidative stress and in vivo chemiluminescence in mouse skin exposed to UVA radiation. *J Photochem Photobiol B* 38:215-9.

Fahlman BM, Krol ES (2009) Inhibition of UVA and UVB radiation-induced lipid oxidation by quercetin. *J Agric Food Chem* 57:5301-5.

FDA (2011) Labeling and Effectiveness Testing; Sunscreen Drug Products for Over-the-Counter Human Use. In: *21 CFR Parts 201 and 310* (35620-65.

Filipe P, Silva JN, Haigle J, Freitas JP, Fernandes A, Santus R*, et al.* (2005) Contrasting action of flavonoids on phototoxic effects induced in human skin fibroblasts by UVA alone or UVA plus cyamemazine, a phototoxic neuroleptic. *Photochem Photobiol Sci* 4:420-8.

Fortes C, Mastroeni S, Melchi F, Pilla MA, Antonelli G, Camaioni D*, et al.* (2008) A protective effect of the Mediterranean diet for cutaneous melanoma. *Int J Epidemiol* 37:1018-29.

Fuchs J, Kern H (1998) Modulation of UV-light-induced skin inflammation by D-alpha-tocopherol and L-ascorbic acid: a clinical study using solar simulated radiation. *Free Radic Biol Med* 25:1006-12.

Fuchs J, Weber S, Podda M, Groth N, Herrling T, Packer L*, et al.* (2003) HPLC analysis of vitamin E isoforms in human epidermis: correlation with minimal erythema dose and free radical scavenging activity. *Free Radic Biol Med* 34:330-6.

Fukuzawa K, Tokumura A, Ouchi S, Tsukatani H (1982) Antioxidant activities of tocopherols on Fe2+-ascorbate-induced lipid peroxidation in lecithin liposomes. *Lipids* 17:511-3.

Garbisa S, Sartor L, Biggin S, Salvato B, Benelli R, Albini A (2001) Tumor gelatinases and invasion inhibited by the green tea flavanol epigallocatechin-3-gallate. *Cancer* 91:822-32.

Gasser P, Lati E, Peno-Mazzarino L, Bouzoud D, Allegaert L, Bernaert H (2008) Cocoa polyphenols and their influence on parameters involved in ex vivo skin restructuring. *Int J Cosmet Sci* 30:339-45.

Gensler HL, Aickin M, Peng YM, Xu M (1996a) Importance of the form of topical vitamin E for prevention of photocarcinogenesis. *Nutr Cancer* 26:183-91.

Gensler HL, Magdaleno M (1991) Topical vitamin E inhibition of immunosuppression and tumorigenesis induced by ultraviolet irradiation. *Nutr Cancer* 15:97-106.

Gensler HL, Timmermann BN, Valcic S, Wachter GA, Dorr R, Dvorakova K, *et al.* (1996b) Prevention of photocarcinogenesis by topical administration of pure epigallocatechin gallate isolated from green tea. *Nutr Cancer* 26:325-35.

Gerrish KE, Gensler HL (1993) Prevention of photocarcinogenesis by dietary vitamin E. *Nutr Cancer* 19:125-33.

Gutierrez-Venegas G, Jimenez-Estrada M, Maldonado S (2007) The effect of flavonoids on transduction mechanisms in lipopolysaccharide-treated human gingival fibroblasts. *Int Immunopharmacol* 7:1199-210.

Halliday GM (2005) Inflammation, gene mutation and photoimmunosuppression in response to UVR-induced oxidative damage contributes to photocarcinogenesis. *Mutat Res* 571:107-20.

Hantke B, Lahmann C, Venzke K, Fischer T, Kocourek A, Windsor LJ, *et al.* (2002) Influence of flavonoids and vitamins on the MMP- and TIMP-expression of human dermal fibroblasts after UVA irradiation. *Photochem Photobiol Sci* 1:826-33.

Heinen MM, Hughes MC, Ibiebele TI, Marks GC, Green AC, van der Pols JC (2007) Intake of antioxidant nutrients and the risk of skin cancer. *Eur J Cancer* 43:2707-16.

Heinrich U, Neukam K, Tronnier H, Sies H, Stahl W (2006) Long-term ingestion of high flavanol cocoa provides photoprotection against UV-induced erythema and improves skin condition in women. *J Nutr* 136:1565-9.

Hellemans L, Corstjens H, Neven A, Declercq L, Maes D (2003) Antioxidant enzyme activity in human stratum corneum shows seasonal variation with an age-dependent recovery. *J Invest Dermatol* 120:434-9.

Jeon SE, Choi-Kwon S, Park KA, Lee HJ, Park MS, Lee JH, *et al.* (2003) Dietary supplementation of (+)-catechin protects against UVB-induced skin damage by modulating antioxidant enzyme activities. *Photodermatol Photoimmunol Photomed* 19:235-41.

Jurkiewicz BA, Bissett DL, Buettner GR (1995) Effect of topically applied tocopherol on ultraviolet radiation-mediated free radical damage in skin. *J Invest Dermatol* 104:484-8.

Kahraman A, Inal ME (2002) Protective effects of quercetin on ultraviolet A light-induced oxidative stress in the blood of rat. *J Appl Toxicol* 22:303-9.

Kang BY, Kim S, Lee KH, Lee YS, Hong I, Lee MO*, et al.* (2008) Transcriptional profiling in human HaCaT keratinocytes in response to kaempferol and identification of potential transcription factors for regulating differential gene expression. *Exp Mol Med* 40:208-19.

Katiyar SK (2008) Grape seed proanthocyanidines and skin cancer prevention: inhibition of oxidative stress and protection of immune system. *Mol Nutr Food Res* 52 Suppl 1:S71-6.

Katiyar SK, Perez A, Mukhtar H (2000) Green tea polyphenol treatment to human skin prevents formation of ultraviolet light B-induced pyrimidine dimers in DNA. *Clin Cancer Res* 6:3864-9.

Katiyar SK, Rupp CO, Korman NJ, Agarwal R, Mukhtar H (1995) Inhibition of 12-O-tetradecanoylphorbol-13-acetate and other skin tumor-promoter-caused induction of epidermal interleukin-1 alpha mRNA and protein expression in SENCAR mice by green tea polyphenols. *J Invest Dermatol* 105:394-8.

Khettab N, Amory MC, Briand G, Bousquet B, Combre A, Forlot P*, et al.* (1988) Photoprotective effect of vitamins A and E on polyamine and oxygenated free radical metabolism in hairless mouse epidermis. *Biochimie* 70:1709-13.

Kim MJ, Ryu GR, Kang JH, Sim SS, Min DS, Rhie DJ*, et al.* (2004) Inhibitory effects of epicatechin on interleukin-1beta-induced inducible nitric oxide synthase expression in RINm5F cells and rat pancreatic islets by down-regulation of NF-kappaB activation. *Biochem Pharmacol* 68:1775-85.

Kimura S, Warabi E, Yanagawa T, Ma D, Itoh K, Ishii Y*, et al.* (2009) Essential role of Nrf2 in keratinocyte protection from UVA by quercetin. *Biochem Biophys Res Commun* 387:109-14.

Klotz LO, Pellieux C, Briviba K, Pierlot C, Aubry JM, Sies H (1999) Mitogen-activated protein kinase (p38-, JNK-, ERK-) activation pattern induced by extracellular and intracellular singlet oxygen and UVA. *Eur J Biochem* 260:917-22.

Kong CS, Kim YA, Kim MM, Park JS, Kim JA, Kim SK*, et al.* (2008) Flavonoid glycosides isolated from Salicornia herbacea inhibit matrix metalloproteinase in HT1080 cells. *Toxicol In Vitro* 22:1742-8.

Kowalski J, Samojedny A, Paul M, Pietsz G, Wilczok T (2005) Effect of apigenin, kaempferol and resveratrol on the expression of interleukin-1beta and tumor necrosis factor-alpha genes in J774.2 macrophages. *Pharmacol Rep* 57:390-4.

Lambert JD, Kim DH, Zheng R, Yang CS (2006) Transdermal delivery of (-)-epigallocatechin-3-gallate, a green tea polyphenol, in mice. *J Pharm Pharmacol* 58:599-604.

Larsson P, Ollinger K, Rosdahl I (2006) Ultraviolet (UV)A- and UVB-induced redox alterations and activation of nuclear factor-kappaB in human melanocytes-protective effects of alpha-tocopherol. *Br J Dermatol* 155:292-300.

Lee JH, Chung JH, Cho KH (2005) The effects of epigallocatechin-3-gallate on extracellular matrix metabolism. *J Dermatol Sci* 40:195-204.

Li N, Jia X, Chen CY, Blumberg JB, Song Y, Zhang W*, et al.* (2007) Almond consumption reduces oxidative DNA damage and lipid peroxidation in male smokers. *J Nutr* 137:2717-22.

Lin JY, Selim MA, Shea CR, Grichnik JM, Omar MM, Monteiro-Riviere NA*, et al.* (2003) UV photoprotection by combination topical antioxidants vitamin C and vitamin E. *J Am Acad Dermatol* 48:866-74.

Liuzzi GM, Latronico T, Brana MT, Gramegna P, Coniglio MG, Rossano R*, et al.* Structure-dependent inhibition of gelatinases by dietary antioxidants in rat astrocytes and sera of multiple sclerosis patients. *Neurochem Res* 36:518-27.

Lopez-Torres M, Thiele JJ, Shindo Y, Han D, Packer L (1998) Topical application of alpha-tocopherol modulates the antioxidant network and diminishes ultraviolet-induced oxidative damage in murine skin. *Br J Dermatol* 138:207-15.

Marrot L, Meunier JR (2008) Skin DNA photodamage and its biological consequences. *J Am Acad Dermatol* 58:S139-48.

Mavon A, Raufast V, Redoules D (2004) Skin absorption and metabolism of a new vitamin E prodrug, delta-tocopherol-glucoside: in vitro evaluation in human skin models. *J Control Release* 100:221-31.

McArdle F, Rhodes LE, Parslew RA, Close GL, Jack CI, Friedmann PS*, et al.* (2004) Effects of oral vitamin E and beta-carotene supplementation on ultraviolet radiation-induced oxidative stress in human skin. *Am J Clin Nutr* 80:1270-5.

McMillan TJ, Leatherman E, Ridley A, Shorrocks J, Tobi SE, Whiteside JR (2008) Cellular effects of long wavelength UV light (UVA) in mammalian cells. *J Pharm Pharmacol* 60:969-76.

McNaughton SA, Marks GC, Green AC (2005) Role of dietary factors in the development of basal cell cancer and squamous cell cancer of the skin. *Cancer Epidemiol Biomarkers Prev* 14:1596-607.

McVean M, Liebler DC (1997) Inhibition of UVB induced DNA photodamage in mouse epidermis by topically applied alpha-tocopherol. *Carcinogenesis* 18:1617-22.

McVean M, Liebler DC (1999) Prevention of DNA photodamage by vitamin E compounds and sunscreens: roles of ultraviolet absorbance and cellular uptake. *Mol Carcinog* 24:169-76.

Meloni M, Farina A, de Servi B Molecular modifications of dermal and epidermal biomarkers following UVA exposures on reconstructed full-thickness human skin. *Photochem Photobiol Sci* 9:439-47.

Milbury PE, Chen CY, Dolnikowski GG, Blumberg JB (2006) Determination of flavonoids and phenolics and their distribution in almonds. *J Agric Food Chem* 54:5027-33.

Mildner M, Mlitz V, Gruber F, Wojta J, Tschachler E (2007) Hepatocyte growth factor establishes autocrine and paracrine feedback loops for the protection of skin cells after UV irradiation. *J Invest Dermatol* 127:2637-44.

Min YD, Choi CH, Bark H, Son HY, Park HH, Lee S*, et al.* (2007) Quercetin inhibits expression of inflammatory cytokines through attenuation of NF-kappaB and p38 MAPK in HMC-1 human mast cell line. *Inflamm Res* 56:210-5.

Mireles-Rocha H, Galindo I, Huerta M, Trujillo-Hernandez B, Elizalde A, Cortes-Franco R (2002) UVB photoprotection with antioxidants: effects of oral therapy with d-alpha-tocopherol and ascorbic acid on the minimal erythema dose. *Acta Derm Venereol* 82:21-4.

Mitani H, Ryu A, Suzuki T, Yamashita M, Arakane K, Koide C (2007) Topical application of plant extracts containing xanthine derivatives can prevent UV-induced wrinkle formation in hairless mice. *Photodermatol Photoimmunol Photomed* 23:86-94.

Mnich CD, Hoek KS, Virkki LV, Farkas A, Dudli C, Laine E*, et al.* (2009) Green tea extract reduces induction of p53 and apoptosis in UVB-irradiated human skin independent of transcriptional controls. *Exp Dermatol* 18:69-77.

Montenegro L, Bonina F, Rigano L, Giogilli S, Sirigu S (1995) Protective effect evaluation of free radical scavengers on UVB induced human cutaneous erythema by skin reflectance spectrophotometry. *Int J Cosmet Sci* 17:91-103.

Morley N, Clifford T, Salter L, Campbell S, Gould D, Curnow A (2005) The green tea polyphenol (-)-epigallocatechin gallate and green tea can protect human cellular DNA from ultraviolet and visible radiation-induced damage. *Photodermatol Photoimmunol Photomed* 21:15-22.

Nakayama S, Katoh EM, Tsuzuki T, Kobayashi S (2003) Protective effect of alpha-tocopherol-6-O-phosphate against ultraviolet B-induced damage in cultured mouse skin. *J Invest Dermatol* 121:406-11.

Neukam K, Stahl W, Tronnier H, Sies H, Heinrich U (2007) Consumption of flavanol-rich cocoa acutely increases microcirculation in human skin. *Eur J Nutr* 46:53-6.

Noel-Hudson MS, Braut-Boucher F, Robert M, Aubery M, Wepierre J (1997) Comparison of six different methods to assess UVA cytotoxicity on reconstructed epidermis. Relevance of a

fluorimetric assay (the calcein-AM) to evaluate the photoprotective effects of alpha-tocopherol. *Toxicol In Vitro* 11:645-51.

Oh JH, Chung AS, Steinbrenner H, Sies H, Brenneisen P (2004) Thioredoxin secreted upon ultraviolet A irradiation modulates activities of matrix metalloproteinase-2 and tissue inhibitor of metalloproteinase-2 in human dermal fibroblasts. *Arch Biochem Biophys* 423:218-26.

Placzek M, Gaube S, Kerkmann U, Gilbertz KP, Herzinger T, Haen E*, et al.* (2005) Ultraviolet B-induced DNA damage in human epidermis is modified by the antioxidants ascorbic acid and D-alpha-tocopherol. *J Invest Dermatol* 124:304-7.

Poon TS, Barnetson RS, Halliday GM (2003) Prevention of immunosuppression by sunscreens in humans is unrelated to protection from erythema and dependent on protection from ultraviolet a in the face of constant ultraviolet B protection. *J Invest Dermatol* 121:184-90.

Potapenko A, Abijev GA, Pistsov M, Roshchupkin DI, Vladimirov Yu A, Pliquett F*, et al.* (1984) PUVA-induced erythema and changes in mechanoelectrical properties of skin. Inhibition by tocopherols. *Arch Dermatol Res* 276:12-6.

Purba MB, Kouris-Blazos A, Wattanapenpaiboon N, Lukito W, Rothenberg EM, Steen BC*, et al.* (2001) Skin wrinkling: can food make a difference? *J Am Coll Nutr* 20:71-80.

Record IR, Dreosti IE (1998) Protection by black tea and green tea against UVB and UVA + B induced skin cancer in hairless mice. *Mutat Res* 422:191-9.

Record IR, Dreosti IE, Konstantinopoulos M, Buckley RA (1991) The influence of topical and systemic vitamin E on ultraviolet light-induced skin damage in hairless mice. *Nutr Cancer* 16:219-25.

Rhie G, Shin MH, Seo JY, Choi WW, Cho KH, Kim KH*, et al.* (2001) Aging- and photoaging-dependent changes of enzymic and nonenzymic antioxidants in the epidermis and dermis of human skin in vivo. *J Invest Dermatol* 117:1212-7.

Richelle M, Sabatier M, Steiling H, Williamson G (2006) Skin bioavailability of dietary vitamin E, carotenoids, polyphenols, vitamin C, zinc and selenium. *Br J Nutr* 96:227-38.

Rijnkels JM, Moison RM, Podda E, van Henegouwen GM (2003) Photoprotection by antioxidants against UVB-radiation-induced damage in pig skin organ culture. *Radiat Res* 159:210-7.

Ritter EF, Axelrod M, Minn KW, Eades E, Rudner AM, Serafin D*, et al.* (1997) Modulation of ultraviolet light-induced epidermal damage: beneficial effects of tocopherol. *Plast Reconstr Surg* 100:973-80.

Rittie L, Fisher GJ (2002) UV-light-induced signal cascades and skin aging. *Ageing Res Rev* 1:705-20.

Roshchupkin DI, Pistsov MY, Potapenko AY (1979) Inhibition of ultraviolet light-induced erythema by antioxidants. *Arch Dermatol Res* 266:91-4.

Sander CS, Chang H, Hamm F, Elsner P, Thiele JJ (2004) Role of oxidative stress and the antioxidant network in cutaneous carcinogenesis. *Int J Dermatol* 43:326-35.

Sander CS, Chang H, Salzmann S, Muller CS, Ekanayake-Mudiyanselage S, Elsner P*, et al.* (2002) Photoaging is associated with protein oxidation in human skin in vivo. *J Invest Dermatol* 118:618-25.

Saral Y, Uyar B, Ayar A, Naziroglu M (2002) Protective effects of topical alpha-tocopherol acetate on UVB irradiation in guinea pigs: importance of free radicals. *Physiol Res* 51:285-90.

Schoonderwoerd SA, Beijersbergen van Henegouwen GM, Persons KC (1991) Effect of alpha-tocopherol and di-butyl-hydroxytoluene (BHT) on UV-A-induced photobinding of 8-methoxypsoralen to Wistar rat epidermal biomacromolecules in vivo. *Arch Toxicol* 65:490-4.

Selmi C, Mao TK, Keen CL, Schmitz HH, Eric Gershwin M (2006) The anti-inflammatory properties of cocoa flavanols. *J Cardiovasc Pharmacol* 47 Suppl 2:S163-71; discussion S72-6.

Sevin A, Oztas P, Senen D, Han U, Karaman C, Tarimci N, *et al.* (2007) Effects of polyphenols on skin damage due to ultraviolet A rays: an experimental study on rats. *J Eur Acad Dermatol Venereol* 21:650-6.

Shils ME, Shike M, Ross A, Caballero B, Cousins R, (eds) (2006) *Modern Nutrition in Health and Disease*, Lippincott Williams & Williams.

Shindo Y, Witt E, Han D, Epstein W, Packer L (1994) Enzymic and non-enzymic antioxidants in epidermis and dermis of human skin. *J Invest Dermatol* 102:122-4.

Shirakata Y Regulation of epidermal keratinocytes by growth factors. *J Dermatol Sci* 59:73-80.

Sim GS, Lee BC, Cho HS, Lee JW, Kim JH, Lee DH*, et al.* (2007) Structure activity relationship of antioxidative property of flavonoids and inhibitory effect on matrix metalloproteinase activity in UVA-irradiated human dermal fibroblast. *Arch Pharm Res* 30:290-8.

Stahl W, Heinrich U, Jungmann H, Sies H, Tronnier H (2000) Carotenoids and carotenoids plus vitamin E protect against ultraviolet light-induced erythema in humans. *Am J Clin Nutr* 71:795-8.

Steinbrenner H, Ramos MC, Stuhlmann D, Sies H, Brenneisen P (2003) UVA-mediated downregulation of MMP-2 and MMP-9 in human epidermal keratinocytes. *Biochem Biophys Res Commun* 308:486-91.

Suganuma M, Okabe S, Oniyama M, Tada Y, Ito H, Fujiki H (1998) Wide distribution of [3H](-)-epigallocatechin gallate, a cancer preventive tea polyphenol, in mouse tissue. *Carcinogenesis* 19:1771-6.

Thiele JJ, Ekanayake-Mudiyanselage S (2007) Vitamin E in human skin: organ-specific physiology and considerations for its use in dermatology. *Mol Aspects Med* 28:646-67.

Thiele JJ, Traber MG, Packer L (1998) Depletion of human stratum corneum vitamin E: an early and sensitive in vivo marker of UV induced photo-oxidation. *J Invest Dermatol* 110:756-61.

Thiele JJ, Weber SU, Packer L (1999) Sebaceous gland secretion is a major physiologic route of vitamin E delivery to skin. *J Invest Dermatol* 113:1006-10.

Touitou E, Godin B (2008) Skin nonpenetrating sunscreens for cosmetic and pharmaceutical formulations. *Clin Dermatol* 26:375-9.

U.S. Department of Agriculture ARS (2007) USDA National Nutrient Database for Standard Reference, Release 21. <Nutrient Data Laboratory Home Page http://www.ars.usda.gov/nutrientdata> Accessed June 2011.

van der Pols JC, Heinen MM, Hughes MC, Ibiebele TI, Marks GC, Green AC (2009) Serum antioxidants and skin cancer risk: an 8-year community-based follow-up study. *Cancer Epidemiol Biomarkers Prev* 18:1167-73.

Vayalil PK, Mittal A, Hara Y, Elmets CA, Katiyar SK (2004) Green tea polyphenols prevent ultraviolet light-induced oxidative damage and matrix metalloproteinases expression in mouse skin. *J Invest Dermatol* 122:1480-7.

Vicentini FT, Fonseca YM, Pitol DL, Iyomasa MM, Bentley MV, Fonseca MJ Evaluation of protective effect of a water-in-oil microemulsion incorporating quercetin against UVB-induced damage in hairless mice skin. *J Pharm Pharm Sci* 13:274-85.

Vicentini FT, He T, Shao Y, Fonseca MJ, Verri WA, Jr., Fisher GJ, *et al.* Quercetin inhibits UV irradiation-induced inflammatory cytokine production in primary human keratinocytes by suppressing NF-kappaB pathway. *J Dermatol Sci* 61:162-8.

Vicentini FT, Simi TR, Del Ciampo JO, Wolga NO, Pitol DL, Iyomasa MM, *et al.* (2008) Quercetin in w/o microemulsion: in vitro and in vivo skin penetration and efficacy against UVB-induced skin damages evaluated in vivo. *Eur J Pharm Biopharm* 69:948-57.

Vijayababu MR, Arunkumar A, Kanagaraj P, Venkataraman P, Krishnamoorthy G, Arunakaran J (2006) Quercetin downregulates matrix metalloproteinases 2 and 9 proteins expression in prostate cancer cells (PC-3). *Mol Cell Biochem* 287:109-16.

Wang ZY, Huang MT, Ho CT, Chang R, Ma W, Ferraro T, *et al.* (1992) Inhibitory effect of green tea on the growth of established skin papillomas in mice. *Cancer Res* 52:6657-65.

Werninghaus K, Meydani M, Bhawan J, Margolis R, Blumberg JB, Gilchrest BA (1994) Evaluation of the photoprotective effect of oral vitamin E supplementation. *Arch Dermatol* 130:1257-61.

Wu S, Gao J, Dinh QT, Chen C, Fimmel S (2008) IL-8 production and AP-1 transactivation induced by UVA in human keratinocytes: roles of D-alpha-tocopherol. *Mol Immunol* 45:2288-96.

Yaar M, Gilchrest BA (2007) Photoageing: mechanism, prevention and therapy. *Br J Dermatol* 157:874-87.

Young AR (2006) Acute effects of UVR on human eyes and skin. *Prog Biophys Mol Biol* 92:80-5.

Yuen KS, Halliday GM (1997) alpha-Tocopherol, an inhibitor of epidermal lipid peroxidation, prevents ultraviolet radiation from suppressing the skin immune system. *Photochem Photobiol* 65:587-92.

Zingg JM (2007) Modulation of signal transduction by vitamin E. *Mol Aspects Med* 28:481-506.

CHAPTER 3: Methods

3.1 3D human skin tissue

3D human skin tissues were prepared as previously described (Carlson *et al.*, 2008). Briefly, human dermal fibroblasts (HFF) were derived from newborn foreskin and grown in Dulbecco's modified Eagle's medium (Invitrogen, Carlsbad, CA, USA) supplemented with 10% fetal bovine serum (FBS) (Hyclone, Logan, UT, USA). HFFs were mixed with bovine type I collagen (2.5×10^4 cells/mL) and the gels were allowed to contract for 7 days in deep-well polycarbonate tissue culture inserts (Organogenesis, Canton, MA, USA). Subsequently, a total of 5×10^5 human keratinocytes were seeded onto the collagen gel and tissues were then maintained submerged in low calcium epidermal growth media for two days, for an additional two days in normal calcium media and raised to the air-liquid interface for seven days, after which tissues are considered fully developed (Organogenesis, Canton, MA, USA). Experiments were performed 2-4 times on fully developed tissues. For proliferation assays, 20 μg/mL bromodeoxyuridine (BrdU) (Invitrogen, Carlsbad, CA) was added to tissue culture medium 5 h prior to harvesting.

3.2 AT treatment and application

For safety testing, AT (Sigma, St. Louis, MO) was dissolved in dimethyl sulfoxide (DMSO) before application to the media of fully developed tissues at a final concentration of 0, 6.25, 12.5, 25 and 50 μM. DMSO was 0.1% of media. Medium was agitated to ensure homogeneity of treatment. AT was dissolved in 45 μL acetone for topical application of four doses (0, 1, 5, and 25 mg/cm^2). Tissues were incubated for 48 hours with treatment. For absorption time course analysis, tissues were incubated 0 – 48 hours with 9 μM medium or 1 mg/cm^2 topical AT. For analysis of dose-dependent absorption, medium (15 or 25 μM) or topical (0.5 or 1 mg/cm^2) AT doses were incubated for 48 hours.

For photoprotection studies, AT (Sigma, St. Louis, MO) was dissolved in DMSO before application to the medium of fully developed skin tissue at a final concentration of 0 or 25 μM for 48 h. Dose was selected based on previous experiments in 3D skin models assessing morphology, proliferation and apoptosis from a range of doses which are physiologically achievable concentrations in human circulation (Evans JA *et al.*, 2011). DMSO concentration was 0.1% of medium. Medium was agitated by pipetting 8 times to ensure homogeneity of treatment. AT was dissolved in 45 μL acetone for topical application of 0 or 1 mg/cm^2 for 2 h. Dose was selected based on our previous work which established its safety in 3D tissues (Evans JA *et al.*, 2011).

3.3 AP treatment preparation and application

For topical application to the fully developed skin tissue, polyphenols from skins of Nonpareil almonds produced in California were extracted sequentially twice with glacial acetic acid/water/methanol (3.7:46.3:50, v/v/v) over 16 h at 4^{o}C (Chen *et al.*, 2005). Aliquots of dried AP were obtained after solvent removal with N_2 air and stored at -80^{o}C until use. Total phenols were quantified using the Folin-Ciocalteu's reaction (Singleton, 1999) and expressed as micromoles per liter of gallic acid equivalents (GAE). AP were resuspended in 40% acetone/phosphate buffered solution (PBS) for topical application of 45 μL AP at 14 μg/cm^2 GAE. Dose and incubation time were selected based on our previous work which established its safety in 3D tissues (Evans JA *et al.*, 2011).

For medium application, *glucuronide-conjugated* metabolites of quercetin, a major AP, which are generally found in circulation after consumption, were synthesized according to Bolling et al (Bolling *et al.*, 2009). Briefly, pooled human liver microsomal protein (0-1 mg/ml, final concentration, BD Biosciences, San Jose, CA) were preincubated with alamethicin (0.25

μg/ml) at 37°C for 5 min in microcentrifuge tubes containing previously dried quercetin solution (600 μM). A cofactor solution of UDP-glucuronic acid (5 mM, final concentration), magnesium chloride (5 mM, final concentration) and potassium phosphate buffer, pH 7.5 (0.05 mM, final concentration), was added to initiate the reaction in a final assay volume of 0.1 mL. After 3 h incubation at 37°C, the reaction was terminated with 0.1 mL ice cold methanol. After centrifugation at 14,000 × *g* for 5 min, supernatants were dried under a stream of purified nitrogen gas at room temperature and stored at −80°C until use within 2 weeks. The products were reconstituted with 17% methanol in water and quantified by HPLC using a previously established method (Boersma *et al.*, 2002). A Waters Alliance 2695 system (Waters Corp., Milford, MA) with a C18 column (Synergi 10μm Hydro-RP 80A, 4.6 x 250mm) was used. The data is collected and analyzed using Waters Empower 2 Software (copyright 2006, Waters Corp). Mobile phase A consisting of 20 mM phosphate buffer, pH 2.0, and mobile phase B consisting of acetonitrile, were employed to elute quercetin and metabolites. Quercetin and glucuronidated metabolites were quantified using a standard curve established in the absence of UDPGA. Twenty μL of sample was injected at 1 mL/min flow rate of 17% mobile phase B for 2 min and then increased to 25% in 5 min, to 35% in 8 min and to 50% in 5 min. After 3 min at 50%, mobile phase B will be decreased to 17% in 4 min and held for 5 min to equilibrate the column.

Once the products were quantified, dried residue were reconstituted in PBS for application to culture medium at a final concentration of 5 μM for 2 h. The 5 μM dose and 2 h incubation period were selected based physiologically achievable concentrations in human circulation and metabolism kinetics of polyphenols. For vehicle controls, the dry residues from

glucuronidation reaction with quercetin absent were used. Medium with quercetin metabolites was agitated to ensure homogeneity of treatment.

3.4 UVA irradiation

For UV irradiation treatments, medium was removed and the skin samples, which were gently washed with PBS two times on each surface, and samples were transferred to a sterile platform. A 200-W UV radiation source (Lightning Cure 200, Hamamatsu, Japan) was used in combination with a dichroic mirror assembly reflecting most of the visible and infrared wavelengths, to reduce the heat load on the skin, and with UG11 and WG335 filters for wavelength delivery in the UVA range (320 – 400 nm). A liquid light guide was connected to the lamp, conducting the light to the surface of the skin. The light guide was mounted to a stand, parallel to the skin surface, at a distance of 3 cm, which provides the most uniform field of light. UVA dose was 0 or 35 J/cm^2 with an intensity of 75 mW/cm^2 as measured by a radiometer (Fluke 289 True RMS Multimeter, Everett, WA). Tissue inserts were returned to tissue culture trays with fresh media and harvested 96 h post-irradiation for histology analysis and media were collected as well.

3.5 Tissue Harvesting and Morphology Assessment

Tissues were analyzed for morphology, proliferation and apoptosis. At harvesting, tissues were divided into three equal portions for separate preservation and tissue medium was collected and stored at -80ºC until analysis. One third was fixed in formalin, embedded in paraffin, and serially sectioned at 6 μm. Histological sections were stained with hematoxylin and eosin (H&E), images were captured using a Nikon Eclipse 80i microscope (Nikon Instruments Inc., Melville, NY, USA) equipped with a SPOT RT camera (Diagnostic Instruments, Sterling Heights, MI, USA) and analyzed using Spot Advanced software (Diagnostic Instruments,

Sterling Heights, MI, USA). Morphologic assessment of H&E stained tissue cross sections included qualitative evaluation of 1) organization of basal layer, 2) presence of fibroblasts and 3) development of epidermis. A separate third of tissue was snap frozen in O.C.T. compound (Sakura Finetek USA, Torrance, CA, USA) by liquid nitrogen after immersion in 2 M sucrose solution at 4ºC for at least 24 hours. The remaining third of tissue was snap frozen in O.C.T. compound (Sakura Finetek USA, Torrance, CA, USA) by liquid nitrogen after immersion in 4% paraformaldehyde (to enable identification of terminal deoxynucleotidyl transferase mediated dUTP nick-end labeling [TUNEL]-positive cells) for 1h and 2 M sucrose solution at 4ºC for at least 24 h, serial sectioned at 6 μm, and mounted onto gelatin-chrome alum coated slides.

3.6 Immunohistochemical and immunofluorescence analysis

Immunohistochemical staining of BrdU was performed on paraffin-embedded tissues sectioned at 6 μm thickness using monoclonal antibodies against BrdU (Roche, Indianapolis, IN) and Vectastain ABC kit (Vector Labs, Burlingame, CA). The number of BrdU-positive cells was determined and expressed as a percentage of total cells in the basal layer.

Immunohistochemical staining of cytokeratin-10 positive cells was performed on paraffin-embedded tissues sectioned at 6 μm thickness, immersed in 0.1% sodium citrate at 100ºC for 15 m for antigen retrieval then incubated with monoclonal antibody against cytokeratin-10 (Abcam, Cambridge, MA) and Vectastain ABC kit (Vector Labs, Burlingame, CA).

The TUNEL assay was used to identify apoptotic cells. Tissue soaked in 4% paraformaldehyde prior to freezing were sectioned at 6 μm thickness, permeabilized with 0.1% triton in 0.1% sodium citrate then incubated with the TUNEL reaction mixture (Roche, Indianapolis, IN) for 1 h at 37^{o}C in the dark and counterstained with DAPI (40,6-diamidino-2-

phenylindole. The percentage of TUNEL-positive cells was calculated from the number of these cells divided by the total number of cells counted in the entire epithelium.

3.7 AT quantitation

A portion of each tissue was fixed in formalin before paraffin embedding, sectioning and H&E staining. The remainder of the tissue was separated into dermal and epidermal compartments with forceps, weighed and stored separately at -80ºC until analysis. Tocopherol extraction and analysis by HPLC was performed on the medium and epidermal and dermal layers of tissue. Tissues were extracted as previously described with minor modifications (Foote *et al.*, 2009; Peng *et al.*, 1993). Skin was incubated with collagenase (50 mg/mL; Sigma, St. Louis, MO) at 37°C for 1 h followed by homogenization (IKA Ultra-Turrax T8, Wilmington, NC), and incubation with protease (20 mg/mL; Sigma, St. Louis, MO) at 37°C for 0.5 h. 1% SDS in ethanol was added and the sample was extracted with hexane and dried under nitrogen. Medium samples (100 µl) were extracted with 3 ml of chloroform/methanol (2:1) followed by 3 ml of hexane and dried under nitrogen. All samples were resuspended in 50 µl ethanol of which 25 µl was injected into the HPLC. The reverse phase HPLC is performed using a Waters Alliance 2695 system (Waters Corp., Milford, MA) and a C30 carotenoid column (3 µm, 150 x 3.0 mm, Bischoff, Leonberg, Germany). The data was collected and analyzed using Waters Empower 2 Software (copyright 2006, Waters Corp). The HPLC mobile phase was methanol:methyl-tert-butyl ether:water (83:15:2, v:v:v, with 1.5% ammonium acetate in H_2O, solvent A) and methanol:methyl-tert-butyl ether:water (8:90:2, v:v:v, with 1% ammonium acetate in H_2O, solvent B). The gradient procedure at a flow rate of 0.4 mL/min at 16°C was as follows: The procedure began at 100% solvent A for 3 min before going to 80% solvent A and 20% solvent B over a 7 min linear gradient. This was followed by a 8 min linear gradient to 45% solvent A and

55% solvent B, followed by a 15 min linear gradient to 5% solvent A and 95% solvent B. The solvent flow was held at 5% solvent A and 95% solvent B for 4 minutes, then a 2 min linear gradient to 100% solvent A. The system was held at 100% solvent A for 10 min for equilibration back to initial conditions. HPLC grade ethanol, methyl-tert-butyl ether, ammonium acetate (analytical grade) were purchased from Sigma-Aldrich Company (St. Louis, MO). Water was obtained from Water Purification Systems (Millipore Corp., Bilerica, MA). Results were adjusted by an internal standard (retinyl acetate) recovery. AT was quantified by determining peak areas in the HPLC chromatograms at 292 nm calibrated against known amounts of standards. The spectrophotometer detector is set at 292 nm and 340 for quantitation of tocopherols and internal standard, respectively.

3.8 Ferric reducing antioxidant power (FRAP) Assay

Total antioxidant capacity in the harvested medium was measured using the FRAP assay as previously described (Benzie and Strain, 1996). Reagents included 300 mM acetate buffer, pH 3.6 (3.1 g $C_2H_3NaO_2 \cdot 3H_2O$ and 16 ml $C_2H_4O_2$ per liter of buffer solution); 10 mM TPTZ (2,4,6-tripyridyl-*s*-triazine, Sigma, St. Louis, MO) in 40 mM HCl; 20 mM $FeCl_3 \cdot 6H_2O$. Working FRAP reagent was prepared as required by mixing 25ml acetate buffer, 2.5 ml TPTZ solution, and 2.5 ml $FeCl_3 \cdot 6H_2O$ solution. Trolox concentrations in the range of 31.25–1000 μM (Sigma, St. Louis, MO) were used for calibration. Thirty μL of medium, blank (H_2O) or standards were added to non-UV disposable cuvettes followed by 90 μL H_2O and 900 μL of working FRAP reagent and incubated for 60 min at room temperature. The absorbance was measured at 593 nm using a spectrophotometer (Shimadzu UV-1601, Japan). Reported values are adjusted for the FRAP value of medium not incubated with tissue.

3.9 Enzyme-linked immunosorbent assay (ELISA)

To assess protein secretion, tissue culture media were harvested and processed using commercial DuoSet HGF, IL-1α and KGF ELISA kit (R&D Systems, Minneapolis, MN, USA) and MMP-2 human ELISA kit (Invitrogen, Carlsbad, CA). Medium was assayed in duplicate.

References

Benzie IF, Strain JJ (1996) The ferric reducing ability of plasma (FRAP) as a measure of "antioxidant power": the FRAP assay. *Anal Biochem* 239:70-6.

Boersma MG, van der Woude H, Bogaards J, Boeren S, Vervoort J, Cnubben NH*, et al.* (2002) Regioselectivity of phase II metabolism of luteolin and quercetin by UDP-glucuronosyl transferases. *Chem Res Toxicol* 15:662-70.

Bolling BW, Court MH, Blumberg JB, Chen CY (2009) The kinetic basis for age-associated changes in quercetin and genistein glucuronidation by rat liver microsomes. *J Nutr Biochem*.

Carlson MW, Alt-Holland A, Egles C, Garlick JA (2008) Three-dimensional tissue models of normal and diseased skin. *Curr Protoc Cell Biol* Chapter 19:Unit 19 9.

Chen CY, Milbury PE, Lapsley K, Blumberg JB (2005) Flavonoids from almond skins are bioavailable and act synergistically with vitamins C and E to enhance hamster and human LDL resistance to oxidation. *J Nutr* 135:1366-73.

Evans JA, Chen C-YO, Garlick J, Wang X-D, Johnson EJ (2011) Feasibility of nutrient photoprotection studies in a three-dimensional human skin tissue model: Using alpha tocopherol. *FASEB J* 25.

Foote JA, Ranger-Moore JR, Einspahr JG, Saboda K, Kenyon J, Warneke J*, et al.* (2009) Chemoprevention of human actinic keratoses by topical DL-alpha-tocopherol. *Cancer Prev Res (Phila Pa)* 2:394-400.

Peng YM, Peng YS, Lin Y (1993) A nonsaponification method for the determination of carotenoids, retinoids, and tocopherols in solid human tissues. *Cancer Epidemiol Biomarkers Prev* 2:139-44.

Singleton VL, R. Orthofer, R.M. Lamuela-Ravent, (ed) (1999) *Analysis of Total Phenols and Other Oxidation Substrates and Antioxidants by Means of Folin-Ciocalteu Reagent*, Academic Press: New York.

CHAPTER 4

Examination of a Three-Dimensional Skin Tissue Model for Nutrient and UVA Studies, Using alpha-Tocopherol as an Example

Abstract

Introduction: Alpha-tocopherol (AT) has previously shown promise as a photoprotectant. This study aimed to determine the feasibility of AT uptake in a 3-dimensional (3D) skin model and assessment of ultraviolet A (UVA) irradiation.

Methods: AT was applied to medium (0 – 50 μM) or topically (0 – 25 mg/cm^2) for up to 48 h. Skin absorption of AT was quantified in dermis and epidermis by RP-HPLC with UV detection after proteolysis and standard lipid extraction. Optimal dose and incubation time for each treatment were selected based on maximal nutrient absorption while maintaining healthy skin tissue parameters (morphology, proliferation and apoptosis). Tissue was exposed to ultraviolet A (UVA) irradiation at 0 – 100 J/cm^2 and morphology (from hematoxylin & eosin stain) and apoptosis (by TUNEL assay) were assessed after 48 - 96 h.

Results: Skin AT content increased in dose- and time-dependent manners. After 48 h medium incubation with 25 μM AT, dermal and epidermal concentrations of AT were approximately 3 and 30 ng/mg wet weight, respectively, comparable to those found in human skin. After 2 h incubation with 1 mg/cm^2 topical AT, dermal and epidermal concentrations of AT were 1 and 37 μg/mg wet weight, respectively. In a dose-dependent, reproducible manner, UVA induced apoptosis and morphologic changes.

Conclusion: AT is absorbed into both compartments of this skin model from medium and topical application and UVA damage was reproducible and dose-dependent. Our results lend to

the feasibility of using this model to investigate the mechanisms of action of these treatments in 3D skin models.

Introduction

Skin is the largest organ in the human body. It is exposed to environmental insult of which UV light is thought to be the most harmful (Lippens *et al.*, 2009). UV exposure can cause oxidative stress, inflammation, erythema, breakdown of the extracellular matrix, wrinkling and skin cancer (Boelsma *et al.*, 2001; Iddamalgoda *et al.*, 2008; Mudgil *et al.*, 2003). In fact, cumulative sun exposure is one of the most important risk factors for both nonmelanoma and melanoma skin cancers (Gloster and Brodland, 1996; Miller and Mihm, 2006). There are many ways to protect oneself from UV exposure including avoidance of the sun, wearing protective clothing (hats, long-sleeved shirts, treated fabrics, etc), and topical sunscreen. However, the potential for dietary UV protection is a relatively recent concept. Compared to topical sunscreens which require reapplication and have localized effects, dietary methods are thought to provide continual whole body protection.

Many nutrients (tocopherols, carotenoids and polyphenols) have shown promise as photoprotectants in clinical, animal and monolayer cell culture studies (Sies and Stahl, 2004). Currently, most studies of nutrient photoprotection are conducted in one of these research models, each with its own limitations. Conducting these studies in human skin *in vivo* is difficult because it requires scar-inducing skin biopsies and can be costly. Bioavailability and metabolism of nutrients in modeled animals are different from humans, as well as their skin structure. Monolayer cultures do not mimic *in vivo* conditions, in terms of stratification, differentiation, proliferation and signaling pathways, as well as the three-dimensional (3D) human skin tissue model. This novel *in vitro* skin tissue model provides a unique opportunity to

assess histological, biochemical and molecular outcomes under conditions similar to those found *in vivo*.

Our goal is to determine if such a model can be applied to nutrient and UVA studies, using alpha-tocopherol (AT) as an example. To evaluate the feasibility of the 3D skin tissue model, we will assess absorption of AT into epidermal and dermal compartments and the induction of damage to tissue by UVA exposure.

Methods and Materials

3D human skin tissues were prepared as previously described (Carlson *et al.*, 2008). Briefly, human dermal fibroblasts (HFF) were derived from newborn foreskin and grown in Dulbecco's modifed Eagle's medium (Invitrogen, Carlsbad, CA, USA) supplemented with 10% fetal bovine serum (Hyclone, Logan, UT, USA). HFFs were mixed with bovine type I collagen (2.5×10^4 cells/mL) and the gels were allowed to contract for 7 days in deep-well polycarbonate tissue culture inserts (Organogenesis, Canton, MA, USA). A total of 5×10^5 human keratinocytes were seeded onto the collagen gel and tissues were then maintained submerged in low calcium epidermal growth media for 2 days, for an additional 2 days in normal calcium media, and raised to the air-liquid interface for 7 days, after which tissues is considered fully developed (Organogenesis, Canton, MA, USA). Experiments were performed 1-4 times, depending on tissue availability. For proliferation assays, 20 µg/mL bromodeoxyuridine (BrdU) (Invitrogen, Carlsbad, CA) was added to tissue culture medium 5 h prior to harvesting.

AT treatment

For safety testing, AT (Sigma, St. Louis, MO) was dissolved in dimethyl sulfoxide (DMSO) before application to the medium at a final concentration of 0, 6.25, 12.5, 25 and 50 µM. Doses were selected based on physiologically achievable concentrations in human

circulation. DMSO was 0.1% of media. Medium was agitated by pipetting to ensure homogeneity of treatment. AT was dissolved in 45 μL acetone for topical application of four doses (0, 1, 5, and 25 mg/cm^2). Doses were selected based on previously tested doses in human and animal studies (Chung *et al.*, 2002; Lopez-Torres *et al.*, 1998). Tissues were incubated for up to 48 hours with treatment. For absorption time course analysis, tissues were incubated 0 – 48 hours with 9 μM medium or 1 mg/cm^2 topical AT. For analysis of dose-dependent absorption, medium (15 or 25 μM) or topical (0.5 or 1 mg/cm^2) AT doses were incubated for 48 hours.

UV irradiation

For UV irradiation, medium was removed and the skin samples, which were gently washed with PBS twice on each surface, were transferred to a sterile platform. A 200-W UV radiation source (Lightning Cure 200, Hamamatsu, Japan) was used in combination with a dichroic mirror assembly reflecting most of the visible and infrared wavelengths, to reduce the heat load on the skin, and with UG11 and WG335 filters for wavelength delivery in the UVA range (320 – 400 nm). A liquid light guide was connected to the lamp, conducting the light to the surface of the skin. The light guide was mounted onto a stand, parallel to the skin surface, at a distance of 3 cm, which provides the more uniform field of light. UVA dose ranged 0-100 J with an intensity of 75 mW/cm^2 as measured by a radiometer (Fluke 289 True RMS Multimeter, Everett, WA). Tissue inserts were returned to tissue culture trays, incubated with fresh medium and harvested 48 – 96 hrs post-irradiation for histology analysis.

Safety assessment

For safety assessment, tissues were analyzed for morphology, proliferation and apoptosis. At harvesting, tissues were divided into two equal portions for separate preservation. One part was fixed in formalin, embedded in paraffin, and serially sectioned at 6 μm. Histological sections

were stained with hematoxylin and eosin (H&E), images were captured using a Nikon Eclipse 80i microscope (Nikon Instruments Inc., Melville, NY, USA) equipped with a SPOT RT camera (Diagnostic Instruments, Sterling Heights, MI, USA) and analyzed using Spot Advanced software (Diagnostic Instruments, Sterling Heights, MI, USA). Morphologic assessment of H&E stained tissue cross sections included qualitative evaluation of 1) organization of basal layer, 2) presence of fibroblasts and 3) development of epidermis. A second tissue portion was used for the measurement of apoptotic cells using terminal deoxynucleotidyl transferase mediated dUTP nick-end labeling [TUNEL] assay was immersed in 4% paraformaldehyde for 1 h and 2 M sucrose solution at 4ºC for at least 24 h and snap frozen in O.C.T. compound (Sakura Finetek USA, Torrance, CA, USA) by liquid nitrogen and serial sectioned at 6 μm, and mounted onto gelatin-chrome alum coated slides.

Immunohistochemical and immunofluorescence analysis

Immunohistochemical staining of BrdU was performed on paraffin-embedded tissues sectioned at 6 μm thickness using monoclonal antibodies against BrdU (Roche, Indianapolis, IN) and Vectastain ABC kit (Vector Labs, Burlingame, CA). The number of BrdU-positive cells was determined and expressed as a percentage of total cells in the basal layer.

The TUNEL assay was used to identify apoptotic cells. Frozen tissues sectioned at 6 μm thickness were first permeabilized with 0.1% triton in 0.1% sodium citrate then incubated with the TUNEL reaction mixture (Roche, Indianapolis, IN) for 1 h at 37^{o}C in the dark and counterstained with DAPI (40,6-diamidino-2-phenylindole). The percentage of TUNEL-positive cells was calculated from the number of these cells divided by the total number of cells counted in the entire epithelium.

AT quantitation

A portion of each tissue was fixed in formalin before paraffin embedding, sectioning and H&E staining. The remainder of the tissue was separated into dermal and epidermal compartments with forceps, weighed and stored separately at -80ºC until analysis. Tocopherol extraction and analysis by HPLC was performed on the medium and epidermal and dermal layers of tissue. Tissues were extracted as previously described with minor modifications (Foote *et al.*, 2009; Peng *et al.*, 1993). Skin was incubated with collagenase (50 mg/mL; Sigma, St. Louis, MO) at 37°C for 1 h followed by homogenization (IKA Ultra-Turrax T8, Wilmington, NC) and incubation with protease (20 mg/mL; Sigma, St. Louis, MO) at 37°C for 0.5 h. 1% SDS in ethanol was added and the sample was extracted with hexane and dried under nitrogen. Medium samples (100 µl) were extracted with 3 mL of chloroform/methanol (2:1) followed by 3 mL of hexane and dried under nitrogen. All samples were resuspended in 50 µl ethanol of which 25 µl was injected into the HPLC. The reverse phase HPLC was performed using a Waters Alliance 2695 system (Waters Corp., Milford, MA) and a C30 carotenoid column (3 µm, 150 x 3.0 mm, Bischoff, Leonberg, Germany). The data was collected and analyzed using Waters Empower 2 Software (copyright 2006, Waters Corp). The HPLC mobile phase was methanol:methyl-tert-butyl ether:water (83:15:2, v:v:v, with 1.5% ammonium acetate in H_2O, solvent A) and methanol:methyl-tert-butyl ether:water (8:90:2, v:v:v, with 1% ammonium acetate in H_2O, solvent B). The gradient procedure at a flow rate of 0.4 mL/min at 16°C was as follows: The procedure began at 100% solvent A for 3 min before going to 80% solvent A and 20% solvent B over a 7 min linear gradient. This was followed by a 8 min linear gradient to 45% solvent A and 55% solvent B, followed by a 15 min linear gradient to 5% solvent A and 95% solvent B. The solvent flow was held at 5% solvent A and 95% solvent B for 4 minutes, then a 2 min linear

gradient to 100% solvent A. The system was held at 100% solvent A for 10 min for equilibration back to initial conditions. HPLC grade ethanol, methyl-tert-butyl ether, ammonium acetate (analytical grade) were purchased from Sigma-Aldrich Company (St. Louis, MO). Water was obtained from Water Purification Systems (Millipore Corp., Bilerica, MA). Results were adjusted by an internal standard (retinyl acetate) recovery. AT was quantified by determining peak areas in the HPLC chromatograms at 292 nm calibrated against known amounts of standards. The spectrophotometer detector was set at 292 nm and 340 for quantitation of tocopherols and internal standard, respectively.

Results

Safety of AT treatments

Morphology

Tissues incubated for 48 h with AT doses ranging 6.25 μM – 50 μM medium and 1-5 mg/cm^2 topical had organized basal layers, fibroblasts were present and the epithelia were fully developed, comparable to control tissues (**Figures 1 and 2**). Vehicle controls of DMSO and acetone had comparable morphology to untreated controls as well. Tissue treated topically with the highest AT dose of 25 mg/cm^2 demonstrated less developed epithelium (Figure 2).

Proliferation

Compared to DMSO controls, tissues treated with 12.5, 25 and 50 μM AT in medium for 48 h in medium had greater percent BrdU positive basal cells by 56, 118 and 38%, respectively, while DMSO alone induced a 34% decrease compared to untreated controls (**Figure 3**). Compared to acetone controls, topical AT treatment of 1, 5 and 25 mg/cm^2 over 48 h had fewer percent BrdU positive basal cells by 13, 12 and 48%. The proliferation data indicate that all

treatments and vehicles are safe, but the decreased proliferation from topical 25 mg/cm^2 is not optimal for skin health.

Apoptosis

All treatments had apoptotic response no different from control tissues, with the exception of the DMSO vehicle which increased percent apoptotic keratinocytes from 0.4 to 8% (**Figure 4**). This effect was negated in the presence of AT treatment. The apoptosis data indicate that all nutrient treatments and vehicles are safe.

AT absorption

After safe AT doses were established, time- and dose-response absorption experiments were conducted. Skin AT concentrations increased with time after medium and topical treatments, except the dermis appeared to become saturated at 2 ng and 1 μg per mg wet weight with the medium and topical doses, respectively (**Figure 5 & 6**).

After higher medium AT dose (25 μM v. 15 μM) concentrations were greater in both epidermis (40%) and dermis (127%). After higher topical dose (1 mg/cm^2 v. 0.5 mg/cm^2), concentration were greater in the dermis (884%). The dermis appeared to become saturated from topical treatment as an increase in dermal concentration was not observed from the higher dose (**Figure 7**). Final AT concentrations from 1 mg/cm^2 topical doses were 1251 and 300 fold greater than those achieved from 25 μM medium dose in the epidermis and dermis, respectively.

UV damage

Morphology

Compared to sham irradiated tissues, the morphology was unchanged at doses below 35 J/cm^2 at both 48 and 96 h postirradiation (**Figure 8 & 9**). At this 35 J/cm^2 dose and above,

deterioration of morphologic parameters including organization of basal layer, presence of fibroblasts and development of epidermis were observed.

Apoptosis

At 48 h after irradiation, the percentage of apoptotic cells was similar to sham irradiated tissues at doses up to 35 and 40 J/cm^2 in the dermis and epidermis, respectively (**Figure 10**). Percent apoptotic cells increased with doses above these thresholds, except in the dermis where it was fairly constant at doses between 50 and 100 J/cm^2. At 96 h after irradiation, dermal apoptosis was greater than in sham irradiated tissues for all doses of 30 J/cm^2 and greater (**Figure 11**). At 96 h after irradiation, similar to the 48 h timepoint, epidermal apoptosis did not differ from sham irradiated tissue at doses less than 40 J/cm^2 and increased in a linear fashion with greater doses.

Discussion

The goal of this study was to determine the feasibility of the use of a 3D skin tissue model for nutrient and UVA studies. Because tissue models mimic *in vivo* conditions better than animal and monolayer cell models and allow for easy analysis of histological, biochemical and molecular outcomes, they could be an invaluable tool in the growing fields of skin nutrition and photoprotection. This model uniquely allows for application of nutrients to medium, mimicking delivery from blood circulation after oral consumption of nutrients, and topically. Towards this goal, we have investigated the safety and absorption of AT in this model as well as the effects of UVA irradiation on skin tissue. While this is a study with limited replication, it provides useful information for future studies.

AT treatment

Morphology, proliferation and apoptosis data combined indicate 25 mg AT applied topically does not optimize skin conditions. All other nutrient treatments and vehicles were found to be suitable for subsequent studies. We also found that AT is absorbed into both the dermis and epidermis of this model in time and dose-dependent manners. AT concentrations achieved in the 3D skin tissue model from medium treatment were similar to the concentrations measured in human skin (7 and 13 ng/mg wet weight in dermal and epidermal compartments, respectively (Shindo *et al.*, 1994)), further supporting the comparability of 3D skin models to human *in vivo* conditions. To our knowledge, AT absorption into a 3D skin model has not been previously reported, but Mavon et al (Mavon *et al.*, 2004) demonstrated absorption of AT acetate (2.45 $\mu g/cm^2$) in a 3D epidermal model from topical application.

It should be noted that the barrier function of 3D skin models is thought to be lesser than in humans (Van Gele *et al.*) and AT is delivered primarily to the skin's surface via sebum secretions by the sebaceous glands (Thiele *et al.*, 1999). While the barrier function varies and these glands are not present in our model, we are able to obtain physiologically relevant concentrations of AT. This safety and absorption data establishes the feasibility of conducting studies on the potential benefits of nutrients using 3D skin models as an *in vitro* model of human skin.

UVA damage

We chose to investigate UVA damage because its effect on skin damage has been understudied compared to that of UVB. Because UVA is a longer wavelength, it is able to penetrate into the dermis, while shorter UVB rays do not. The effects of UVA are considered to be cumulative and can have significant consequences, including cancer and photoaging. In our

study, UVA damage was reproducible and apoptosis increased in a dose-dependent manner within a certain dose range bracketed by plateau zones. Our observation of UVA-induced apoptosis in both epidermal and dermal compartments coincides with ability of UVA to penetrate the dermis.

For our future studies evaluating the photoprotection of AT, a UVA dose (35 J/cm^2) was selected that induced nontoxic damage to the tissue. This dose is equivalent to <5 hours of midday sun exposure in Mediterranean countries (Fourtanier *et al.*, 2008). These results are similar to what has been found in other 3D skin models from UVA exposure, including induction of upper dermal apoptosis (Bernerd and Asselineau, 1998), further validating use of this model in UVA studies.

The results we present here indicate the applicability of this skin model to the study of AT and UVA damage. It is conceivable that the model can be used to investigate other nutrients and their photoprotection against UVB (Mudgil *et al.*, 2003). Of interest would be the evaluation of other fat-soluble nutrients as well as water-soluble compounds such as carotenoids and polyphenols that have been suggested as photoprotectants (Sies and Stahl, 2004). Given the synergistic biologic activity combinations of these nutrients can have (Chen *et al.*, 2005; Fuhrman *et al.*, 2000), of further interest would be the study of combinations of nutrients on photoprotection using this skin tissue model. Finally, this model allows for investigation of mechanism of action than human studies.

References

Bernerd F, Asselineau D (1998) UVA exposure of human skin reconstructed in vitro induces apoptosis of dermal fibroblasts: subsequent connective tissue repair and implications in photoaging. *Cell Death Differ* 5:792-802.

Boelsma E, Hendriks HF, Roza L (2001) Nutritional skin care: health effects of micronutrients and fatty acids. *Am J Clin Nutr* 73:853-64.

Carlson MW, Alt-Holland A, Egles C, Garlick JA (2008) Three-dimensional tissue models of normal and diseased skin. *Curr Protoc Cell Biol* Chapter 19:Unit 19 9.

Chen CY, Milbury PE, Lapsley K, Blumberg JB (2005) Flavonoids from almond skins are bioavailable and act synergistically with vitamins C and E to enhance hamster and human LDL resistance to oxidation. *J Nutr* 135:1366-73.

Chung JH, Seo JY, Lee MK, Eun HC, Lee JH, Kang S, *et al.* (2002) Ultraviolet modulation of human macrophage metalloelastase in human skin in vivo. *J Invest Dermatol* 119:507-12.

Foote JA, Ranger-Moore JR, Einspahr JG, Saboda K, Kenyon J, Warneke J, *et al.* (2009) Chemoprevention of human actinic keratoses by topical DL-alpha-tocopherol. *Cancer Prev Res (Phila Pa)* 2:394-400.

Fourtanier A, Moyal D, Seite S (2008) Sunscreens containing the broad-spectrum UVA absorber, Mexoryl SX, prevent the cutaneous detrimental effects of UV exposure: a review of clinical study results. *Photodermatol Photoimmunol Photomed* 24:164-74.

Fuhrman B, Volkova N, Rosenblat M, Aviram M (2000) Lycopene synergistically inhibits LDL oxidation in combination with vitamin E, glabridin, rosmarinic acid, carnosic acid, or garlic. *Antioxid Redox Signal* 2:491-506.

Gloster HM, Jr., Brodland DG (1996) The epidemiology of skin cancer. *Dermatol Surg* 22:217-26.

Iddamalgoda A, Le QT, Ito K, Tanaka K, Kojima H, Kido H (2008) Mast cell tryptase and photoaging: possible involvement in the degradation of extra cellular matrix and basement membrane proteins. *Arch Dermatol Res* 300 Suppl 1:S69-76.

Lippens S, Hoste E, Vandenabeele P, Agostinis P, Declercq W (2009) Cell death in the skin. *Apoptosis* 14:549-69.

Lopez-Torres M, Thiele JJ, Shindo Y, Han D, Packer L (1998) Topical application of alpha-tocopherol modulates the antioxidant network and diminishes ultraviolet-induced oxidative damage in murine skin. *Br J Dermatol* 138:207-15.

Mavon A, Raufast V, Redoules D (2004) Skin absorption and metabolism of a new vitamin E prodrug, delta-tocopherol-glucoside: in vitro evaluation in human skin models. *J Control Release* 100:221-31.

Miller AJ, Mihm MC, Jr. (2006) Melanoma. *N Engl J Med* 355:51-65.

Mudgil AV, Segal N, Andriani F, Wang Y, Fusenig NE, Garlick JA (2003) Ultraviolet B irradiation induces expansion of intraepithelial tumor cells in a tissue model of early cancer progression. *J Invest Dermatol* 121:191-7.

Peng YM, Peng YS, Lin Y (1993) A nonsaponification method for the determination of carotenoids, retinoids, and tocopherols in solid human tissues. *Cancer Epidemiol Biomarkers Prev* 2:139-44.

Shindo Y, Witt E, Han D, Epstein W, Packer L (1994) Enzymic and non-enzymic antioxidants in epidermis and dermis of human skin. *J Invest Dermatol* 102:122-4.

Sies H, Stahl W (2004) Nutritional protection against skin damage from sunlight. *Annu Rev Nutr* 24:173-200.

Thiele JJ, Weber SU, Packer L (1999) Sebaceous gland secretion is a major physiologic route of vitamin E delivery to skin. *J Invest Dermatol* 113:1006-10.

Van Gele M, Geusens B, Brochez L, Speeckaert R, Lambert J Three-dimensional skin models as tools for transdermal drug delivery: challenges and limitations. *Expert Opin Drug Deliv* 8:705-20.

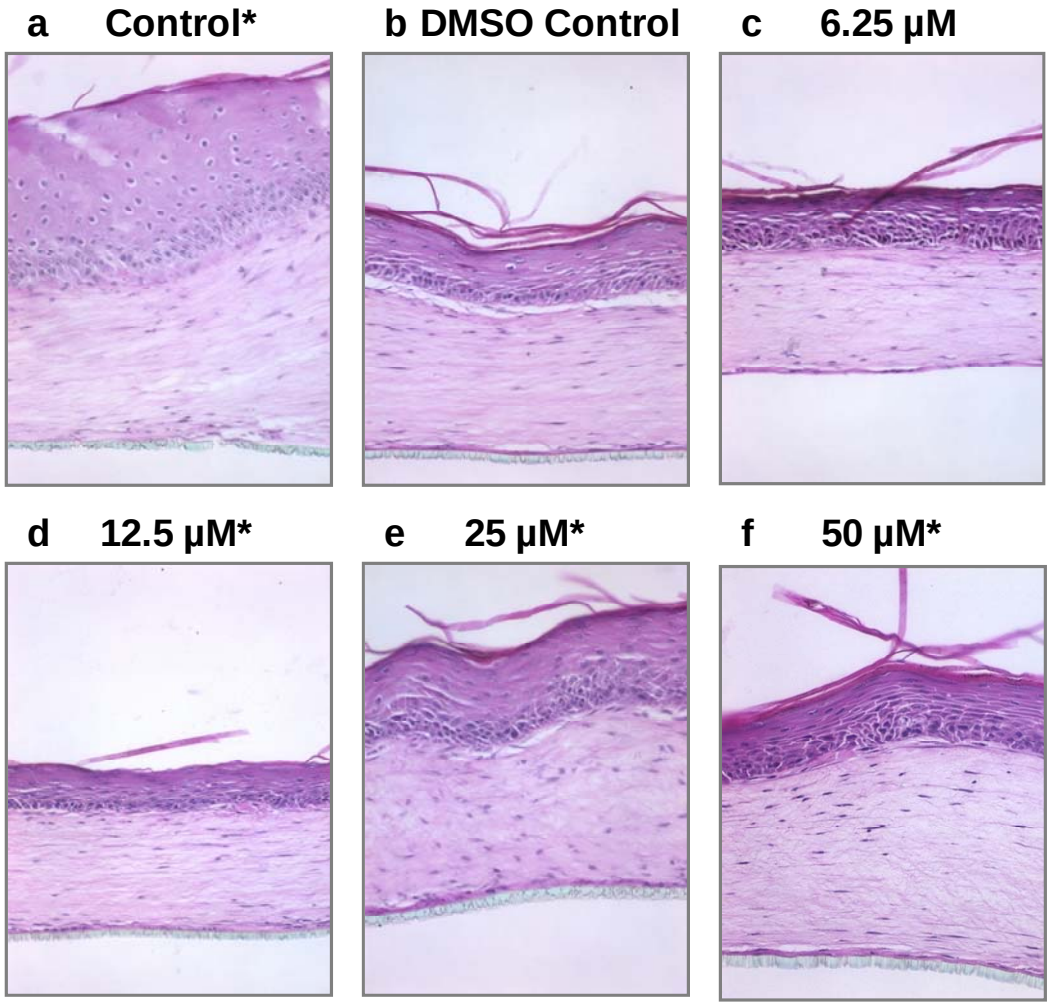

Figure 1. No deterioration of morphology from medium AT treatment in 3D tissues. Hematoxylin and eosin stained cross sections from 3D tissues after 48 hour incubation with AT mediu treatment at a range of concentrations (a) untreated, (b) 0.1% DMSO, vehicle control, (c) 6.25 µM, (d) 12.5 µM, (e) 25 µM, and (f) 50 µM. Representative images are shown. *n=2, otherwise n=1

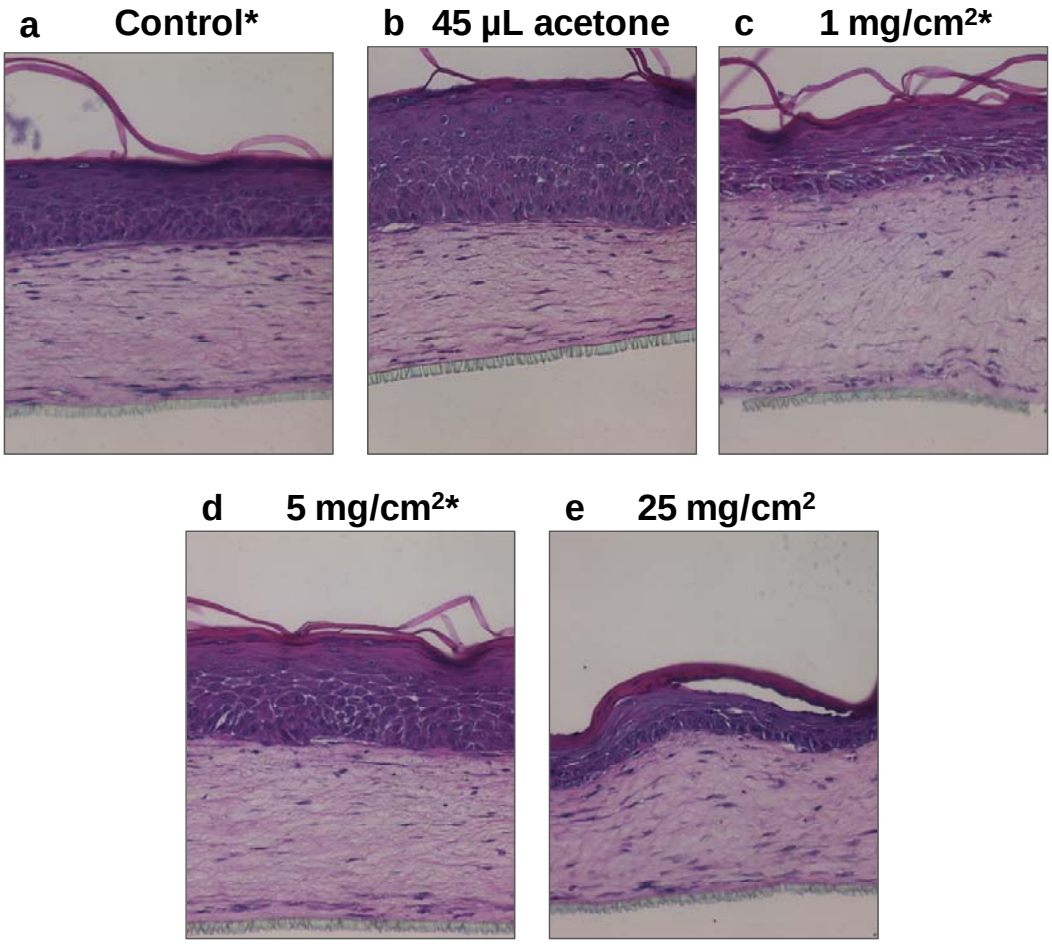

Figure 2. **No deterioration of morphology from topical AT treatment <25 mg/cm^2 in 3D tissues.** Morphology analysis of hematoxylin and eosin stained cross sections from 3D tissues after 48 hour incubation with topical AT treatment at a range of concentrations (a) untreated, (b) 45 µL acetone, vehicle control, (c) 1 mg/cm^2, (d) 5 mg/cm^2 and (e) 25 mg/cm^2. Representative images are shown. *n=2, otherwise n=1

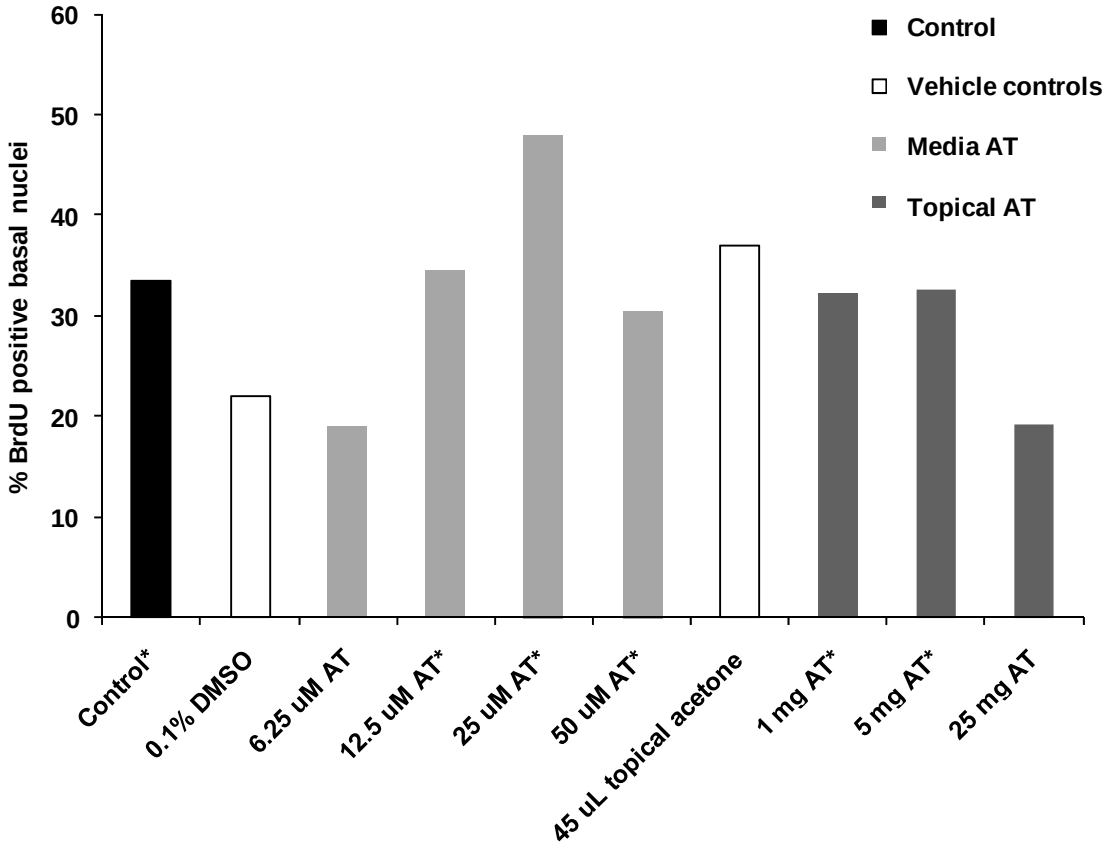

Figure 3. **AT can modulate proliferation in 3D tissues.** Percent BrdU positive basal cells (mean) in control (black), vehicle control (white), medium AT (light gray) and topical AT (dark gray) treated tissues at indicated concentrations after 48 h incubation. *n=2, otherwise n=1

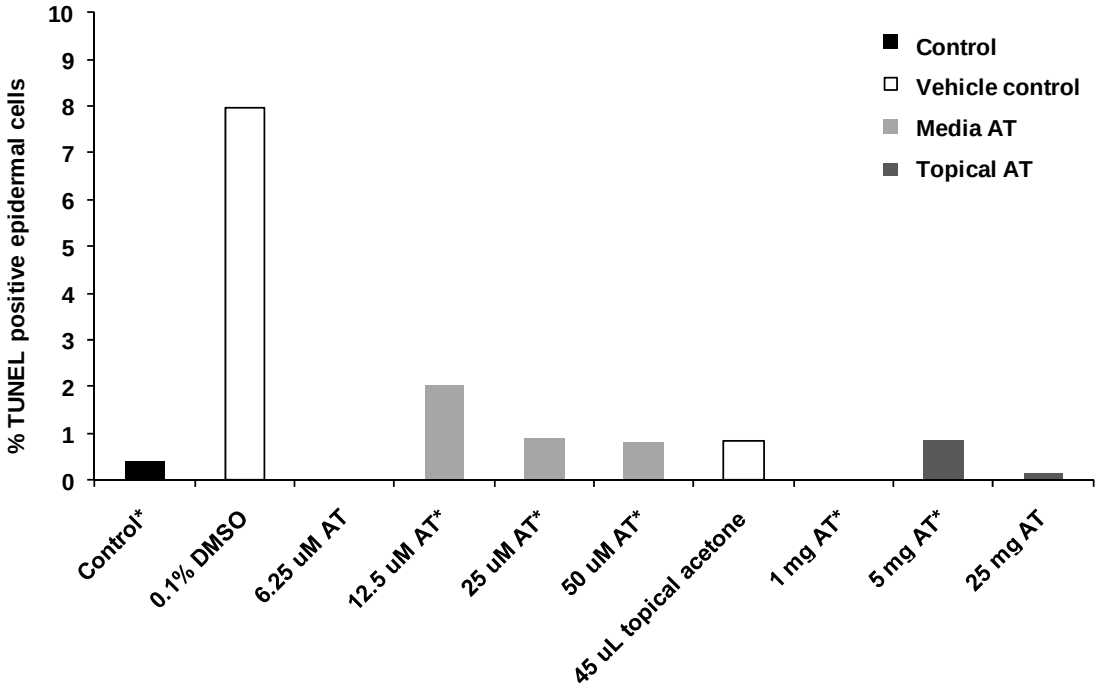

Figure 4. **AT does not induce epidermal apoptosis in 3D tissues.** Percent apoptotic keratinocytes (mean) as assessed by TUNEL in control (black), vehicle control (white), medium AT (light gray) and topical AT (dark gray) treated tissues at indicated concentrations after 48 h incubation. *n=2, otherwise n=1

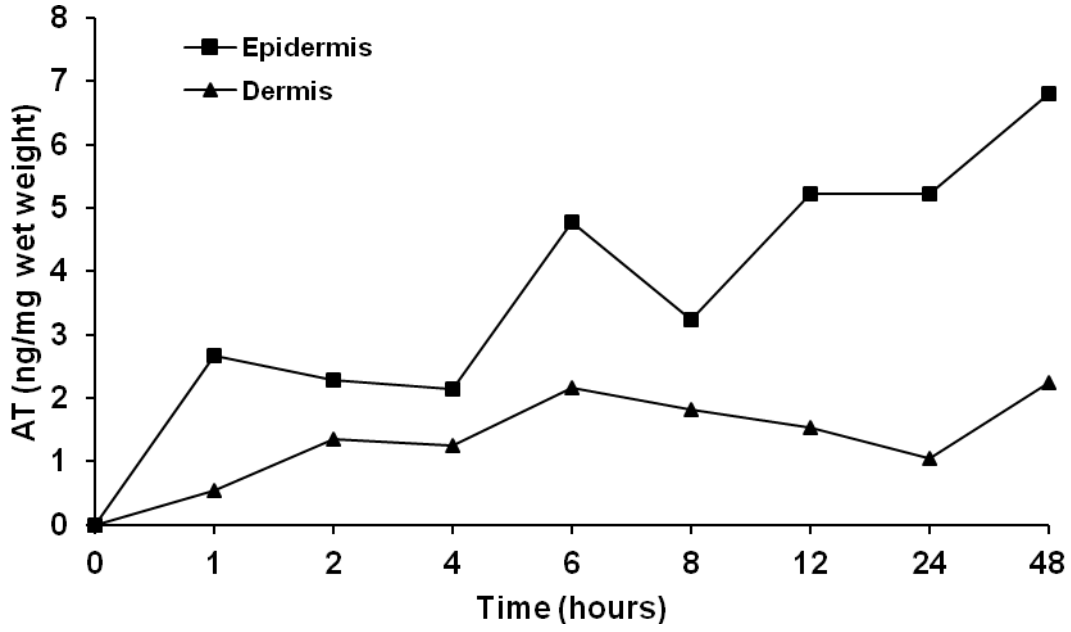

Figure 5. Medium AT is absorbed into the epidermal and dermal compartment of 3D tissues in a time-dependent manner. AT concentrations (mean) in the epidermis (square) and dermis (triangle) after 0, 1, 2, 4, 6, 8, 12, 24 and 48 hours medium incubation with 9 μM medium AT, quantitated by HPLC. n=2

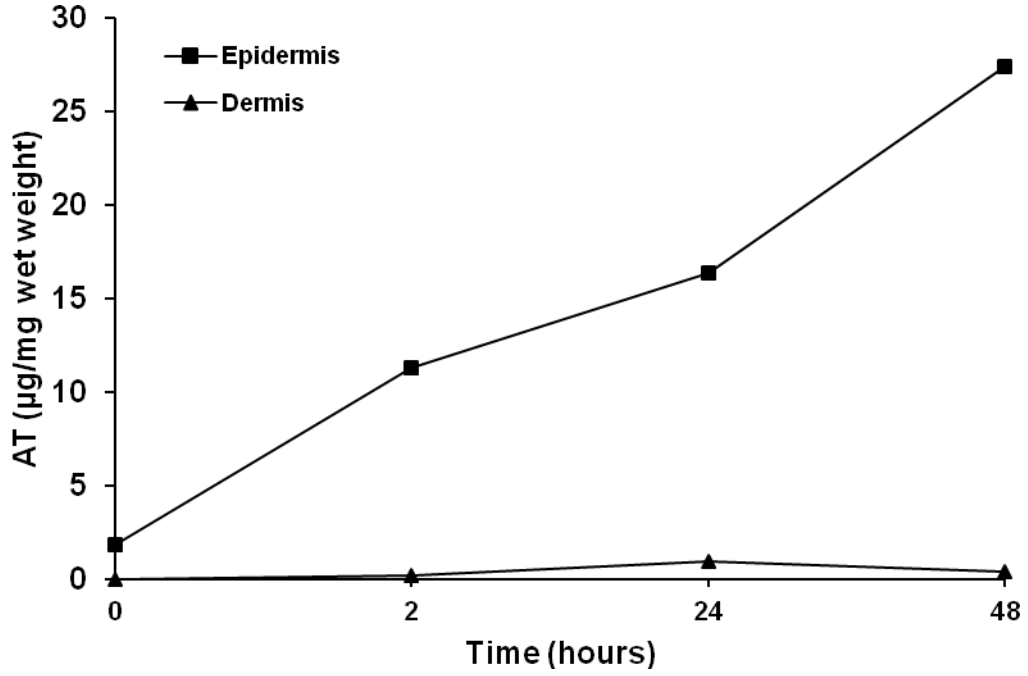

Figure 6. Topical AT is absorbed into the epidermal and dermal compartment of 3D tissues in a time-dependent manner. AT concentrations (mean) in the epidermis (square) and dermis (triangle) after 0, 2, 24 and 48 hours topical incubation with 1 mg/cm^2 AT, quantified by HPLC. n=2

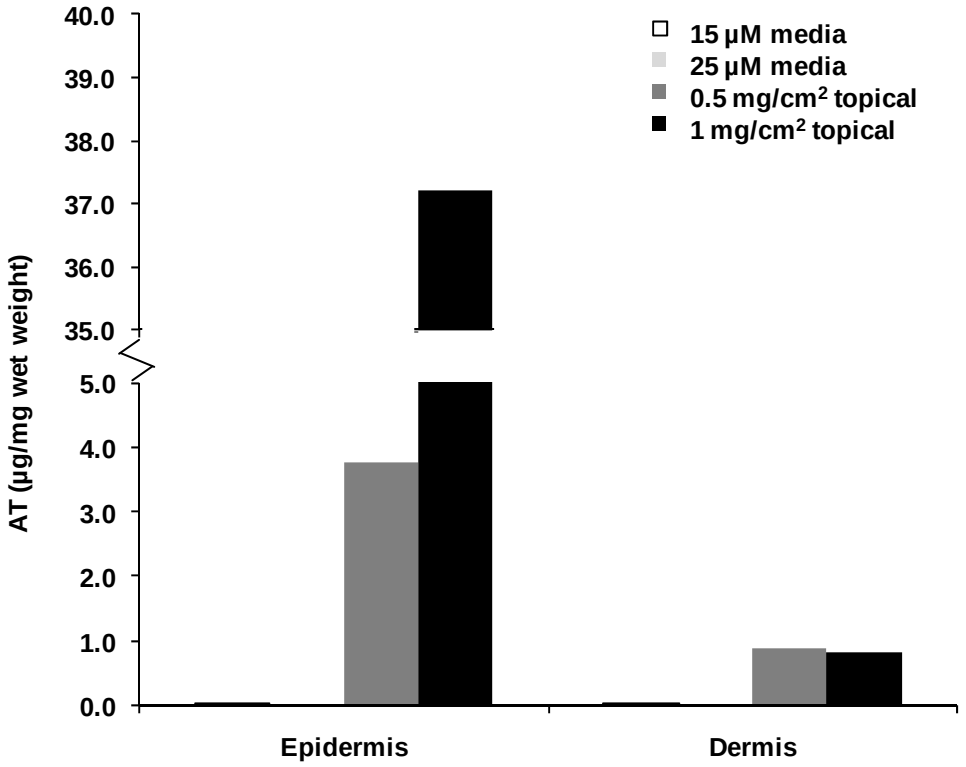

Figure 7. Absorption of medium and topical AT into 3D tissues. AT concentrations (mean) in the epidermis and dermis after 48 h medium incubation with 15 µM (white), 25 µM (light gray), 0.5 mg/cm^2 (dark gray) and 1 mg/cm^2 (black) AT, quantified by HPLC. n=2

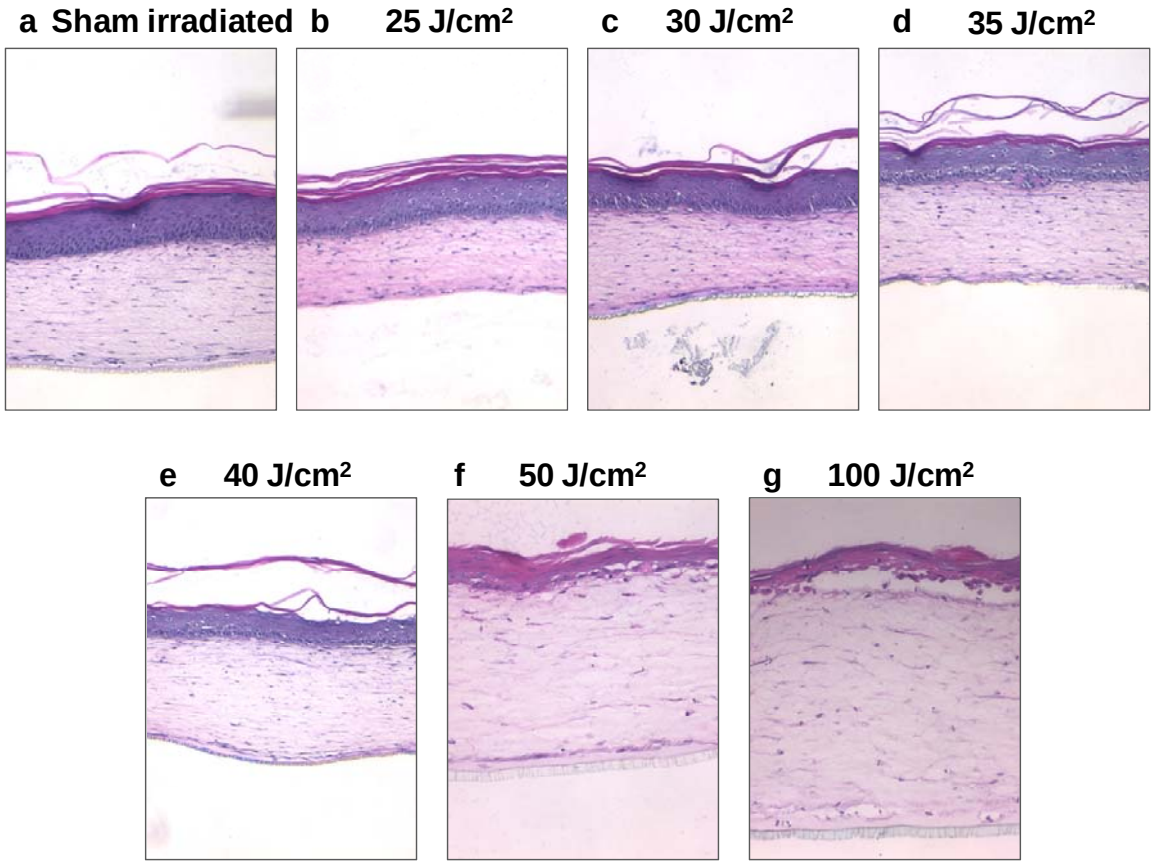

Figure 8. UVA irradiation alters morphology in a dose-dependent manner in 3D tissues after 48 hours. Morphology analysis of hematoxylin and eosin stained cross sections from 3D tissues 48 hour after UVA irradiation (a) sham; n=4, (b) 25; n=4 (c) 30; n=2, (d) 35; n=2, (e) 40; n=3, (f) 50; n=1 and (g) 100 J/cm^2; n=3. Representative images are shown.

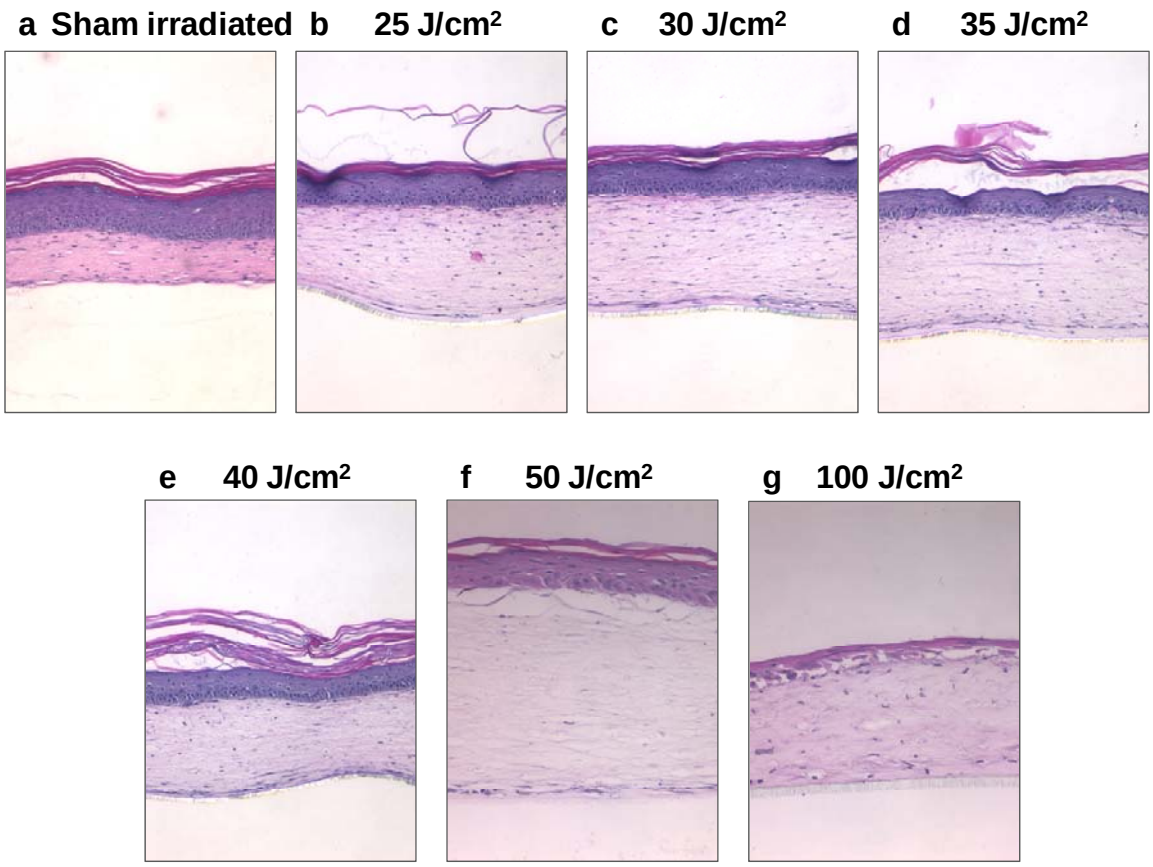

Figure 9. UVA irradiation alters morphology in a dose-dependent manner in 3D tissues after 96 hours. Morphology analysis of hematoxylin and eosin stained cross sections from 3D tissues 96 hour after UVA irradiation (a) sham; n=2, (b) 25; n=2 (c) 30; n=1 (d) 35; n=2, (e) 40; n=1, (f) 50; n=1 and (h) 100 J/cm^2; n=1. Representative images are shown.

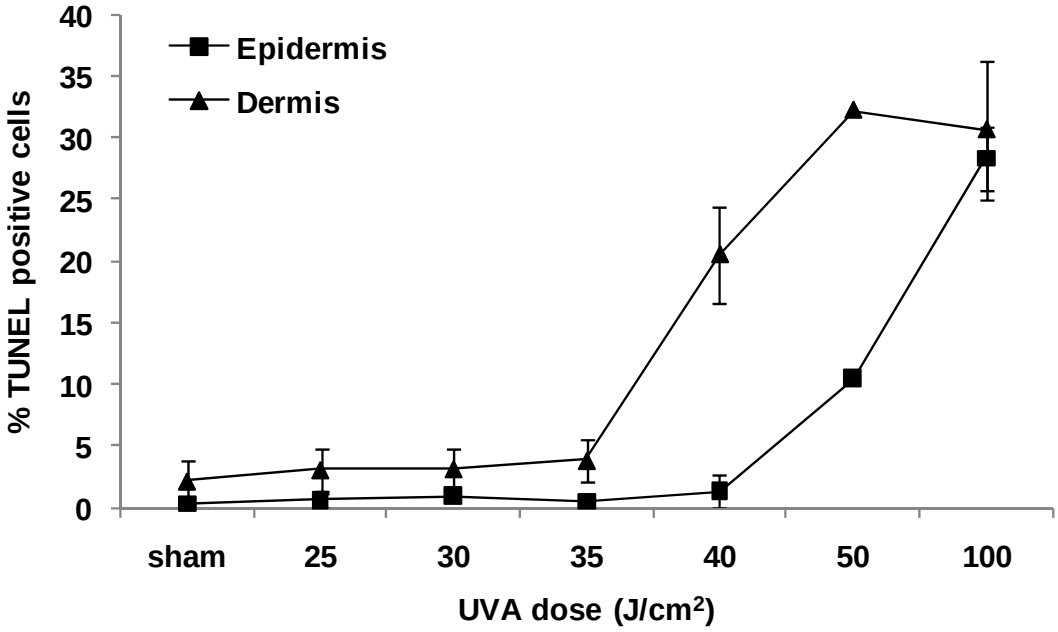

Figure 10. UVA irradiation induces apoptosis in 3D tissues 48 hours after irradiation. Percent apoptotic cells (mean ± SEM) as assessed by TUNEL in the epidermis (square) and dermis (triangle) 48 h after sham (n=4), 25 (n=4), 30 (n=2), 35 (n=2), 40 (n=3), 50 (n=1) and 100 (n=3) J/cm^2 UVA irradiation.

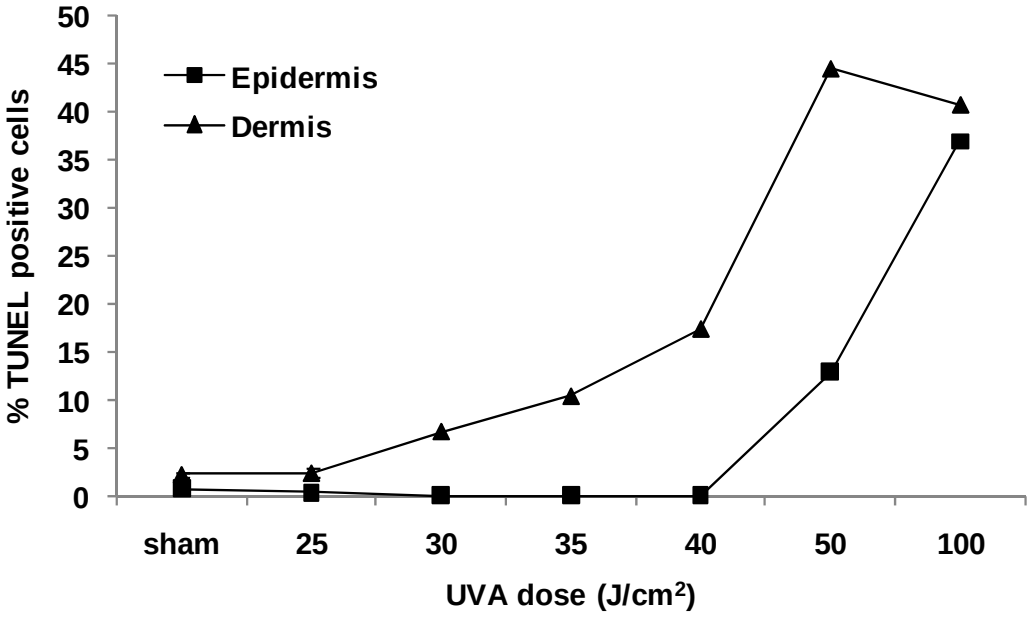

Figure 11. UVA irradiation induces apoptosis in a dose-dependent manner in 3D tissues 96 hours after irradiation. Percent apoptotic cells (mean) as assessed by TUNEL in the epidermis (square) and dermis (triangle) 96 h after sham (n=2), 25 (n=2), 30 (n=1), 35 (n=2), 40 (n=1), 50 (n=1) and 100 (n=1) J/cm^2 UVA irradiation.

CHAPTER 5

The Photoprotective Effects of alpha-Tocopherol in a Three-Dimensional Human Skin Tissue Model

Abstract

Introduction: Alpha-tocopherol (AT) has previously shown promise as a photoprotectant. This study aimed to assess the photoprotection of these nutrients in a 3-dimensinal (3D) human skin tissue model with ultraviolet-A (UVA) irradiation.

Methods and Materials: AT was applied to medium or topically (25 μM and 1 mg/cm^2, respectively). Optimal dose and incubation time for each treatment were selected based on maximal nutrient absorption while maintaining healthy skin tissue parameters (morphology, proliferation and apoptosis). After nutrient incubation, tissues were UVA irradiated (35 J/cm^2) and photodamage was assessed in comparison to control tissues after 96 h. Photodamage was assessed by morphological outcomes (basal layer organization, fibroblast presence, and epidermal development) observed in hemotoxylin and eosin-stained tissue cross-sections; proliferation of basal cells by bromodeoxyuridine incorporation assay; apoptosis by TUNEL assay; differentiation by cytokeratin-10 immunohistochemistry; antioxidant capacity by ferric reducing antioxidant power assay; and protein secretion fibroblast growth factors and matrix metalloprotease (MMP)-2.

Results: Nutrient treatments alone did not induce significant changes in the percentage of apoptotic fibroblasts or morphologic parameters. Topical AT treatment alone stimulated hepatocyte growth factor (HGF; 132%), keratinocyte growth factor (KGF; 132%) and interleukin-1 alpha. However, UVA irradiation increased apoptotic fibroblasts by approximately 12 fold and decreased proliferating basal keratinocytes by 60%, compared to control tissues. Negative morphologic changes were also observed at 96 h after irradiation, including

disappearance of fibroblasts in the upper dermis, disorganized basal layer and less developed epithelium. UVA delayed keratinocyte differentiation, suppressed secretion of HGF and induced secretion of MMP-2. UVA-induced morphological deterioration was partially prevented by pretreatment of medium and topical AT. Tissues pretreated with AT medium and topical treatments had increased proliferating basal keratinocytes (46 and 31%, respectively) and decreased apoptotic fibroblasts (39 and 65%, respectively), compared to corresponding vehicle treated tissues after UVA irradiation. UVA-induced delayed keratinocyte differentiation was attenuated by both pretreatments. Pretreatment with medium and topical AT attenuated increased HGF secretion (77 and 147%, respectively), compared to corresponding vehicle controls after UVA irradiation. Pretreatment with medium and topical AT modulated MMP-2 secretion (+12 and +20%, respectively), compared to corresponding vehicle controls after UVA irradiation.

Conclusions: Both medium and topical AT treatments provided some degree of photoprotection from UVA. Our results showing the absorption of AT and protective effects of medium and topical AT on morphology, proliferation, apoptosis, differentiation and protein secretion lends to the feasibility of using this model to investigate the mechanisms of action of these treatments in photoprotection. These data may have positive implications for the use of dietary and topical AT to prevent sun damage.

Introduction

Skin is the largest organ in the human body. It is exposed to environmental insult of which UV light is thought to be the most harmful (Lippens *et al.*, 2009). UV exposure can cause oxidative stress, inflammation, erythema, breakdown of the extracellular matrix, wrinkling and skin cancer (Boelsma *et al.*, 2001; Iddamalgoda *et al.*, 2008; Mudgil *et al.*, 2003). In fact, cumulative sun exposure is one of the most important risk factors for both nonmelanoma and

melanoma skin cancers (Gloster and Brodland, 1996; Miller and Mihm, 2006). At the earth's surface, we are exposed to both UVA and shorter wave, higher energy UVB. A majority of photodamage research has focused on UVB but recent research has revealed that UVA damage can be significant, including DNA mutations and altered DNA repair, immune function, cell integrity, and cell cycle regulation (Mouret *et al.*, 2006; Ridley *et al.*, 2009; Runger and Kappes, 2008; Waster and Ollinger, 2009). UVA is known to penetrate further than UVB, into the dermal layer (Bernerd and Asselineau, 2008). This is reflected in the revised FDA regulations for sunscreen, where "Broad Spectrum SPF" values will reflect both UVA and UVB protection equally (FDA, 2011). There are many ways to protect oneself from UV damage including avoidance of the sun, wearing protective clothing (hats, long-sleeved shirts, treated fabrics, etc), and topical sunscreen. However, the potential for nutrient UV protection via diet and topical application is a relatively recent concept. Compared to topical sunscreens which require reapplication and have localized effects, dietary methods are thought to provide continual whole body protection.

Vitamin E (VE) refers to a family of eight nutrients of which α-tocopherol (AT) is the most abundant and biologically active form in the human body. This essential lipophilic nutrient is well known for its role as a chain-breaking antioxidant during lipid peroxidation and it protects polyunsaturated fatty acids in cell membranes from oxidation. AT concentrations in skin can be increased with oral (5 fold increase of deuterated AT in skin surface lipid) or topical delivery (>20 fold increase) (Lopez-Torres *et al.*, 1998; Thiele and Ekanayake-Mudiyanselage, 2007) and are decreased by 50% in the stratum corneum with UV exposure (Rijnkels *et al.*, 2003). AT is found in human skin at approximately 7 and 13 ng/mg wet weight in dermal and epidermal

compartments, respectively (Shindo *et al.*, 1994). AT's activity as an antioxidant, combined with its presence in human skin, provide biologic plausibility for its role as a photoprotectant in skin.

AT has been shown as a photoprotectant in clinical, epidemiological, animal and *in vitro* research. In humans, dietary AT was found protective of UV-induced erythema and lipid peroxidation (McArdle *et al.*, 2004; Mireles-Rocha *et al.*, 2002) but combinations with supplemental vitamin C show greater protection. Epidemiological data indicates a weak protective effect of dietary VE in nonmelanoma skin cancer (McNaughton *et al.*, 2005). Animal studies have demonstrated protection of topically applied AT against wrinkling, sunburn cell formation and skin tumor incidence from (Bissett *et al.*, 1990, 1992; Bissett *et al.*, 1989). Because most of these studies have focused on UVB, our knowledge of AT and UVA photoprotection is limited.

A novel *in vitro* 3-dimensional (3D) skin tissue model provides a unique platform to assess histological, biochemical and molecular outcomes under conditions similar to those found *in vivo*. We have previously demonstrated the time and dose-dependent absorption of AT into the 3D skin model as well as dose-dependent UVA damage (Evans JA *et al.*, 2011). The current study examined the potential UVA photoprotection provided by pretreatment of AT topically applied or added to medium to mimic dietary delivery, as assessed by morphology, proliferation, apoptosis, differentiation, antioxidant capacity and protein secretion. The overall objective of this work is to establish feasibility in using the 3D skin tissue model in photoprotective studies involving nutrients.

Methods and Materials

3D human skin tissues were prepared as previously described (Carlson *et al.*, 2008). Briefly, human dermal fibroblasts (HFF) were derived from newborn foreskin and grown in

Dulbecco's modified Eagle's medium (Invitrogen, Carlsbad, CA, USA) supplemented with 10% fetal bovine serum (Hyclone, Logan, UT, USA). HFFs were mixed with bovine type I collagen (2.5×10^4 cells/mL) and the gels were allowed to contract for 7 days in deep-well polycarbonate tissue culture inserts (Organogenesis, Canton, MA, USA). Subsequently, a total of 5×10^5 human keratinocytes were seeded onto the collagen gel and tissues were then maintained submerged in low calcium epidermal growth media for 2 days, for an additional 2 days in normal calcium media and raised to the air-liquid interface for seven days, after which tissues is considered fully developed (Organogenesis, Canton, MA, USA). Experiments were performed 2-4 times on fully developed tissues. For proliferation assays, 20 μg/mL bromodeoxyuridine (BrdU) (Invitrogen, Carlsbad, CA) was added to tissue culture medium 5 h prior to harvesting.

AT treatment

AT (Sigma, St. Louis, MO) was dissolved in dimethyl sulfoxide (DMSO) before application to the media of fully developed skin tissues at a final concentration of 0 or 25 μM for 48 h. Dose was selected based on previous experiments in 3D skin models assessing morphology, proliferation and apoptosis from a range of doses which are physiologically achievable concentrations in human circulation (Evans JA *et al.*, 2011). DMSO concentration was 0.1% of medium. Medium was agitated by pipetting 8 times to ensure homogeneity of treatment. AT was dissolved in 45 μL acetone for topical application of 0 or 1 mg/cm^2 for 2 h. Dose was selected based on our previous work which established its safety in 3D tissues (Evans JA *et al.*, 2011).

UV irradiation

At the end of topical and medium treatment, medium was removed and the skin samples, which were gently washed with PBS two times on each surface, were transferred to a sterile

platform. A 200-W UV radiation source (Lightning Cure 200, Hamamatsu, Japan) was used in combination with a dichroic mirror assembly reflecting most of the visible and infrared wavelengths, to reduce the heat load on the skin, and with UG11 and WG335 filters for wavelength delivery in the UVA range (320 – 400 nm). A liquid light guide was connected to the lamp, conducting the light to the surface of the skin. The light guide was mounted to a stand, parallel to the skin surface, at a distance of 3 cm, which provides the most uniform field of light. UVA dose was 0 or 35 J/cm^2 with an intensity of 75 mW/cm^2 as measured by a radiometer (Fluke 289 True RMS Multimeter, Everett, WA). Tissue inserts were returned to tissue culture trays after the UVA treatment with fresh medium and harvested 96 h post-irradiation for histology analysis and media were collected as well.

Tissue Harvesting and Morphology Assessment

At the end of 96-h post irradiation, tissues were analyzed for morphology, proliferation and apoptosis. At harvesting, tissues were divided into 3 equal portions for separate preservation and tissue media were collected and stored at -80ºC until analysis. One third of tissue was fixed in formalin, embedded in paraffin, and serially sectioned at 6 μm. Histological sections were stained with hematoxylin and eosin (H&E), images were captured using a Nikon Eclipse 80i microscope (Nikon Instruments Inc., Melville, NY, USA) equipped with a SPOT RT camera (Diagnostic Instruments, Sterling Heights, MI, USA) and analyzed using Spot Advanced software (Diagnostic Instruments, Sterling Heights, MI, USA). Morphologic assessment of H&E stained tissue cross sections included qualitative evaluation of 1) organization of basal layer, 2) presence of fibroblasts and 3) development of epidermis. A separate third of tissue was snap frozen in O.C.T. compound (Sakura Finetek USA, Torrance, CA, USA) by liquid nitrogen after immersion in 2 M sucrose solution at 4ºC for at least 24 hours. The remaining third of tissue used

for the measurement of apoptotic cells using terminal deoxynucleotidyl transferase mediated dUTP nick-end labeling [TUNEL] assay was immersed in 4% paraformaldehyde for 1 h and 2 M sucrose solution at 4ºC for at least 24 h and snap frozen in O.C.T. compound (Sakura Finetek USA, Torrance, CA, USA) by liquid nitrogen and serial sectioned at 6 µm, and mounted onto gelatin-chrome alum coated slides.

Immunohistochemical and immunofluorescence analysis

Immunohistochemical staining of BrdU as a marker of proliferation was performed on paraffin-embedded tissues sectioned at 6 µm thickness using monoclonal antibodies against BrdU (Roche, Indianapolis, IN) and Vectastain ABC kit (Vector Labs, Burlingame, CA). The number of BrdU-positive basal keratinocytes was determined by counting and expressed as a percentage of total cells in the basal layer.

Immunohistochemical staining of cytokeratin 10 was performed on paraffin-embedded tissues sectioned at 6 µm thickness. Cytokeratins, filament proteins, play a critical role in differentiation and tissue specialization and function to maintain the overall structural integrity of epithelial cells. Tissue was immersed in 0.1% sodium citrate at 100ºC for 15 min for antigen retrieval, incubated with monoclonal antibody against cytokeratin 10 (Abcam, Cambridge, MA) and developed with Vectastain ABC kit (Vector Labs, Burlingame, CA).

The TUNEL assay was used to identify apoptotic cells (Mudgil *et al.*, 2003). Tissue samples soaked in 4% paraformaldehyde prior to freezing were sectioned at 6 µm thickness, permeabilized with 0.1% triton in 0.1% sodium citrate, incubated with the TUNEL reaction mixture (Roche, Indianapolis, IN) for 1 h at 37^{o}C in the dark and counterstained with DAPI (40,6-diamidino-2-phenylindole). The percentage of TUNEL-positive cells was calculated from the number of these cells divided by the total number of cells counted in the entire epithelium.

Ferric reducing antioxidant power (FRAP) Assay

Total antioxidant capacity in the harvested medium was measured using the FRAP assay as previously described (Benzie and Strain, 1996). Reagents included 300 mM acetate buffer, pH 3.6 (3.1 g $C_2H_3NaO_2 \cdot 3H_2O$ and 16 mL $C_2H_4O_2$ per liter of buffer solution); 10 mM TPTZ (2,4,6-tripyridyl-s-triazine, Sigma, St. Louis, MO) in 40 mM HCl; 20 mM $FeCl_3 \cdot 6H_2O$. Working FRAP reagent was prepared as required by mixing 25 mL acetate buffer, 2.5 mL TPTZ solution, and 2.5 mL $FeCl_3 \cdot 6H_2O$ solution. Trolox concentrations in the range of 31.25–1000 μM (Sigma, St. Louis, MO) were used for calibration. Thirty μL of medium, blank (H_2O) or standards were added to non-UV disposable cuvettes followed by 90 μL H_2O and 900 μL of working FRAP reagent and incubated for 60 min at room temperature. The absorbance was measured at 593 nm using a spectrophotometer (Shimadzu UV-1601, Japan). Reported values are adjusted for the FRAP value of medium not incubated with tissue.

Enzyme-linked immunosorbent assay (ELISA)

To assess protein secretion, tissue culture media were harvested and processed using commercial DuoSet HGF, IL-1α and KGF ELISA kit (R&D Systems, Minneapolis, MN, USA) and MMP-2 human ELISA kit (Invitrogen, Carlsbad, CA). Medium was assayed in duplicate.

Statistics

Results are expressed as mean $\pm$ SEM. Due to limited replication, comparison of experimental conditions are largely descriptive and statistical analysis was not performed.

Results

Morphology

UVA irradiation (35 J/cm^2) induced morphologic changes in the 3D skin tissue including keratinocyte invasion into the dermal matrix, disorganized basal layer of epidermis, less

epidermal development and fibroblast loss (**Figure 1b**) that was not seen in non-irradiated control tissues (Figure 1a). Sham irradiated tissues treated with vehicle controls (medium or topical; Figures 1d and h) were comparable to untreated controls. Tissues pretreated with 25 μM medium or 1 mg/cm^2 topical AT (Figure 1f & j) were less damaged than vehicle controls after UVA treatment but not as healthy as non-irradiated tissues. Tissues receiving nutrient treatments alone (Figure 1c & g) were comparable to untreated controls.

Proliferation

Basal cell proliferation of UVA treated tissues was 60% less than that of untreated tissues (**Figure 2**). Sham irradiated tissues treated with medium vehicle (DMSO) had 28% greater proliferation than untreated controls, while topical vehicle did not induce an effect. Tissues treated with 25 μM or 1 mg/cm^2 AT had 12 and 13% lower proliferation, respectively, than corresponding vehicle and sham irradiated controls. Tissues pretreated with medium or topical doses had 46 and 31% greater proliferation, respectively, compared to vehicle treated tissues after UVA exposure.

Apoptosis

Dermal apoptosis of UVA treated tissues was approximately 12 times that of untreated tissues (**Figure 3**). Nutrient and sham irradiated vehicle control tissues (medium or topical) were comparable to untreated controls. Apoptosis of tissues pretreated with 25 μM or 1 mg/cm^2 AT was 39 and 65% less, respectively, than that of vehicle controls after UVA exposure.

Differentiation

UVA exposure delayed keratinocyte differentiation (**Figure 4b**), as indicated by cytokeratin-10 presence, which was attenuated by medium and topical AT pretreatment (Figure

4f & j). Nutrient and sham irradiated vehicle controls (medium or topical) were comparable to untreated controls.

FRAP

All treated tissues had media trolox equivalent values greater than control (**Figure 5**). AT treatment of 25 μM or 1 mg/cm^2 led to 8 and 26% greater trolox equivalents in media of treated tissues, respectively, compared to corresponding vehicle and sham irradiated controls. Tissues pretreated with 25 μM or 1 mg/cm^2 AT had 122 and 18% greater media trolox equivalents, respectively, compared to vehicle and sham irradiated controls after UVA exposure.

Protein Secretion

Tissues exposed to UVA had approximately 30% decreased HGF media concentrations compared to controls (**Figure 6**). Sham irradiated tissues treated with topical vehicle (acetone) had 39% lower HGF media concentrations than untreated controls, while medium vehicle did not induce an effect. Twenty five μM or 1 mg/cm^2 AT treated tissues had 12% less and 132% greater HGF, respectively compared to vehicle and sham irradiated controls. Tissues pretreated with 25 μM or 1 mg/cm^2 AT had 77 and 147% greater media HGF concentrations, respectively, compared to vehicle controls after UVA exposure.

KGF medium concentration was 14% greater in tissues exposed to UVA compared to untreated controls (**Figure 7**). Sham irradiated tissues treated with topical vehicle (acetone) had 24% lower KGF medium concentration than untreated controls. One mg/cm^2 AT treated tissues had 132% greater KGF medium concentration compared to vehicle and sham irradiated control. Tissues pretreated with 1 mg/cm^2 AT had 25% greater KGF compared to vehicle control after UVA irradiation. KGF medium concentration was not detectable in tissues treated with medium vehicle and sham irradiated or 25 μM medium AT and UVA irradiated.

IL-1α concentrations in media were only detected in tissues treated with 1 mg/cm^2 AT alone or in combination with UVA irradiation (data not shown).

Tissues exposed to UVA had approximately 21% increased MMP-2 media concentrations compared to controls (**Figure 8**). Sham irradiated tissues treated with vehicle controls (medium or topical) were comparable to untreated controls. Twenty five μM medium or 1 mg/cm^2 topical AT treated tissues had 21% less and 22% greater MMP-2 secretion, respectively, compared to vehicle and sham irradiated controls. Tissues pretreated with 25 μM or 1 mg/cm^2 AT had 12 and 20% greater MMP-2 secretion, respectively, compared to vehicle controls after UVA exposure.

Discussion

The primary goal of this research was to evaluate the feasibility of using a 3D skin tissue model in studies assessing the photoprotectiveness of nutrients. To this end, AT was selected for our evaluation because of its role as an antioxidant and its presence in human skin tissue.

Potential UVA photoprotection was examined in 3D skin tissue treated with topical AT or AT added to medium to mimic dietary nutrient delivery. We have previously demonstrated that a dose of 35 J/cm^2 UVA (equivalent to <5 h midday summer sun exposure) to the 3D skin tissue model is damaging but nontoxic (Evans JA *et al.*, 2011). In the present study, we examined UVA damage in this 3D skin model from the most global perspective of morphology, narrowing in on specific tissue parameters of interest using immunohistochemical analysis (proliferation, apoptosis, differentiation) and finally examining proteins thought to be involved in the cellular cross-talk that regulates these processes. While this is a study with limited replication, our results suggest that this is a feasible research tool in future studies evaluating the mechanisms by which foods or specific nutrients are photoprotective.

UVA induced unhealthy morphologic changes, reflected by decreased basal cell proliferation and HGF secretions, increased dermal apoptosis and MMP-2 secretions and delayed differentiation, which is consistent with the literature (Bernerd and Asselineau, 1998, 2008; de Laat *et al.*, 1997; de Laat *et al.*, 1996; Oh *et al.*, 2004). As fibroblasts are the principal source of HGF and KGF secretions (Shirakata), the observed HGF decreases likely reflect the fibroblast loss. Others have found UVA to stimulate IL-1α in an epidermal model of normal human keratinocytes 24 h after 20, 40 and 60 J/cm^2 (Noel-Hudson *et al.*, 1997). Because media IL-1α concentrations were below the detection limit in both untreated and UVA irradiated tissues of our study, we cannot determine if there was a response. It is possible that IL-1α response is short-term and would have returned to homeostatic conditions at the 96 h time point that we used in our study. However, when assessed 2, 4, 24 and 168 h post-irradiation, IL-1α gene expression was not stimulated by low dose UVA (2, 6 or 12 J/cm^2) in a 3D human skin model (Meloni *et al.*).

UVA damage was attenuated, with the exception of changes in MMP-2 secretion, with topical or medium AT treatment. In concordance with our results, pretreatment with topical AT reduced cell death in an epidermal model (Noel-Hudson *et al.*, 1997). Our MMP-2 AT response results may contradict previous research showing medium AT pretreatment partially inhibited UVA-induced MMP-2 activity in human dermal fibroblasts (both monolayer and in collagen gel) (Hantke *et al.*, 2002). This contradiction may be attributed to different MMP-2 measures (secretion compared to activity), their use of a lower UVA dose (10 J/cm^2) and higher medium AT concentration (150 μM) but importantly, their system did not include keratinocytes. Fibroblast response is known to be altered in the presence of adjacent keratinocytes due to the epithelial-mesenchymal cross-talk (Smola *et al.*, 1993). The small, but significant nutrient

photoprotection observed in our study is consistent with what others have found in humans (Richelle *et al.*, 2006; Sies and Stahl, 2004).

Because AT does not directly absorb UVA waves, we believe its mechanism of action to be indirect via antioxidant activity against UVA-induced damage or interaction with cellular signaling. Our results showed pretreatment with AT increased antioxidant status measured by the FRAP assay after UVA irradiation compared to controls. Wu et al. found that AT prevented UVA-induced lipid peroxidation and NADPH oxidase activation through AP-1 in primary human keratinocytes (Wu *et al.*, 2008) and AT has been shown to prompt glutathione production in HaCaT keratinocytes (Masaki *et al.*, 2002).

Medium v. topical

While both treatments provided photoprotection, differences in outcome measures were observed between the medium and topical AT treated tissues. Topical treatment alone stimulated HGF and MMP-2 secretions while medium treatment was suppressive, in comparison to corresponding vehicle treated, sham irradiated tissues. Pretreatment of topical AT provided greater protection from UVA-induced changes than medium treatment, including apoptosis, delayed differentiation and decreased HGF secretion. Also, the morphology after UVA irradiation shows healthier fibroblasts in topical treated tissues than medium treated. Tissues pretreated with topical AT before UVA irradiation, showed less KGF secretion into the medium, the opposite of observation in media of AT pretreated tissues. Topical AT alone and in combination with UVA uniquely induced IL-1α secretion, which was below the range of detection in all other samples. It has previously been shown that UVA and IL-1α induced secretion of HGF in human dermal fibroblasts acts in an autocrine manner to prevent apoptosis (Mildner *et al.*, 2007). It is possible that this mechanism is at play here as well. The differential

response to medium and topical treatment is likely due to the greater skin AT concentration achieved from topical application. In previous experiments using the doses of the current study, epidermal and dermal concentrations of AT were more than 1000 and 300 fold greater, respectively from topical AT application (Evans JA *et al.*, 2011). It is possible to apply a much greater AT dose topically than to the medium, similar to comparing application of a cosmetic product to dietary consumption of the same compound. However, when the same absolute amount (100 mg) of AT was applied topically or to the medium of an epidermal model, protection from UVA-induced cell death was attenuated only by topical treatment (Noel-Hudson *et al.*, 1997). Evidence from many UV studies strongly supports topical AT as a photoprotectant but comparison between oral and topical application is uncommon (Thiele and Ekanayake-Mudiyanselage, 2007). However in a clinical trial investigating oral, topical and combined application of other fat-soluble compounds, combined application provided the most benefit (Palombo *et al.*, 2007).

Currently, most studies of nutrient photoprotection are conducted in humans, animals or monolayer models, although each with its own limitations. Conducting these studies in human skin *in vivo* is difficult because it requires scar-inducing skin biopsies. Bioavailability and metabolism of nutrients in modeled animals are different from humans, as well as their skin structure. Monolayer cultures do not mimic *in vivo* physiologies, in terms of stratification, differentiation, proliferation and signaling pathways as well as the 3D human skin tissue model. This novel *in vitro* 3D skin tissue model provides a unique opportunity to assess histological, biochemical and molecular outcomes under conditions similar to those found *in vivo* and could be an invaluable tool in the growing fields of skin nutrition and photoprotection. Our ability to establish that the AT applications were absorbed in this skin tissue model and the subsequent

effects on morphology, proliferation, apoptosis and differentiation lends to the feasibility of using this model to investigate the mechanisms of action of nutrients in photoprotection.

References

Benzie IF, Strain JJ (1996) The ferric reducing ability of plasma (FRAP) as a measure of "antioxidant power": the FRAP assay. *Anal Biochem* 239:70-6.

Bernerd F, Asselineau D (1998) UVA exposure of human skin reconstructed in vitro induces apoptosis of dermal fibroblasts: subsequent connective tissue repair and implications in photoaging. *Cell Death Differ* 5:792-802.

Bernerd F, Asselineau D (2008) An organotypic model of skin to study photodamage and photoprotection in vitro. *J Am Acad Dermatol* 58:S155-9.

Bissett DL, Chatterjee R, Hannon DP (1990) Photoprotective effect of superoxide-scavenging antioxidants against ultraviolet radiation-induced chronic skin damage in the hairless mouse. *Photodermatol Photoimmunol Photomed* 7:56-62.

Bissett DL, Chatterjee R, Hannon DP (1992) Protective effect of a topically applied anti-oxidant plus an anti-inflammatory agent against ultraviolet radiation-induced chronic skin damage in the hairless mouse. *J Soc Cosmet Chem* 43:85-92.

Bissett DL, Hillebrand GG, Hannon DP (1989) The hairless mouse as a model of skin photoaging: its use to evaluate photoprotective materials. *Photodermatol* 6:228-33.

Boelsma E, Hendriks HF, Roza L (2001) Nutritional skin care: health effects of micronutrients and fatty acids. *Am J Clin Nutr* 73:853-64.

Carlson MW, Alt-Holland A, Egles C, Garlick JA (2008) Three-dimensional tissue models of normal and diseased skin. *Curr Protoc Cell Biol* Chapter 19:Unit 19 9.

de Laat A, Kroon ED, de Gruijl FR (1997) Cell cycle effects and concomitant p53 expression in hairless murine skin after longwave UVA (365 nm) irradiation: a comparison with UVB irradiation. *Photochem Photobiol* 65:730-5.

de Laat A, van Tilburg M, van der Leun JC, van Vloten WA, de Gruijl FR (1996) Cell cycle kinetics following UVA irradiation in comparison to UVB and UVC irradiation. *Photochem Photobiol* 63:492-7.

Evans JA, Chen C-YO, Garlick J, Wang X-D, EJ J (2011) Feasibility of nutrient photoprotection studies in a three-dimensional human skin tissue model: Using alpha tocopherol. *FASEB J* 25.

FDA (2011) Labeling and Effectiveness Testing; Sunscreen Drug Products for Over-the-Counter Human Use. In: *21 CFR Parts 201 and 310* (35620-65.

Gloster HM, Jr., Brodland DG (1996) The epidemiology of skin cancer. *Dermatol Surg* 22:217-26.

Hantke B, Lahmann C, Venzke K, Fischer T, Kocourek A, Windsor LJ, *et al.* (2002) Influence of flavonoids and vitamins on the MMP- and TIMP-expression of human dermal fibroblasts after UVA irradiation. *Photochem Photobiol Sci* 1:826-33.

Iddamalgoda A, Le QT, Ito K, Tanaka K, Kojima H, Kido H (2008) Mast cell tryptase and photoaging: possible involvement in the degradation of extra cellular matrix and basement membrane proteins. *Arch Dermatol Res* 300 Suppl 1:S69-76.

Lippens S, Hoste E, Vandenabeele P, Agostinis P, Declercq W (2009) Cell death in the skin. *Apoptosis* 14:549-69.

Lopez-Torres M, Thiele JJ, Shindo Y, Han D, Packer L (1998) Topical application of alpha-tocopherol modulates the antioxidant network and diminishes ultraviolet-induced oxidative damage in murine skin. *Br J Dermatol* 138:207-15.

Masaki H, Okano Y, Ochiai Y, Obayashi K, Akamatsu H, Sakurai H (2002) alpha-tocopherol increases the intracellular glutathione level in HaCaT keratinocytes. *Free Radic Res* 36:705-9.

McArdle F, Rhodes LE, Parslew RA, Close GL, Jack CI, Friedmann PS, *et al.* (2004) Effects of oral vitamin E and beta-carotene supplementation on ultraviolet radiation-induced oxidative stress in human skin. *Am J Clin Nutr* 80:1270-5.

McNaughton SA, Marks GC, Green AC (2005) Role of dietary factors in the development of basal cell cancer and squamous cell cancer of the skin. *Cancer Epidemiol Biomarkers Prev* 14:1596-607.

Meloni M, Farina A, de Servi B Molecular modifications of dermal and epidermal biomarkers following UVA exposures on reconstructed full-thickness human skin. *Photochem Photobiol Sci* 9:439-47.

Mildner M, Mlitz V, Gruber F, Wojta J, Tschachler E (2007) Hepatocyte growth factor establishes autocrine and paracrine feedback loops for the protection of skin cells after UV irradiation. *J Invest Dermatol* 127:2637-44.

Miller AJ, Mihm MC, Jr. (2006) Melanoma. *N Engl J Med* 355:51-65.

Mireles-Rocha H, Galindo I, Huerta M, Trujillo-Hernandez B, Elizalde A, Cortes-Franco R (2002) UVB photoprotection with antioxidants: effects of oral therapy with d-alpha-tocopherol and ascorbic acid on the minimal erythema dose. *Acta Derm Venereol* 82:21-4.

Mouret S, Baudouin C, Charveron M, Favier A, Cadet J, Douki T (2006) Cyclobutane pyrimidine dimers are predominant DNA lesions in whole human skin exposed to UVA radiation. *Proc Natl Acad Sci U S A* 103:13765-70.

Mudgil AV, Segal N, Andriani F, Wang Y, Fusenig NE, Garlick JA (2003) Ultraviolet B irradiation induces expansion of intraepithelial tumor cells in a tissue model of early cancer progression. *J Invest Dermatol* 121:191-7.

Noel-Hudson MS, Braut-Boucher F, Robert M, Aubery M, Wepierre J (1997) Comparison of six different methods to assess UVA cytotoxicity on reconstructed epidermis. Relevance of a fluorimetric assay (the calcein-AM) to evaluate the photoprotective effects of alpha-tocopherol. *Toxicol In Vitro* 11:645-51.

Oh JH, Chung AS, Steinbrenner H, Sies H, Brenneisen P (2004) Thioredoxin secreted upon ultraviolet A irradiation modulates activities of matrix metalloproteinase-2 and tissue inhibitor of metalloproteinase-2 in human dermal fibroblasts. *Arch Biochem Biophys* 423:218-26.

Palombo P, Fabrizi G, Ruocco V, Ruocco E, Fluhr J, Roberts R, *et al.* (2007) Beneficial long-term effects of combined oral/topical antioxidant treatment with the carotenoids lutein and zeaxanthin on human skin: a double-blind, placebo-controlled study. *Skin Pharmacol Physiol* 20:199-210.

Richelle M, Sabatier M, Steiling H, Williamson G (2006) Skin bioavailability of dietary vitamin E, carotenoids, polyphenols, vitamin C, zinc and selenium. *Br J Nutr* 96:227-38.

Ridley AJ, Whiteside JR, McMillan TJ, Allinson SL (2009) Cellular and sub-cellular responses to UVA in relation to carcinogenesis. *Int J Radiat Biol* 85:177-95.

Rijnkels JM, Moison RM, Podda E, van Henegouwen GM (2003) Photoprotection by antioxidants against UVB-radiation-induced damage in pig skin organ culture. *Radiat Res* 159:210-7.

Runger TM, Kappes UP (2008) Mechanisms of mutation formation with long-wave ultraviolet light (UVA). *Photodermatol Photoimmunol Photomed* 24:2-10.

Shindo Y, Witt E, Han D, Epstein W, Packer L (1994) Enzymic and non-enzymic antioxidants in epidermis and dermis of human skin. *J Invest Dermatol* 102:122-4.

Shirakata Y Regulation of epidermal keratinocytes by growth factors. *J Dermatol Sci* 59:73-80.

Sies H, Stahl W (2004) Nutritional protection against skin damage from sunlight. *Annu Rev Nutr* 24:173-200.

Smola H, Thiekotter G, Fusenig NE (1993) Mutual induction of growth factor gene expression by epidermal-dermal cell interaction. *J Cell Biol* 122:417-29.

Thiele JJ, Ekanayake-Mudiyanselage S (2007) Vitamin E in human skin: organ-specific physiology and considerations for its use in dermatology. *Mol Aspects Med* 28:646-67.

Waster PK, Ollinger KM (2009) Redox-dependent translocation of p53 to mitochondria or nucleus in human melanocytes after UVA- and UVB-induced apoptosis. *J Invest Dermatol* 129:1769-81.

Wu S, Gao J, Dinh QT, Chen C, Fimmel S (2008) IL-8 production and AP-1 transactivation induced by UVA in human keratinocytes: roles of D-alpha-tocopherol. *Mol Immunol* 45:2288-96.

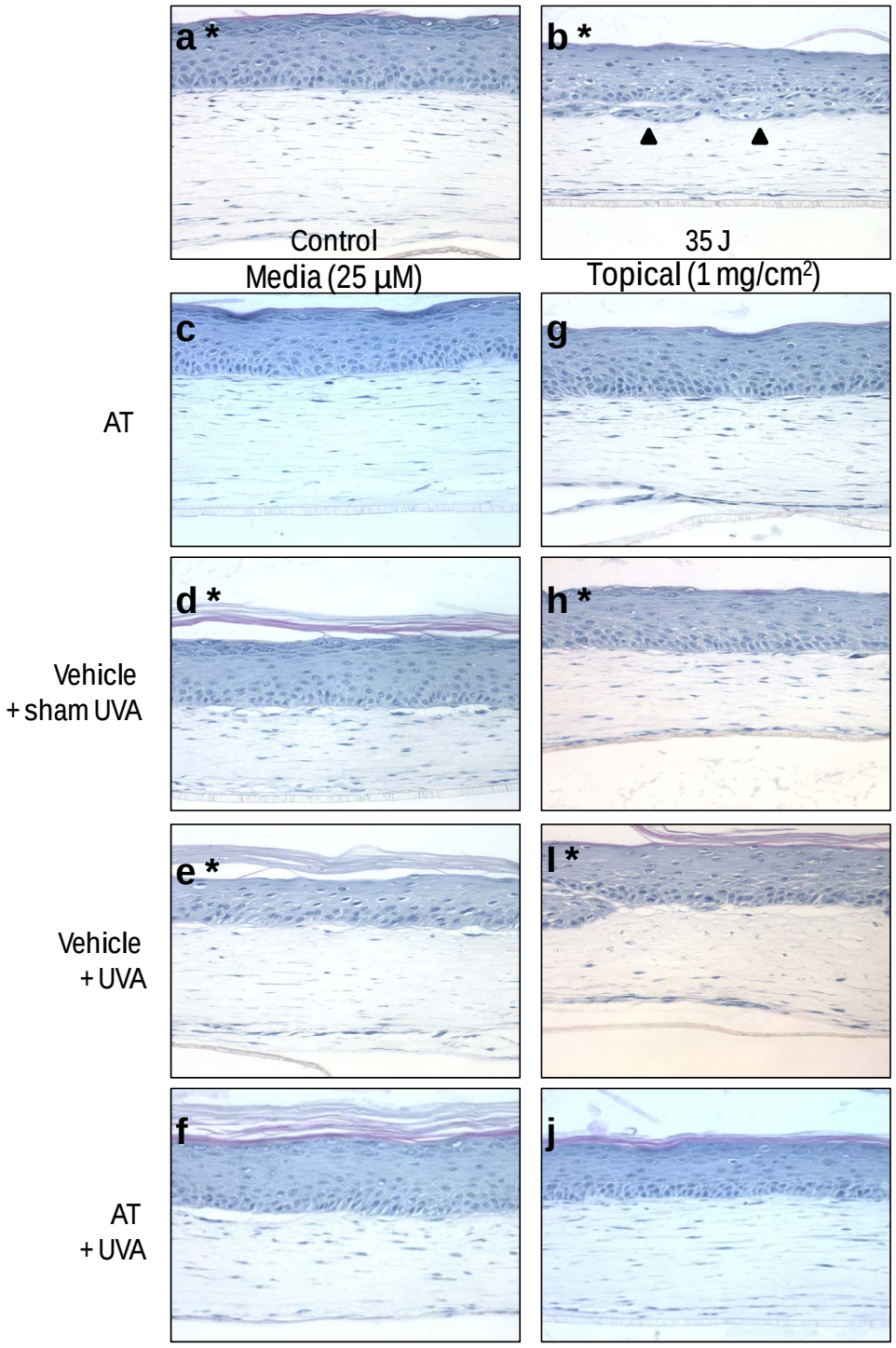

Figure 1. AT partially prevents deterioration of morphology from UVA irradiation in 3D tissues. Hematoxylin and eosin stained cross sections from 3D tissues 96 hours after UVA (35 J/cm^2) irradiation which was preceded by 48 hour incubation with medium (c.-f.) and 2 hour

incubation topical (g.-j.) AT treatment as follows (a) untreated, (b) UVA, (c) 25 μM AT, (d) vehicle[1] and sham irradiated (e) vehicle[1] and UVA irradiated, (f) 25 μM AT and UVA irradiated, (g) 1 mg/cm^2 topical AT, (h) vehicle[2] and sham irradiated, (i) vehicle[2] and UVA irradiated and (j) 1 mg/cm^2 topical AT and UVA irradiated. UVA irradiated tissues showed cellular invasion into the matrix (arrows), disappearance of fibroblasts in the upper dermis, disorganization in the basal layer and less developed epithelia. Both medium and topical AT partially prevented these alterations. Representative images are shown. *n=2, otherwise n=4.

[1]Medium AT vehicle is DMSO of (0.1% of medium volume).

[2]Topical AT vehicle consists of 45 μL of acetone.

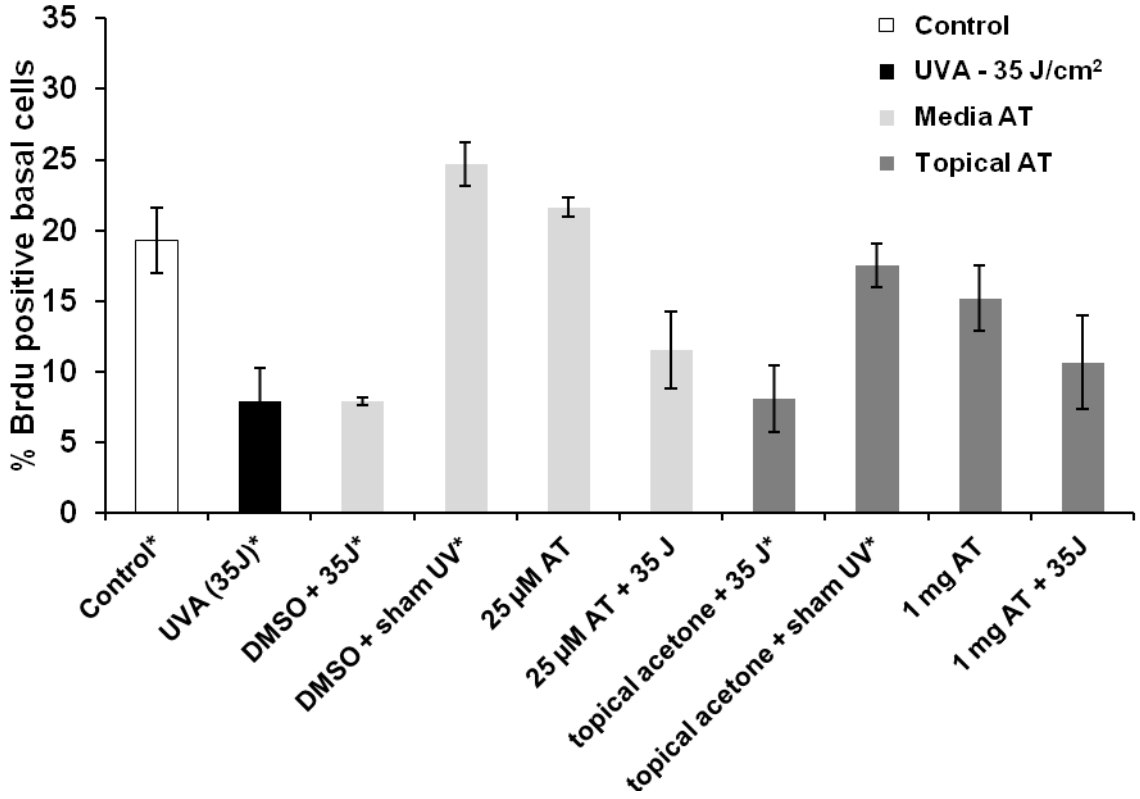

Figure 2. **AT and UVA modulate proliferation in 3D tissues.** Proliferation was measured as the percentage of total basal keratinocytes that were BrdU-positive (mean ± SEM) 96 h after irradiation in 3D tissues with the following conditions: untreated control (white); UVA irradiated (35 J/cm^2; black); medium AT (vehicle[1] + UVA/sham irradiated and 25 µM AT + UVA/sham irradiated (light gray)); and topical AT (vehicle[2] + UVA/sham irradiated and 1 mg/cm^2 AT + UVA/sham irradiated (dark gray)). *n=2, otherwise n=4.

[1]Medium AT vehicle is DMSO of (0.1% of medium volume).

[2]Topical AT vehicle consists of 45 µL of acetone.

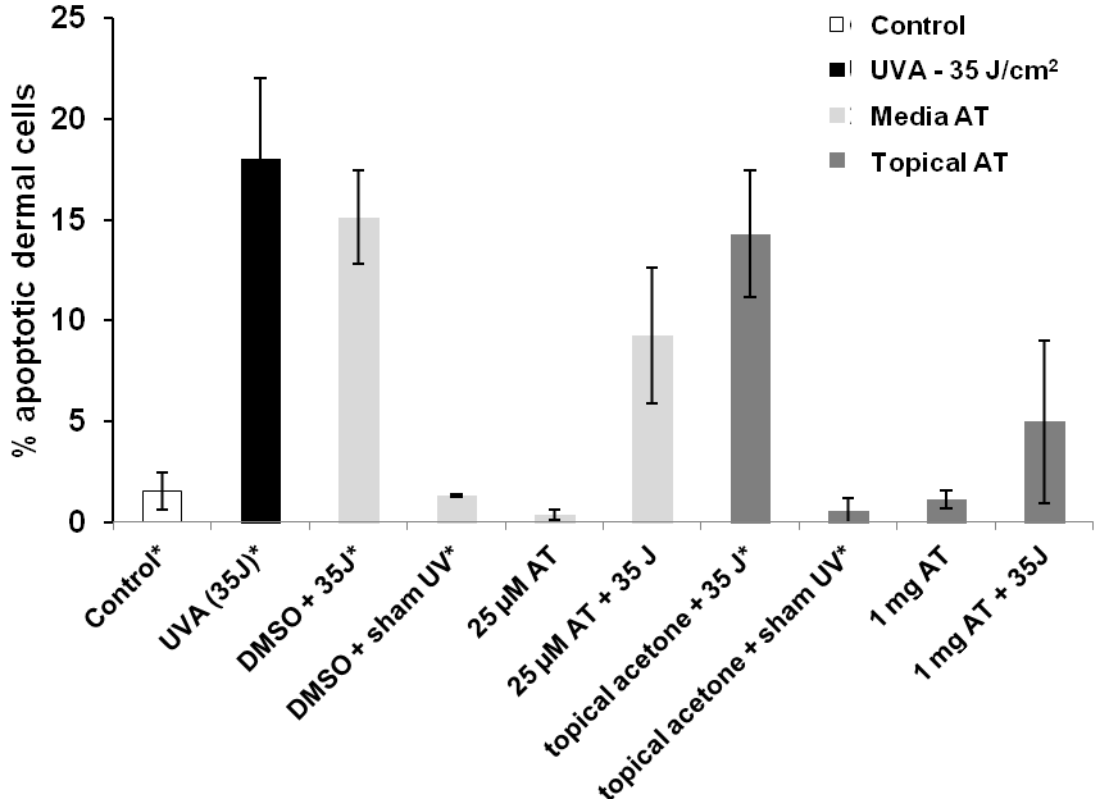

Figure 3. AT partially prevents UVA-induced dermal apoptosis in 3D tissues. Apoptosis was measured as the percentage of total fibroblasts that were TUNEL-positive (mean ± SEM) 96 h after irradiation in medium of 3D tissues with the following conditions: untreated control (white); UVA irradiated (35 J/cm^2; black); medium AT (vehicle[1] + UVA/sham irradiated and 25 µM AT + UVA/sham irradiated (light gray)); and topical AT (vehicle[2] + UVA/sham irradiated and 1 mg/cm^2 AT + UVA/sham irradiated (dark gray)). *n=2, otherwise n=4.

[1]Medium AT vehicle is DMSO of (0.1% of medium volume).

[2]Topical AT vehicle consists of 45 µL of acetone.

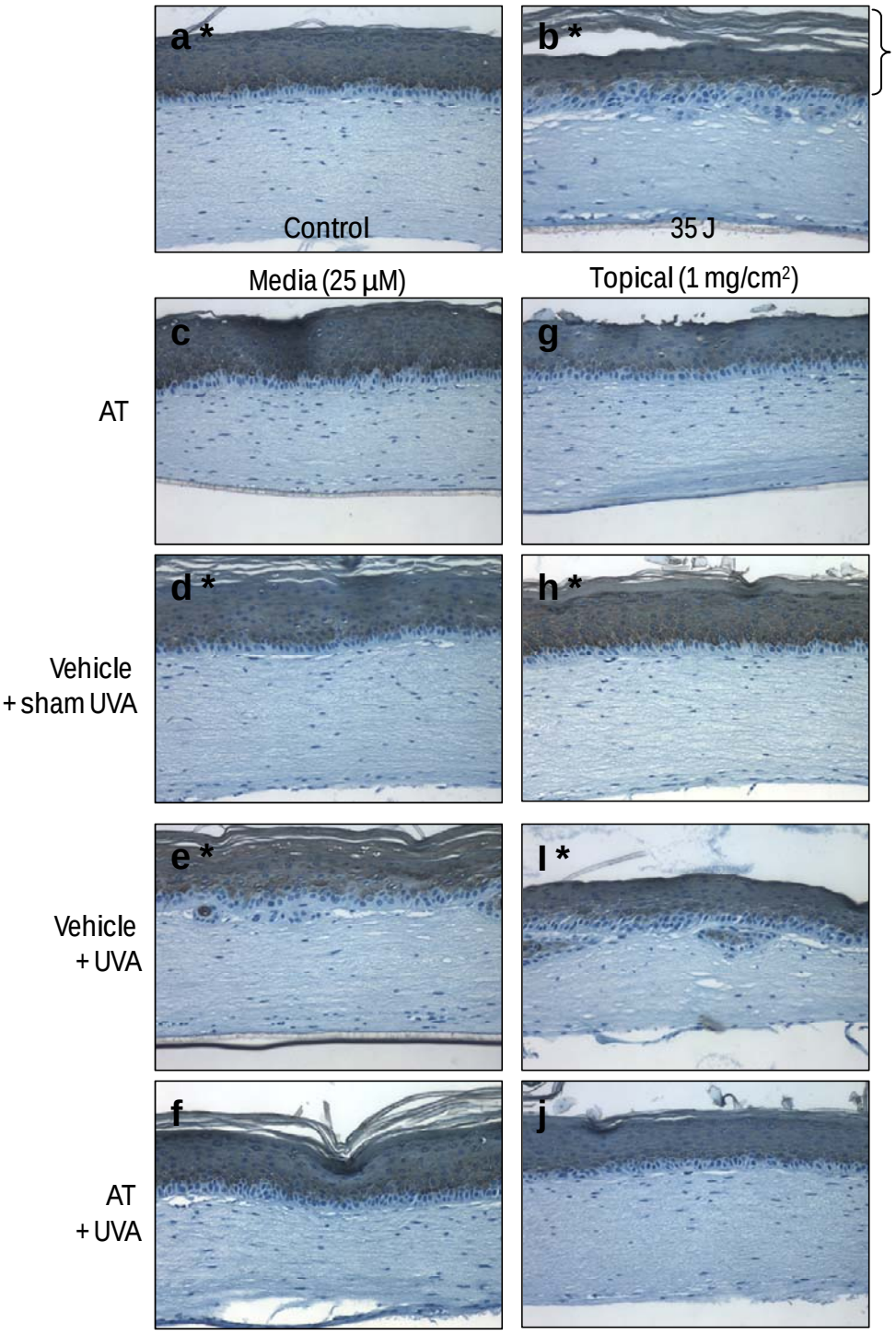

Figure 4. AT partially prevents keratinocyte differentiation delay induced by UVA irradiation in 3D tissues. Cytokeratin-10 stained cross sections from 3D tissues 96 hours UVA (35 J/cm^2) irradiation which was preceded by 2 hour incubation with medium (c.-f.) and topical (g.-j.) AT treatment as follows (a) untreated, (b) UVA, (c) 25 µM AT, (d) vehicle[1] and sham

irradiated (e) vehicle[1] and UVA irradiated, (f) 25 μM AT and UVA irradiated, (g) 1 mg/cm^2 topical AT, (h) vehicle[2] and sham irradiated, (i) vehicle[2] and UVA irradiated and (j) 1 mg/cm^2 topical AT and UVA irradiated. Cytokeratin-10 stained tissues are evaluated by visual comparison for presence of stain relative to the basal layer (example stain indicated by bracket). UVA irradiated tissues showed delayed differentiation. Both medium and topical AT partially prevented this delay. Representative images are shown. *n=2, otherwise n=4.

[1]Medium AT vehicle is DMSO of (0.1% of medium volume).

[2]Topical AT vehicle consists of 45 μL of acetone.

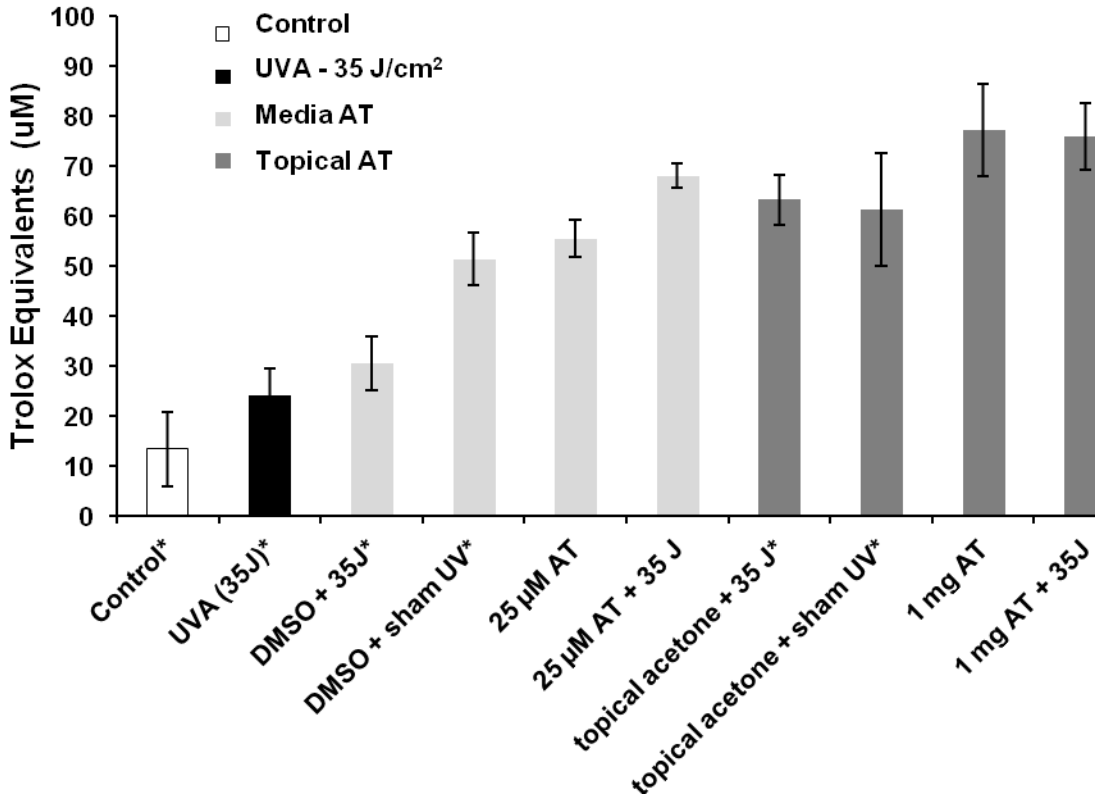

Figure 5. UVA irradiation, AT treatment and vehicles increase antioxidant capacity in 3D tissues. Antioxidant capacity (mean ± SEM) as assessed by FRAP assay 96 h after irradiation in medium of 3D tissues with the following conditions: untreated control (white); UVA irradiated (35 J/cm^2; black); medium AT (vehicle[1] + UVA/sham irradiated and 25 µM AT + UVA/sham irradiated (light gray)); and topical AT (vehicle[2] + UVA/sham irradiated and 1 mg/cm^2 AT + UVA/sham irradiated (dark gray)). *n=2, otherwise n=4.

[1]Medium AT vehicle is DMSO of (0.1% of medium volume).

[2]Topical AT vehicle consists of 45 µL of acetone.

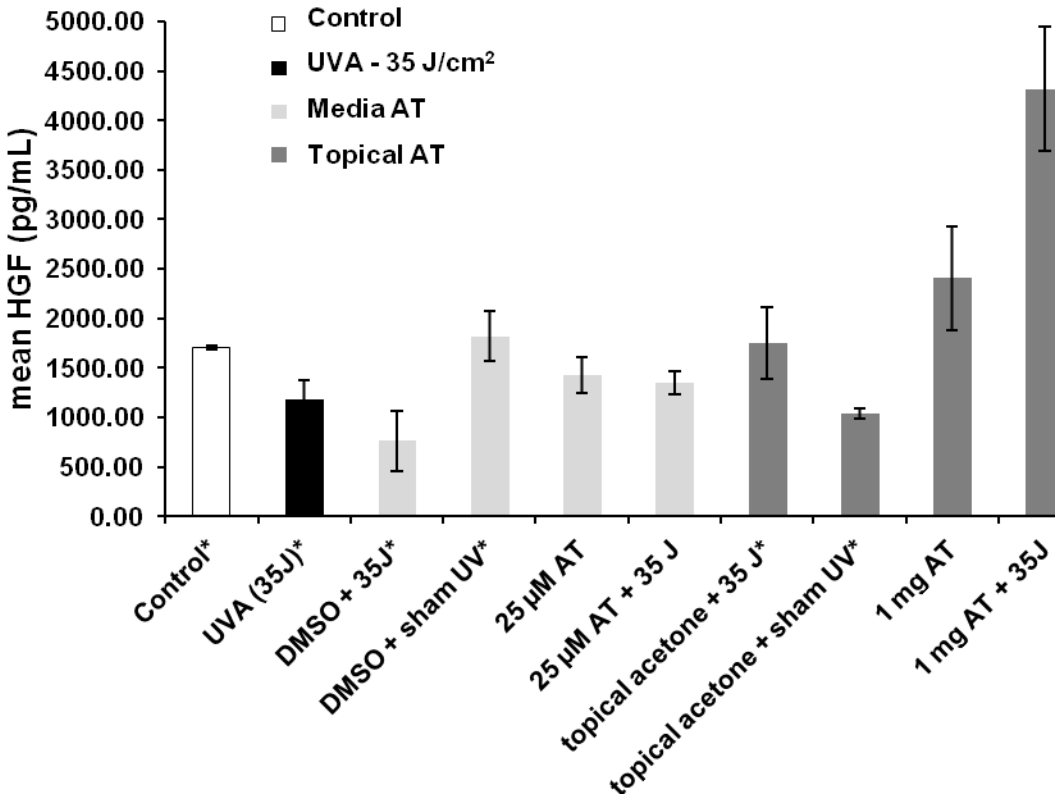

Figure 6. **AT pretreatment attenuates UVA suppression of HGF secretion in 3D tissues.** HGF concentration (mean ± SEM) as assessed by ELISA 96 h after irradiation in medium of 3D tissues with the following conditions: untreated control (white); UVA irradiated (35 J/cm^2; black); medium AT (vehicle[1] + UVA/sham irradiated and 25 µM AT + UVA/sham irradiated (light gray)); and topical AT (vehicle[2] + UVA/sham irradiated and 1 mg/cm^2 AT + UVA/sham irradiated (dark gray)). *n=2, otherwise n=4.

[1]Medium AT vehicle is DMSO of (0.1% of medium volume).

[2]Topical AT vehicle consists of 45 µL of acetone.

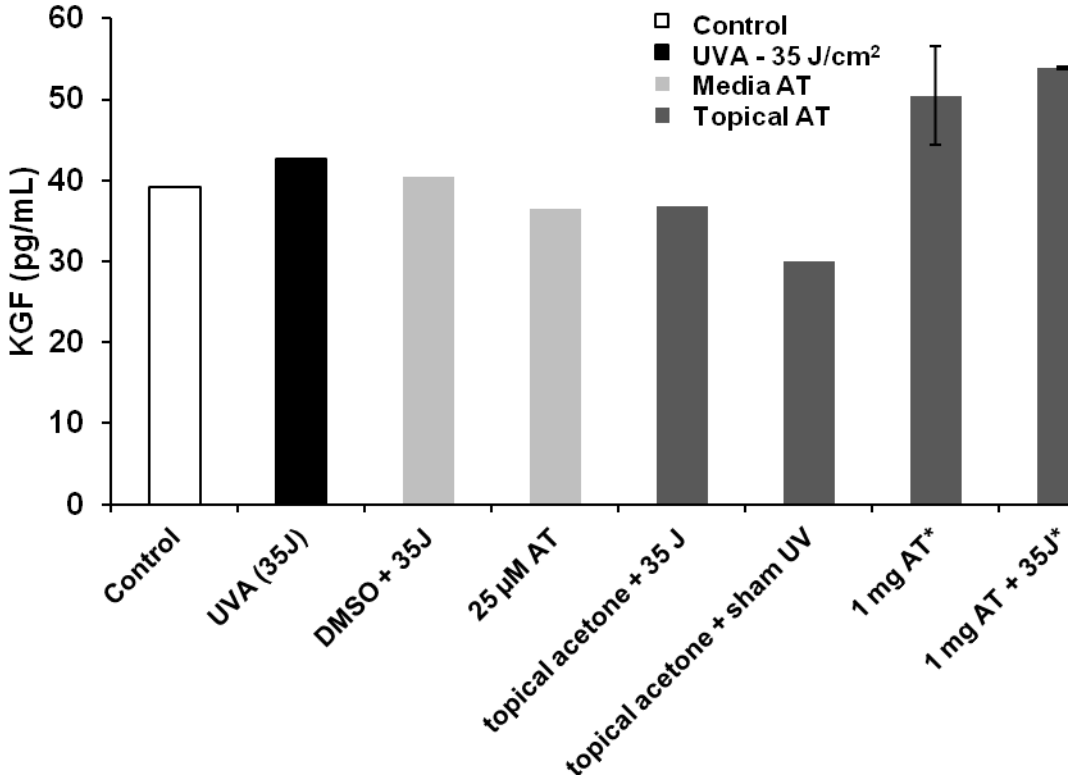

Figure 7. **UVA induces KGF secretion in 3D tissues.** KGF concentration (mean ± SEM) as assessed by ELISA 96 h after irradiation in medium of 3D tissues with the following conditions: untreated control (white); UVA irradiated (35 J/cm^2; black); medium AT (vehicle[1] + UVA/sham irradiated and 25 µM AT + UVA/sham irradiated (light gray)); and topical AT (vehicle[2] + UVA/sham irradiated and 1 mg/cm^2 AT + UVA/sham irradiated (dark gray)). KGF secretion was greater in UVA irradiated while topical AT enhanced this response in treated 3D tissues. *n=2, otherwise n=1.

[1]Medium AT vehicle is DMSO of (0.1% of medium volume).

[2]Topical AT vehicle consists of 45 µL of acetone.

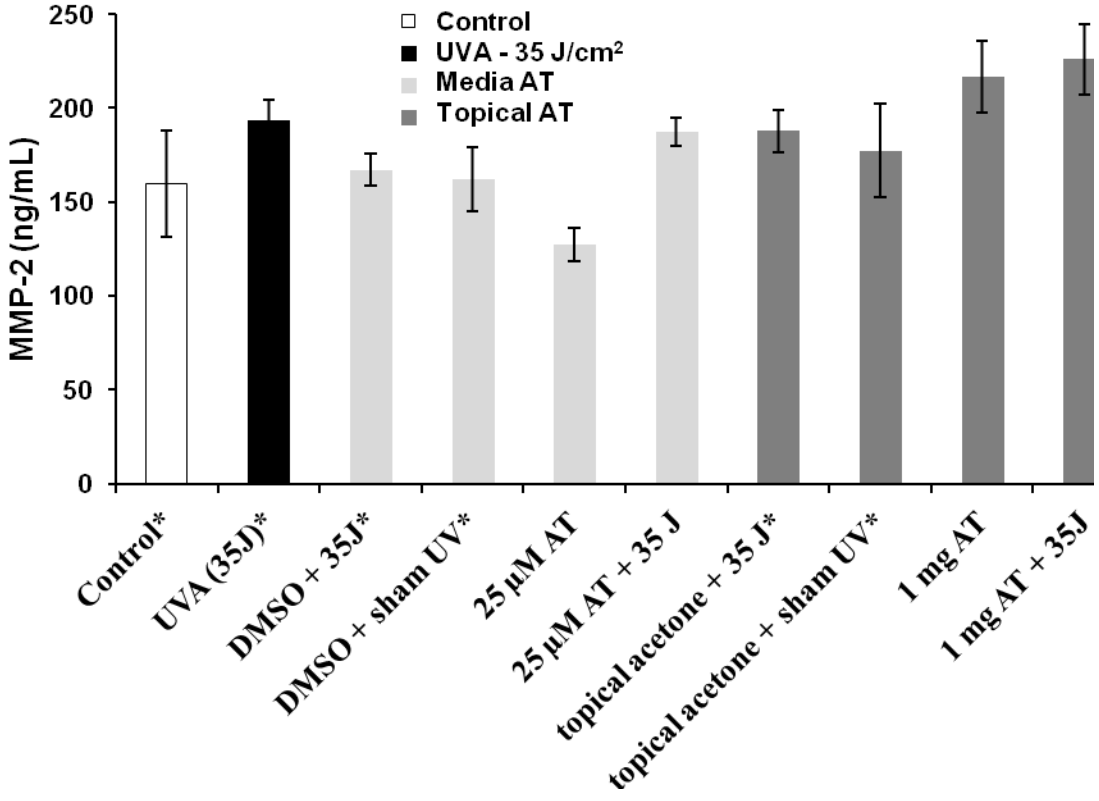

Figure 8. **AT and UVA induce MMP-2 secretion in 3D tissues.** MMP-2 concentration (mean ± SEM) as assessed by ELISA 96 h after irradiation in medium of 3D tissues with the following conditions: untreated control (white); UVA irradiated (35 J/cm^2; black); medium AT (vehicle[1] + UVA/sham irradiated and 25 µM AT + UVA/sham irradiated (light gray)); and topical AT (vehicle[2] + UVA/sham irradiated and 1 mg/cm^2 AT + UVA/sham irradiated (dark gray)). MMP-2 secretion was greater in UVA irradiated and AT + UVA treated 3D tissues. *n=2, otherwise n=4.

[1]Medium AT vehicle is DMSO of (0.1% of medium volume).

[2]Topical AT vehicle consists of 45 µL of acetone.

CHAPTER 6

The Photoprotective Effects of Almond Polyphenols in a Three-Dimensional Human Skin Tissue Model

Abstract

Introduction: Almonds contain the polyphenols (AP), which have shown promise as photoprotectants. This study aimed to assess the photoprotection of these nutrients in a 3-dimensinal (3D) human skin tissue model with ultraviolet-A (UVA) irradiation.

Methods and Materials: AP was applied to medium or topically (5 μM and 14 μg/cm^2, respectively). Optimal dose and incubation time for each treatment were selected based on maintenance of healthy skin tissue parameters (morphology, proliferation and apoptosis) and physiologic relevancy. After nutrient incubation, tissues were UVA irradiated (35 J/cm^2) and photodamage was assessed in comparison to control tissues after 96 h. Photodamage was assessed by morphological outcomes (basal layer organization, fibroblast presence, and epidermal development) observed in hemotoxylin and eosin-stained tissue cross-sections; proliferation of basal cells by bromodeoxyuridine incorporation assay; apoptosis by TUNEL assay; differentiation by cytokeratin-10 immunohistochemistry; antioxidant capacity by ferric reducing antioxidant power assay; and protein secretion fibroblast growth factors and matrix metalloprotease (MMP)-2.

Results: Nutrient treatments alone did not induce significant changes in the percentage of apoptotic fibroblasts or morphologic parameters. Topical AP alone increased percent proliferating basal keratinocytes (19%). However, UVA irradiation increased apoptotic fibroblasts by approximately 12 fold and decreased proliferating basal keratinocytes by 60%, compared to control tissues. Negative morphologic changes were also observed at 96 h after

irradiation, including disappearance of fibroblasts in the upper dermis, disorganized basal layer and less developed epithelium. UVA delayed keratinocyte differentiation, suppressed secretion of HGF and induced secretion of MMP-2. Morphologic deterioration was partially prevented by pretreatment of both medium and topical AP. Tissues pretreated with medium and topical AP had increased proliferating basal keratinocytes (27 and 83%, respectively) and decreased apoptotic fibroblasts (19 and 50%, respectively), compared to corresponding vehicle treated tissues after UVA irradiation. UVA-induced delayed keratinocyte differentiation was attenuated by both pretreatments. Pretreatment with topical AP attenuated MMP-2 secretion (33%, respectively), compared to corresponding vehicle controls after UVA irradiation. AP medium vehicle displayed protection from UVA-induced morphologic damage and delayed-keratinocyte differentiation.

Conclusions: Medium and topical AP treatments provided some degree of photoprotection from UVA, but chemicals used in the 5 μM AP vehicle displayed a photoprotective effect. Our results showing the protective effects of topical AP on morphology, proliferation, apoptosis, differentiation and protein secretion lends to the feasibility of using this model to investigate the mechanisms of action of these treatments in photoprotection. These data may have positive implications for the use of topical almond phytonutrients to prevent sun damage.

Introduction

Skin is the largest organ in the human body. It is exposed to environmental insult of which UV light is thought to be the most harmful (Lippens *et al.*, 2009). UV exposure can cause oxidative stress, inflammation, erythema, breakdown of the extracellular matrix, wrinkling and skin cancer (Boelsma *et al.*, 2001; Iddamalgoda *et al.*, 2008; Mudgil *et al.*, 2003). In fact, cumulative sun exposure is one of the most important risk factors for both nonmelanoma and

melanoma skin cancers (Gloster and Brodland, 1996; Miller and Mihm, 2006). At the earth's surface, we are exposed to both UVA and shorter wave, higher energy UVB. A majority of photodamage research has focused on UVB but recent research has revealed that UVA damage can be significant, including DNA mutations and altered DNA repair, immune function, cell integrity, and cell cycle regulation (Mouret *et al.*, 2006; Ridley *et al.*, 2009; Runger and Kappes, 2008; Waster and Ollinger, 2009). UVA is known to penetrate further than UVB into the dermal layer (Bernerd and Asselineau, 2008). This is reflected in the revised FDA regulations for sunscreen, where "Broad Spectrum SPF" values will reflect both UVA and UVB protection equally (FDA, 2011). There are many ways to protect oneself from UV damage including avoidance of the sun, wearing protective clothing (hats, long-sleeved shirts, treated fabrics, etc), and topical sunscreen. However, the potential for nutrient, dietary and topical, UV protection is a relatively recent concept. Compared to topical sunscreens which require reapplication and have localized effects, dietary methods are thought to provide continual whole body protection.

Flavonoids are a family of over 5000 compounds found in plants and involved in protection against excess light in plants. Flavonoids are also thought to contribute to the prevention of UV damage in humans (Stahl and Sies, 2007). Predominant almond polyphenols (AP) include the flavonoids isorhamnetin, catechin, kaempferol, epicatechin and quercetin (Milbury *et al.*, 2006). Individual AP compounds have been reported to be radical scavengers, UVA absorbent, cytoprotective, anti-inflammatory, anti-apoptotic, and to inhibit DNA damage and to affect cellular signaling pathways (Fahlman and Krol, 2009; Kang *et al.*, 2008; Selmi *et al.*, 2006). Collectively, APs act *in vitro* as antioxidants and induce quinine reductase activity, a marker of chemoprevention (Chen and Blumberg, 2008). Addition of almonds to human diet has reduced biomarkers of oxidative stress in male smokers (Li *et al.*, 2007). Absorption of

isorhamnetin and quercetin from a plant extract into a multilayer membrane system has been reported (Getie *et al.*, 2002). Accumulation of EGCG, a similar polyphenol and common tea catechin, was documented in mice skin via a topical or oral administration (Lambert *et al.*, 2006; Suganuma *et al.*, 1998). However, absorption of APs to human skin has not been tested.

Polyphenol rich foods or extracts have been found to have photoprotective activity in clinical, epidemiological and *in vitro* research. In a clinical trial, long-term, daily ingestion of a cocoa beverage rich in catechin and epicatechin decreased UV-induced erythema by 25% after 12 wks (Heinrich *et al.*, 2006) while topical application of a plant extract containing isorhamnetin, quercetin and kaempferol significantly decreased erythema when applied after UVB irradiation (Aquino *et al.*, 2002). Epidemiologic evidence suggests a negative association between flavonoid-rich dietary factors, including daily tea drinking, high consumption of vegetables, particularly carrots, cruciferous and leafy vegetables, and fruits, especially citrus and melanoma incidence (Fortes *et al.*, 2008). In the "Food Habits in Later Life" study, tea consumption was negatively correlated with actinic skin damage in (Purba *et al.*, 2001). Topical quercetin treatment was found protective of UVB-induced oxidative stress in mouse skin as well (Casagrande *et al.*, 2006).

A novel *in vitro* 3-dimensional (3D) skin tissue model provides a unique opportunity to assess histological, biochemical and molecular outcomes under conditions similar to those found *in vivo*. We have previously demonstrated dose-dependent UVA damage (Evans JA *et al.*, 2011). The current study examined the potential UVA photoprotection provided by pretreatment of topically applied AP or glucuronidated quercetin into medium to mimic metabolites found in circulation after consumption of almond polyphenols, as assessed by morphology, proliferation, apoptosis, differentiation, antioxidant capacity and protein secretion. The overall objective of this

work is to establish feasibility in using a 3D skin tissue model in photoprotective studies involving polyphenols.

Methods and Materials

3D human skin tissues were prepared as previously described (Carlson *et al.*, 2008). Briefly, human dermal fibroblasts (HFF) were derived from newborn foreskin and grown in Dulbecco's modified Eagle's medium (Invitrogen, Carlsbad, CA, USA) supplemented with 10% fetal bovine serum (Hyclone, Logan, UT, USA). HFFs were mixed with bovine type I collagen (2.5×10^4 cells/mL) and the gels were allowed to contract for 7 days in deep-well polycarbonate tissue culture inserts (Organogenesis, Canton, MA, USA). A total of 5 x 10^5 human keratinocytes were seeded onto the collagen gel and tissues were then maintained submerged in low calcium epidermal growth media for 2 days, for an additional 2 days in normal calcium media and raised to the air-liquid interface for 7 days, after which tissues is considered fully developed (Organogenesis, Canton, MA, USA). Experiments were performed 2-4 times. For proliferation assays, 20 μg/mL bromodeoxyuridine (BrdU) (Invitrogen, Carlsbad, CA) was added to tissue culture medium 5 h prior to harvesting.

AP treatment preparation and application

For topical application to the fully developed skin tissue, polyphenols from skins of Nonpareil almonds produced in California were extracted sequentially twice with glacial acetic acid/water/methanol (3.7:46.3:50, v/v/v) over 16 h at 4^{o}C (Chen *et al.*, 2005). Aliquots of dried AP were obtained after solvent removal with N_2 air and stored at -80^{o}C until use. Total phenols were quantified using the Folin-Ciocalteu's reaction (Singleton, 1999) and expressed as micromoles per liter of gallic acid equivalents (GAE). AP were resuspended in 40% acetone/phosphate buffered solution (PBS) for topical application of 45 μL AP at 14 μg/cm^2

GAE. Dose and incubation time were selected based on our previous work which established its safety in 3D tissues (Evans JA *et al.*, 2011).

For medium application, *glucuronide-conjugated* metabolites of quercetin, a major AP, which are generally found in circulation after consumption, were synthesized according to Bolling et al (Bolling *et al.*, 2009). Briefly, pooled human liver microsomal protein (0-1 mg/ml, final concentration, BD Biosciences, San Jose, CA) were preincubated with alamethicin (0.25 μg/ml) at 37°C for 5 min in microcentrifuge tubes containing previously dried quercetin solution (600 μM). A cofactor solution of UDP-glucuronic acid (5 mM, final concentration), magnesium chloride (5 mM, final concentration) and potassium phosphate buffer, pH 7.5 (0.05 mM, final concentration), was added to initiate the reaction in a final assay volume of 0.1 mL. After 3 h incubation at 37°C, the reaction was terminated with 0.1 mL ice cold methanol. After centrifugation at 14,000 × *g* for 5 min, supernatants were dried under a stream of purified nitrogen gas at room temperature and stored at −80°C until use within 2 weeks. The products were reconstituted with 17% methanol in water and quantified by HPLC using a previously established method (Boersma *et al.*, 2002). A Waters Alliance 2695 system (Waters Corp., Milford, MA) with a C18 column (Synergi 10μm Hydro-RP 80A, 4.6 x 250mm) was used. The data is collected and analyzed using Waters Empower 2 Software (copyright 2006, Waters Corp). Mobile phase A consisting of 20 mM phosphate buffer, pH 2.0, and mobile phase B consisting of acetonitrile, were employed to elute quercetin and metabolites. Quercetin and glucuronidated metabolites were quantified using a standard curve established in the absence of UDPGA. Twenty μL of sample was injected at 1 mL/min flow rate of 17% mobile phase B for 2 min and then increased to 25% in 5 min, to 35% in 8 min and to 50% in 5 min. After 3 min at

50%, mobile phase B was decreased to 17% in 4 min and held for 5 min to equilibrate the column.

Once the products were quantified, dried residue were reconstituted in PBS for application to culture medium at a final concentration of 5 μM for 2 h. The 5 μM dose and 2 h incubation period were selected based physiologically achievable concentrations in human circulation and metabolism kinetics of polyphenols. For vehicle controls, the dry residues from glucuronidation reaction with quercetin absent were used. Medium with quercetin metabolites was agitated to ensure homogeneity of treatment.

UV irradiation

For UV irradiation treatments, medium was removed and the skin samples, which were gently washed with PBS two times on each surface, and samples were transferred to a sterile platform. A 200-W UV radiation source (Lightning Cure 200, Hamamatsu, Japan) was used in combination with a dichroic mirror assembly reflecting most of the visible and infrared wavelengths, to reduce the heat load on the skin, and with UG11 and WG335 filters for wavelength delivery in the UVA range (320 – 400 nm). A liquid light guide was connected to the lamp, conducting the light to the surface of the skin. The light guide was mounted to a stand, parallel to the skin surface, at a distance of 3 cm, which provides the most uniform field of light. UVA dose was 0 or 35 J/cm^2 with an intensity of 75 mW/cm^2 as measured by a radiometer (Fluke 289 True RMS Multimeter, Everett, WA). Tissue inserts were returned to tissue culture trays with fresh media and harvested 96 h post-irradiation for histology analysis and media were collected as well.

Tissue Harvesting and Morphology Assessment

Tissues were analyzed for morphology, proliferation and apoptosis. At harvesting, tissues were divided into three equal portions for separate preservation and tissue medium was collected and stored at -80ºC until analysis. One third was fixed in formalin, embedded in paraffin, and serially sectioned at 6 μm. Histological sections were stained with hematoxylin and eosin (H&E), images were captured using a Nikon Eclipse 80i microscope (Nikon Instruments Inc., Melville, NY, USA) equipped with a SPOT RT camera (Diagnostic Instruments, Sterling Heights, MI, USA) and analyzed using Spot Advanced software (Diagnostic Instruments, Sterling Heights, MI, USA). Morphologic assessment of H&E stained tissue cross sections included qualitative evaluation of 1) organization of basal layer, 2) presence of fibroblasts and 3) development of epidermis. A separate third of tissue was snap frozen in O.C.T. compound (Sakura Finetek USA, Torrance, CA, USA) by liquid nitrogen after immersion in 2 M sucrose solution at 4ºC for at least 24 hours. The remaining third of tissue used for the measurement of apoptotic cells using terminal deoxynucleotidyl transferase mediated dUTP nick-end labeling [TUNEL] assay was immersed in 4% paraformaldehyde for 1 h and 2 M sucrose solution at 4ºC for at least 24 h and snap frozen in O.C.T. compound (Sakura Finetek USA, Torrance, CA, USA) by liquid nitrogen and serial sectioned at 6 μm, and mounted onto gelatin-chrome alum coated slides.

Immunohistochemical and immunofluorescence analysis

Immunohistochemical staining of BrdU was performed on paraffin-embedded tissues sectioned at 6 μm thickness using monoclonal antibodies against BrdU (Roche, Indianapolis, IN) and Vectastain ABC kit (Vector Labs, Burlingame, CA). The number of BrdU-positive cells was determined and expressed as a percentage of total cells in the basal layer.

Immunohistochemical staining of cytokeratin-10 positive cells was performed on paraffin-embedded tissues sectioned at 6 μm thickness, immersed in 0.1% sodium citrate at 100ºC for 15 m for antigen retrieval then incubated with monoclonal antibody against cytokeratin-10 (Abcam, Cambridge, MA) and Vectastain ABC kit (Vector Labs, Burlingame, CA).

The TUNEL assay was used to identify apoptotic cells (Mudgil *et al.*, 2003). Tissue soaked in 4% paraformaldehyde prior to freezing were sectioned at 6 μm thickness, permeabilized with 0.1% triton in 0.1% sodium citrate then incubated with the TUNEL reaction mixture (Roche, Indianapolis, IN) for 1 h at 37^{o}C in the dark and counterstained with DAPI (40,6-diamidino-2-phenylindole). The percentage of TUNEL-positive cells was calculated from the number of these cells divided by the total number of cells counted in the entire epithelium.

Ferric reducing antioxidant power (FRAP) Assay

Total antioxidant capacity was measured using the FRAP assay as previously described (Benzie and Strain, 1996). Reagents included 300 mM acetate buffer, pH 3.6 (3.1 g $C_2H_3NaO_2 \cdot 3H_2O$ and 16 mL $C_2H_4O_2$ per liter of buffer solution); 10 mM TPTZ (2,4,6-tripyridyl-s-triazine, Sigma, St. Louis, MO) in 40 mM HCl; 20 mM $FeCl_3 \cdot 6H_2O$. Working FRAP reagent was prepared as required by mixing 25 mL acetate buffer, 2.5 mL TPTZ solution and 2.5 mL $FeCl_3 \cdot 6H_2O$ solution. Aqueous solutions of known Trolox concentration, in the range of 31.25–1000 μM (Sigma, St. Louis, MO), were used for calibration. Thirty μL of medium, blank (H_2O) or standard were added to non-UV disposable cuvettes followed by 90 μL H_2O and 900 μL of FRAP reagent and incubated for 60 m at room temperature. The absorbance was measured at 593 nm on a spectrophotometer (Shimadzu UV-1601, Japan). Reported values are adjusted for the FRAP value of medium not incubated with tissue.

ELISA (enzyme-linked immunosorbent assay)

To assess protein secretion into the medium, tissue culture supernatants were harvested and processed using commercial DuoSet HGF, IL-1α and KGF ELISA kit (R&D Systems, Minneapolis, MN, USA) and MMP-2 human ELISA kit (Invitrogen, Carlsbad, CA). Medium was assayed in duplicates from 2-4 independent samples.

Statistics

Results are expressed as mean ± SEM. Due to the limited replication of this work, comparison of experimental conditions are largely descriptive and statistical analysis was not performed.

Results

Morphology

UVA irradiation of the 3D skin tissue induced morphologic damage including keratinocyte invasion into the dermal matrix, disorganized basal layer, less epidermal development and fibroblast loss (**Figure 1b**) that was not seen in non-irradiated control tissues (Figure 1a). Sham irradiated tissues treated with vehicle controls (medium or topical; Figures 1d and h) were comparable to untreated controls. Tissues pretreated with medium vehicle and UVA irradiated (Figure 1e) had reduced fibroblast loss and basal layer disorganization as well as better epidermal development than those treated with UVA alone. Tissues pretreated with 5 μM medium or 14 $\mu g/cm^2$ topical AP (Figure 1f & j) were less damaged than vehicle controls after UVA treatment but not as healthy as non-irradiated tissues. Medium AP treated tissues had fewer pyknotic fibroblasts and crowding in the basal layer, compared to vehicle treated tissues after UVA exposure. Tissues receiving nutrient treatments alone (Figure 1c & g) were comparable to

untreated controls, however improved polarity of basal keratinocytes is observed with topical AP treatment.

Proliferation

Basal cell proliferation of UVA treated tissues was 60% less than that found in untreated tissues (**Figure 2**). Sham irradiated tissues treated with medium vehicle had 27% greater proliferation than untreated controls, while topical vehicle did not induce an effect. Tissues with 5 μM or 14 μg/cm^2 treatments had 7% less and 19% greater proliferation, respectively, than the corresponding vehicle and sham irradiated controls. Tissues pretreated with medium or topical doses had 27 and 83% greater proliferation, respectively, compared to the corresponding vehicle treated tissues after UVA exposure.

Apoptosis

Dermal apoptosis of UVA irradiated tissues was approximately 12 times that of untreated tissues (**Figure 3**). Nutrient and sham irradiated tissues treated with vehicle controls (medium or topical) were comparable to untreated controls. Apoptosis of tissues pretreated with 5 μM or 14 μg/cm^2 was 19 and 50% less, respectively, than that of vehicle controls after UVA exposure.

Differentiation

UVA irradiation delayed keratinocyte differentiation (**Figure 4b**), as indicated by cytokeratin-10 presence, which was attenuated by medium and topical AP pretreatment (Figure 4f & j). Nutrient and sham irradiated tissues treated with vehicle controls (medium or topical) were comparable to untreated controls.

FRAP

All treated tissues had media trolox equivalent values greater than control (**Figure 5**). Five μM and 14 μg/cm^2 AP treated tissues had 28% less and 24% greater trolox equivalents,

respectively, compared to corresponding vehicle and sham irradiated controls. Tissues pretreated with 5 μM and 14 μg/cm^2 AP had 20 and 11% less trolox equivalents, respectively, compared to vehicle controls after UVA exposure.

Protein Secretion

Tissues exposed to UVA had 30% lower HGF media concentrations compared to media of untreated tissues (**Figure 6**). All AP and vehicle treated tissues had similar media HGF concentrations, all at least 36% less than untreated tissue medium. All media IL-1α concentrations were below the detection limit (data not shown). KGF concentrations in media were only detected in tissues treated with 5 μM or topical vehicle in combination with UVA (data not shown). These values were approximately 35% lower than UVA irradiated tissues.

MMP-2

Medium MMP-2 concentration was 21% greater in UVA treated tissues compared to control tissues (**Figure 7**). Sham irradiated tissues treated with vehicle controls (medium or topical) were comparable to untreated controls. Media MMP-2 concentrations of 5 μM and 14 μg/cm^2 AP treated tissues were 24% less and 10% greater than corresponding vehicle and sham irradiated controls. Media MMP-2 concentrations of tissues pretreated with 5 μM AP or 14 μg/cm^2 were approximately 3% and 33% less, respectively, compared to corresponding vehicle controls after UVA exposure.

Discussion

The primary goal of this research was to evaluate the feasibility of using a 3D skin tissue model in studies assessing the photoprotection of polyphenols. To our knowledge, APs collectively have not previously been evaluated as photoprotectants.

The potential UVA photoprotection was examined in 3D skin tissue treated with topical AP or glucuronidated quercetin added to medium to mimic metabolites found in circulation after consumption of AP. We have previously demonstrated that a dose of 35 J/cm^2 UVA (equivalent to <5 h midday summer sun exposure) to the 3D skin tissue model could cause nontoxic damage (Evans JA *et al.*, 2011). In the present study, we examined UVA damage in this 3D skin model from the most global perspective of morphology, narrowing in on specific tissue parameters of interest using immunohistochemical analysis (proliferation, apoptosis, differentiation) and finally examining proteins thought to be involved in the cellular cross-talk that regulates these processes. While this is a study with limited replication, our results suggest that this is a feasible research tool in future studies evaluating the mechanisms by which foods or specific nutrients are photoprotective.

UVA induced unhealthy morphologic changes, reflected by decreased basal cell proliferation and HGF secretions, increased dermal apoptosis and MMP-2 secretions and delayed differentiation, which was consistent with the literature (Bernerd and Asselineau, 1998, 2008; de Laat *et al.*, 1997; de Laat *et al.*, 1996; Oh *et al.*, 2004). As fibroblasts are the principal source of HGF and KGF secretions (Shirakata), the observed HGF decreases likely reflect the fibroblast loss. Others have found UVA to stimulate IL-1α in an epidermal model of normal human keratinocytes 24 h after 20, 40 and 60 J/cm^2 (Noel-Hudson *et al.*, 1997). It is possible that IL-1α response is short-term and would have returned to homeostatic conditions at the 96 h time point that we used in our study. However, when assessed 2, 4, 24 and 168 h post-irradiation, IL-1α gene expression was not stimulated by low dose UVA (2, 6 or 12 J/cm^2) in a 3D human skin model (Meloni *et al.*). Because media IL-1α concentrations were below the detection limit in

both untreated and UVA irradiated tissues of our study, we cannot determine if there was a response.

The UVA damage was attenuated, with the exception of changes in protein secretion, with topical and medium treatments of AP. The vehicle for 5 μM AP, consisting of residue from a blank glucuronidation reaction resuspended in PBS, independently increased antioxidant capacity and provided some protection from UVA induced morphology damage and delayed keratinocyte differentiation, though the effect on morphology, proliferation, apoptosis and differentiation were not as strong as 5 μM AP. With this in mind, the observed photoprotective effects of 5 μM AP should be interpreted carefully, considering the interactive contribution of vehicle constituents and quercetin metabolites. In concordance with our results, long-term application of topical green tea treatment in a clinical trial significantly reduced UV-induced apoptosis in keratinocytes (Mnich *et al.*, 2009). Quercetin-3-glucoside and epicatechin reduced UVA induced apoptosis of fibroblasts in a 3D skin model experiment and monolayer human fibroblasts, respectively (Basu-Modak *et al.*, 2003; Dekker *et al.*, 2005). In a UVA exposed artificial skin model, composed of differentiated epidermis on a dermal substitute, pretreatment with topical EGCG decreased activities of MMP-2 (Lee *et al.*, 2005). Quercetin administered intraperitoneally in Sprague-Dawley rats prior to UVA exposure diminished UVA-induced oxidative stress, e.g., increased lipid peroxidation and decreased activities of erythrocyte glutathione peroxidase, glutathione reductase, catalase and superoxide dismutase (Kahraman and Inal, 2002).

While both medium and topically applied AP treatments provided some degree of photoprotection, differences in outcome measures were observed between these treatments. Topical treatment alone stimulated proliferation to a greater extent than medium treatment in

comparison to vehicle treated, sham irradiated tissues. Topical treated tissues also showed less delay in differentiation and MMP-2 secretion than medium treated tissues after UVA exposure. However, the morphology after UVA irradiation shows healthier fibroblasts and more developed epithelia in medium treated tissues. Since chemicals used in the generation of quercetin metabolites displayed a photoprotective effect, the photoproective action of quercetin metabolites at the current concentration of 5 μM was inconclusive. However, our results supported that polyphenols via topical administration provided noticeable photoprotection against UVA, probably due to the additive/synergistic actions of polyphenols in almond skins. While we did not have a definitive answer to possible differences in photoprotective bioefficacy of polyphenols via topical and medium administrations, we speculate that form and concentration of polyphenols in the skin compartments might be accountable for the observed differences. Thus, our results suggest that the topical administration of polyphenols could be a more advantageous route, but effects would be localized to treatment area.

While polyphenols have demonstrated skin health benefits, it is unknown if they act directly via an increase in skin content or indirectly through systemic effects on the vascular system (Richelle *et al.*, 2006). In fact, UVA protection was observed in skin fibroblasts when glucuronide metabolites of the polyphenol hesperidin were applied but not detected inside the cells (Proteggente *et al.*, 2003). In contrast, unconjugated hesperidin was efficiently taken up by cells but provided no UVA protection. More work is warranted to investigate absorption of polyphenols to skin.

The possible photoprotective effect of polyphenols might be attributed to several plausible mechanisms, e.g., UVA absorbance (Fahlman and Krol, 2009), radical scavenging and modulation of cellular signaling and endogenous antioxidant defenses (Fahlman and Krol, 2009;

Kang *et al.*, 2008). Sun protection factor and protection factor-UVA of a 10% (w/w) quercetin emulsion are approximately 12 and 15, respectively, which is greater than some UV filters authorized by the European Union (Choquenet *et al.*, 2008). More research is warranted to investigate the mechanism of photoprotection of polyphenols.

Currently, most studies of nutrient photoprotection are conducted in humans, animals or monolayer models, although each with its own limitations. Conducting these studies in human skin *in vivo* is difficult because it requires scar-inducing skin biopsies. Bioavailability and metabolism of nutrients in modeled animals are different from humans, as well as their skin structure. Monolayer cultures do not mimic *in vivo* physiologies, in terms of stratification, differentiation, proliferation and signaling pathways as well as the 3D human skin tissue model. This novel *in vitro* 3D skin tissue model provides a unique opportunity to assess histological, biochemical and molecular outcomes under conditions similar to those found *in vivo* and could be an invaluable tool in the growing fields of skin nutrition and photoprotection. The small, but significant, nutrient photoprotection observed in our study is consistent with what others have found in humans (Richelle *et al.*, 2006; Sies and Stahl, 2004) and lends to the feasibility of using this model to investigate the mechanisms of action of polyphenols and other phytochemicals in photoprotection.

References

Aquino R, Morelli S, Tomaino A, Pellegrino M, Saija A, Grumetto L*, et al.* (2002) Antioxidant and photoprotective activity of a crude extract of Culcitium reflexum H.B.K. leaves and their major flavonoids. *J Ethnopharmacol* 79:183-91.

Basu-Modak S, Gordon MJ, Dobson LH, Spencer JP, Rice-Evans C, Tyrrell RM (2003) Epicatechin and its methylated metabolite attenuate UVA-induced oxidative damage to human skin fibroblasts. *Free Radic Biol Med* 35:910-21.

Benzie IF, Strain JJ (1996) The ferric reducing ability of plasma (FRAP) as a measure of "antioxidant power": the FRAP assay. *Anal Biochem* 239:70-6.

Bernerd F, Asselineau D (1998) UVA exposure of human skin reconstructed in vitro induces apoptosis of dermal fibroblasts: subsequent connective tissue repair and implications in photoaging. *Cell Death Differ* 5:792-802.

Bernerd F, Asselineau D (2008) An organotypic model of skin to study photodamage and photoprotection in vitro. *J Am Acad Dermatol* 58:S155-9.

Boelsma E, Hendriks HF, Roza L (2001) Nutritional skin care: health effects of micronutrients and fatty acids. *Am J Clin Nutr* 73:853-64.

Boersma MG, van der Woude H, Bogaards J, Boeren S, Vervoort J, Cnubben NH*, et al.* (2002) Regioselectivity of phase II metabolism of luteolin and quercetin by UDP-glucuronosyl transferases. *Chem Res Toxicol* 15:662-70.

Bolling BW, Court MH, Blumberg JB, Chen CY (2009) The kinetic basis for age-associated changes in quercetin and genistein glucuronidation by rat liver microsomes. *J Nutr Biochem*.

Carlson MW, Alt-Holland A, Egles C, Garlick JA (2008) Three-dimensional tissue models of normal and diseased skin. *Curr Protoc Cell Biol* Chapter 19:Unit 19 9.

Casagrande R, Georgetti SR, Verri WA, Jr., Dorta DJ, dos Santos AC, Fonseca MJ (2006) Protective effect of topical formulations containing quercetin against UVB-induced oxidative stress in hairless mice. *J Photochem Photobiol B* 84:21-7.

Chen CY, Blumberg JB (2008) In vitro activity of almond skin polyphenols for scavenging free radicals and inducing quinone reductase. *J Agric Food Chem* 56:4427-34.

Chen CY, Milbury PE, Lapsley K, Blumberg JB (2005) Flavonoids from almond skins are bioavailable and act synergistically with vitamins C and E to enhance hamster and human LDL resistance to oxidation. *J Nutr* 135:1366-73.

Choquenet B, Couteau C, Paparis E, Coiffard LJ (2008) Quercetin and rutin as potential sunscreen agents: determination of efficacy by an in vitro method. *J Nat Prod* 71:1117-8.

de Laat A, Kroon ED, de Gruijl FR (1997) Cell cycle effects and concomitant p53 expression in hairless murine skin after longwave UVA (365 nm) irradiation: a comparison with UVB irradiation. *Photochem Photobiol* 65:730-5.

de Laat A, van Tilburg M, van der Leun JC, van Vloten WA, de Gruijl FR (1996) Cell cycle kinetics following UVA irradiation in comparison to UVB and UVC irradiation. *Photochem Photobiol* 63:492-7.

Dekker P, Parish WE, Green MR (2005) Protection by food-derived antioxidants from UV-A1-induced photodamage, measured using living skin equivalents. *Photochem Photobiol* 81:837-42.

Evans JA, Chen C-YO, Garlick J, Wang X-D, Johnson EJ (2011) Feasibility of nutrient photoprotection studies in a three-dimensional human skin tissue model: Using alpha tocopherol. *FASEB J* 25.

Fahlman BM, Krol ES (2009) Inhibition of UVA and UVB radiation-induced lipid oxidation by quercetin. *J Agric Food Chem* 57:5301-5.

FDA (2011) Labeling and Effectiveness Testing; Sunscreen Drug Products for Over-the-Counter Human Use. In: *21 CFR Parts 201 and 310* (35620-65.

Fortes C, Mastroeni S, Melchi F, Pilla MA, Antonelli G, Camaioni D*, et al.* (2008) A protective effect of the Mediterranean diet for cutaneous melanoma. *Int J Epidemiol* 37:1018-29.

Getie M, Gebre-Mariam T, Rietz R, Neubert RH (2002) Evaluation of the release profiles of flavonoids from topical formulations of the crude extract of the leaves of Dodonea viscosa (Sapindaceae). *Pharmazie* 57:320-2.

Gloster HM, Jr., Brodland DG (1996) The epidemiology of skin cancer. *Dermatol Surg* 22:217-26.

Heinrich U, Neukam K, Tronnier H, Sies H, Stahl W (2006) Long-term ingestion of high flavanol cocoa provides photoprotection against UV-induced erythema and improves skin condition in women. *J Nutr* 136:1565-9.

Iddamalgoda A, Le QT, Ito K, Tanaka K, Kojima H, Kido H (2008) Mast cell tryptase and photoaging: possible involvement in the degradation of extra cellular matrix and basement membrane proteins. *Arch Dermatol Res* 300 Suppl 1:S69-76.

Kahraman A, Inal ME (2002) Protective effects of quercetin on ultraviolet A light-induced oxidative stress in the blood of rat. *J Appl Toxicol* 22:303-9.

Kang BY, Kim S, Lee KH, Lee YS, Hong I, Lee MO*, et al.* (2008) Transcriptional profiling in human HaCaT keratinocytes in response to kaempferol and identification of potential transcription factors for regulating differential gene expression. *Exp Mol Med* 40:208-19.

Lambert JD, Kim DH, Zheng R, Yang CS (2006) Transdermal delivery of (-)-epigallocatechin-3-gallate, a green tea polyphenol, in mice. *J Pharm Pharmacol* 58:599-604.

Lee JH, Chung JH, Cho KH (2005) The effects of epigallocatechin-3-gallate on extracellular matrix metabolism. *J Dermatol Sci* 40:195-204.

Li N, Jia X, Chen CY, Blumberg JB, Song Y, Zhang W*, et al.* (2007) Almond consumption reduces oxidative DNA damage and lipid peroxidation in male smokers. *J Nutr* 137:2717-22.

Lippens S, Hoste E, Vandenabeele P, Agostinis P, Declercq W (2009) Cell death in the skin. *Apoptosis* 14:549-69.

Meloni M, Farina A, de Servi B Molecular modifications of dermal and epidermal biomarkers following UVA exposures on reconstructed full-thickness human skin. *Photochem Photobiol Sci* 9:439-47.

Milbury PE, Chen CY, Dolnikowski GG, Blumberg JB (2006) Determination of flavonoids and phenolics and their distribution in almonds. *J Agric Food Chem* 54:5027-33.

Miller AJ, Mihm MC, Jr. (2006) Melanoma. *N Engl J Med* 355:51-65.

Mnich CD, Hoek KS, Virkki LV, Farkas A, Dudli C, Laine E*, et al.* (2009) Green tea extract reduces induction of p53 and apoptosis in UVB-irradiated human skin independent of transcriptional controls. *Exp Dermatol* 18:69-77.

Mouret S, Baudouin C, Charveron M, Favier A, Cadet J, Douki T (2006) Cyclobutane pyrimidine dimers are predominant DNA lesions in whole human skin exposed to UVA radiation. *Proc Natl Acad Sci U S A* 103:13765-70.

Mudgil AV, Segal N, Andriani F, Wang Y, Fusenig NE, Garlick JA (2003) Ultraviolet B irradiation induces expansion of intraepithelial tumor cells in a tissue model of early cancer progression. *J Invest Dermatol* 121:191-7.

Noel-Hudson MS, Braut-Boucher F, Robert M, Aubery M, Wepierre J (1997) Comparison of six different methods to assess UVA cytotoxicity on reconstructed epidermis. Relevance of a fluorimetric assay (the calcein-AM) to evaluate the photoprotective effects of alpha-tocopherol. *Toxicol In Vitro* 11:645-51.

Oh JH, Chung AS, Steinbrenner H, Sies H, Brenneisen P (2004) Thioredoxin secreted upon ultraviolet A irradiation modulates activities of matrix metalloproteinase-2 and tissue inhibitor of metalloproteinase-2 in human dermal fibroblasts. *Arch Biochem Biophys* 423:218-26.

Proteggente AR, Basu-Modak S, Kuhnle G, Gordon MJ, Youdim K, Tyrrell R*, et al.* (2003) Hesperetin glucuronide, a photoprotective agent arising from flavonoid metabolism in human skin fibroblasts. *Photochem Photobiol* 78:256-61.

Purba MB, Kouris-Blazos A, Wattanapenpaiboon N, Lukito W, Rothenberg EM, Steen BC*, et al.* (2001) Skin wrinkling: can food make a difference? *J Am Coll Nutr* 20:71-80.

Richelle M, Sabatier M, Steiling H, Williamson G (2006) Skin bioavailability of dietary vitamin E, carotenoids, polyphenols, vitamin C, zinc and selenium. *Br J Nutr* 96:227-38.

Ridley AJ, Whiteside JR, McMillan TJ, Allinson SL (2009) Cellular and sub-cellular responses to UVA in relation to carcinogenesis. *Int J Radiat Biol* 85:177-95.

Runger TM, Kappes UP (2008) Mechanisms of mutation formation with long-wave ultraviolet light (UVA). *Photodermatol Photoimmunol Photomed* 24:2-10.

Selmi C, Mao TK, Keen CL, Schmitz HH, Eric Gershwin M (2006) The anti-inflammatory properties of cocoa flavanols. *J Cardiovasc Pharmacol* 47 Suppl 2:S163-71; discussion S72-6.

Shirakata Y Regulation of epidermal keratinocytes by growth factors. *J Dermatol Sci* 59:73-80.

Sies H, Stahl W (2004) Nutritional protection against skin damage from sunlight. *Annu Rev Nutr* 24:173-200.

Singleton VL, R. Orthofer, R.M. Lamuela-Ravent, (ed) (1999) *Analysis of Total Phenols and Other Oxidation Substrates and Antioxidants by Means of Folin-Ciocalteu Reagent*, Academic Press: New York.

Stahl W, Sies H (2007) Carotenoids and flavonoids contribute to nutritional protection against skin damage from sunlight. *Molecular Biotechnology* 37:26-30.

Suganuma M, Okabe S, Oniyama M, Tada Y, Ito H, Fujiki H (1998) Wide distribution of [3H](-)-epigallocatechin gallate, a cancer preventive tea polyphenol, in mouse tissue. *Carcinogenesis* 19:1771-6.

Waster PK, Ollinger KM (2009) Redox-dependent translocation of p53 to mitochondria or nucleus in human melanocytes after UVA- and UVB-induced apoptosis. *J Invest Dermatol* 129:1769-81.

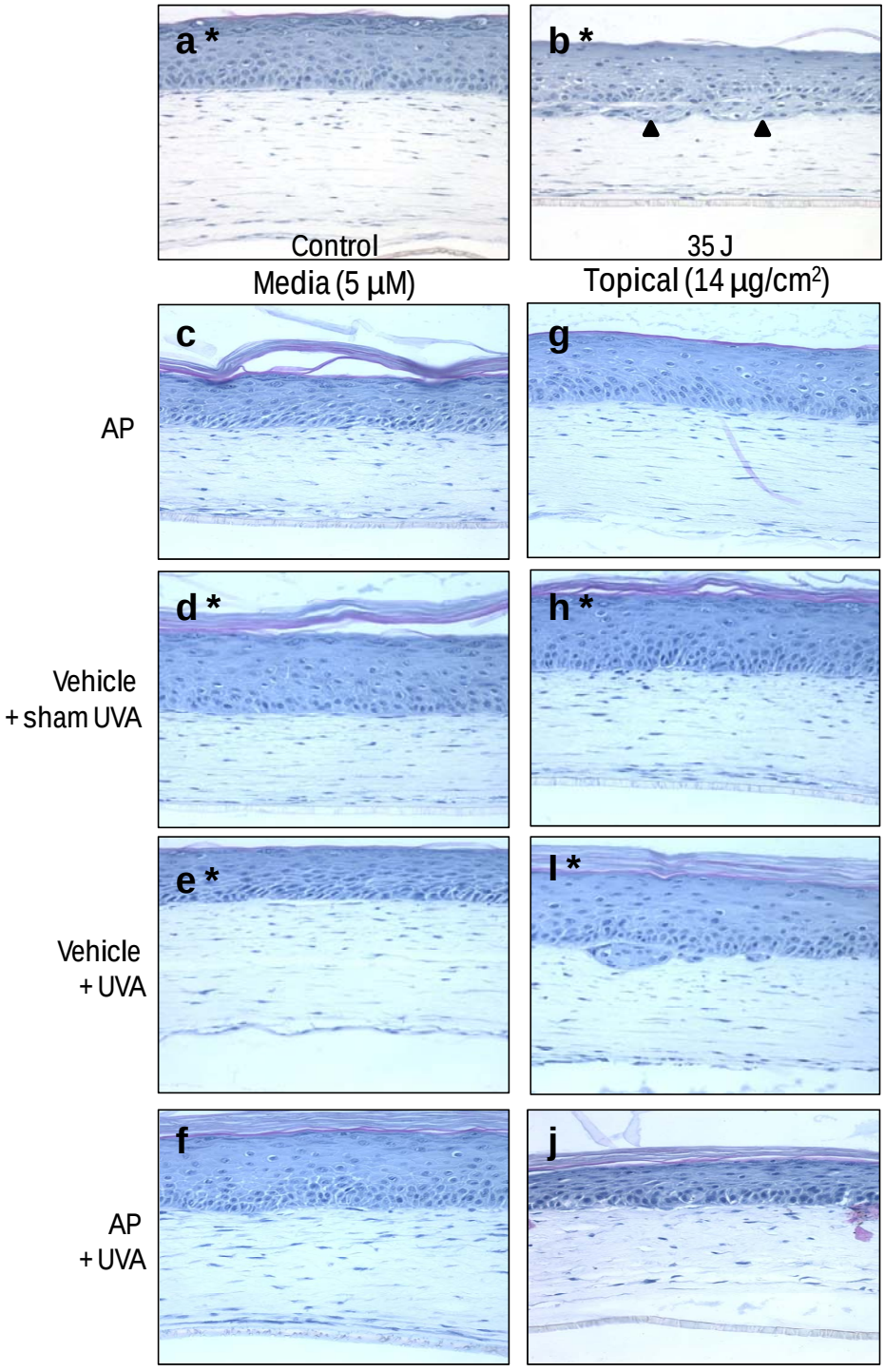

Figure 1. **AP partially prevents deterioration of morphology from UVA irradiation in 3D tissues.** Hematoxylin and eosin stained cross sections from 3D tissues 96 hours after UVA (35 J/cm^2) irradiation which was preceded by 2 hour incubation with medium (c.-f.) and topical (g.-j.) AP treatment as follows (a) untreated, (b) UVA, (c) 5 µM quercetin metabolites[1], (d) vehicle[2]

and sham irradiated (e) vehicle[2] and UVA irradiated, (f) 5 μM quercetin metabolites and UVA irradiated, (g) 14 μg/cm^2 topical AP, (h) vehicle[3] and sham irradiated, (i) vehicle[3] and UVA irradiated and (j) 14 μg/cm^2 topical AP and UVA irradiated. UVA irradiated tissues showed cellular invasion into the matrix (arrows), disappearance of fibroblasts in the upper dermis, disorganization in the basal layer and less developed epithelia. Both medium and topical AP partially prevented these alterations. Representative images are shown. *n=2, otherwise n=4.

[1]Medium AP treatment consisted of glucuronidated quercetin (a predominant polyphenol found in almond skin) to better mimic dietary delivery.

[2]Medium AP vehicle consists of a blank quercetin glucuronidation reaction reconstituted in PBS (1.25% of medium volume).

[3]Topical AP vehicle consists of 45 μL of 40% acetone/PBS.

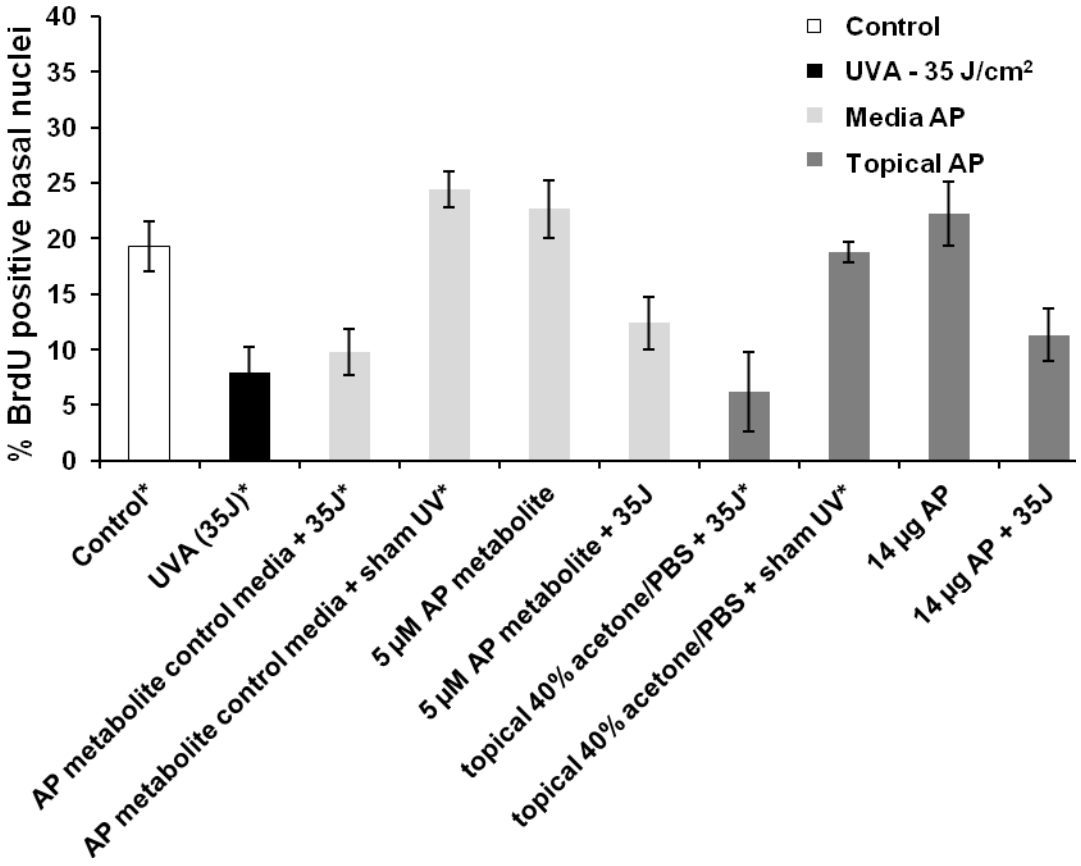

Figure 2. **AP and UVA can modulate proliferation in 3D tissues.** Proliferation was measured as the percentage of total basal keratinocytes that were BrdU-positive (mean ± SEM) 96 h after irradiation in 3D tissues with the following conditions: untreated control (white); UVA irradiated (35 J/cm^2; black); medium AP[1] (vehicle[2] + UVA/sham irradiated and 5 µM quercetin metabolites + UVA/sham irradiated (light gray)); and topical AP (vehicle[3] + UVA/sham irradiated and 14 µg/cm^2 AP + UVA/sham irradiated (dark gray)). *n=2, otherwise n=4

[1]Medium AP treatment consisted of glucuronidated quercetin (a predominant polyphenol found in almond skin) to better mimic dietary delivery.

[2]Medium AP vehicle consists of a blank quercetin glucuronidation reaction reconstituted in PBS (1.25% of medium volume).

[3]Topical AP vehicle consists of 45 µL of 40% acetone/PBS.

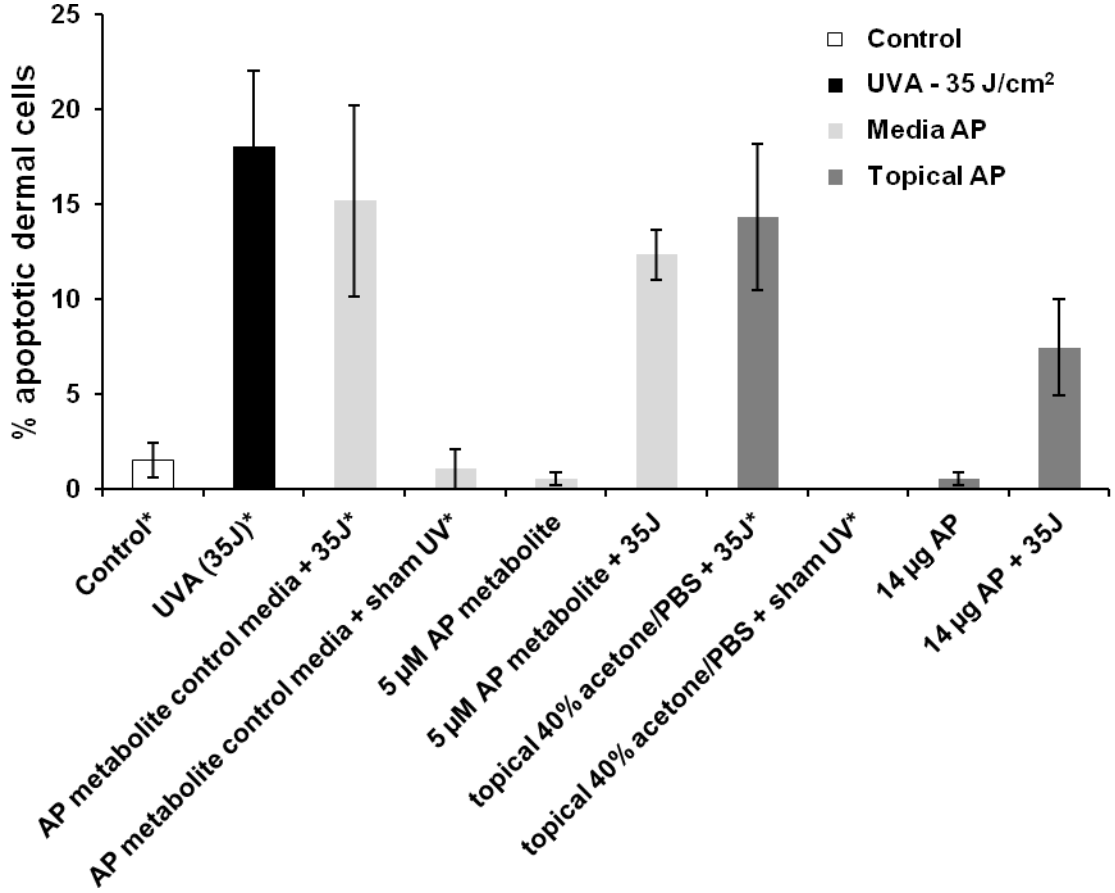

Figure 3. AP partially prevents UVA-induced dermal apoptosis in 3D tissues. Apoptosis was measured as the percentage of total fibroblasts that were TUNEL-positive (mean ± SEM) 96 h after irradiation in 3D tissues with the following conditions: untreated control (white); UVA irradiated (35 J/cm^2; black); medium AP[1] (vehicle[2] + UVA/sham irradiated and 5 µM quercetin metabolites + UVA/sham irradiated (light gray)); and topical AP (vehicle[3] + UVA/sham irradiated and 14 µg/cm^2 AP + UVA/sham irradiated (dark gray)). *n=2, otherwise n=4

[1]Medium AP treatment consisted of glucuronidated quercetin (a predominant polyphenol found in almond skin) to better mimic dietary delivery.

[2]Medium AP vehicle consists of a blank quercetin glucuronidation reaction reconstituted in PBS (1.25% of medium volume).

[3]Topical AP vehicle consists of 45 μL of 40% acetone/PBS.

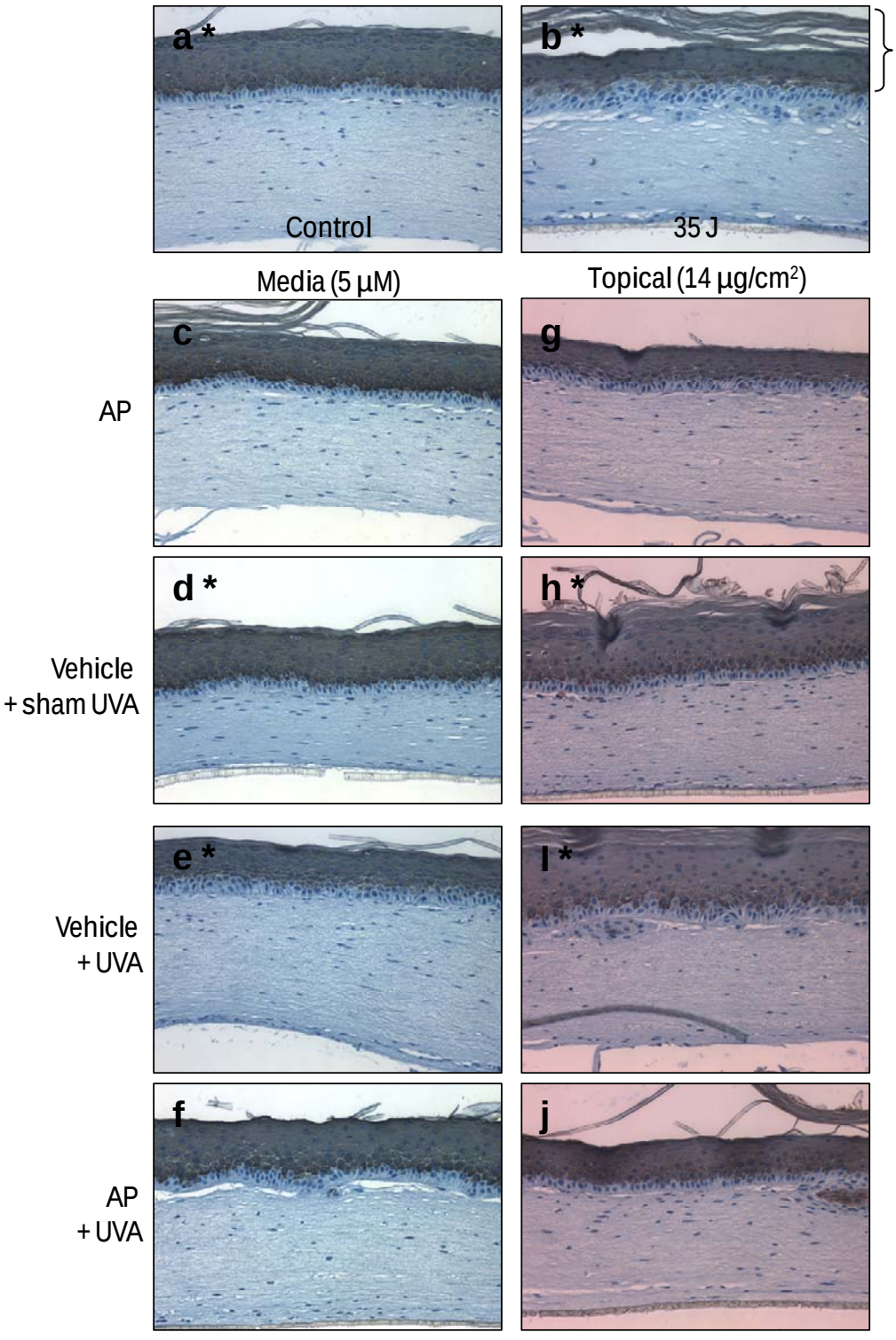

Figure 4. **AP partially prevents keratinocyte differentiation delay induced by UVA irradiation in 3D tissues.** Cytokeratin-10 stained cross sections from 3D tissues 96 hours UVA

(35 J/cm^2) irradiation which was preceded by 2 hour incubation with medium (c.-f.) and topical (g.-j.) AP treatment as follows (a) untreated, (b) UVA, (c) 5 μM quercetin metabolites[1], (d) vehicle[2] and sham irradiated (e) vehicle[2] and UVA irradiated, (f) 5 μM quercetin metabolites and UVA irradiated, (g) 14 μg/cm^2 topical AP, (h) vehicle[3] and sham irradiated, (i) vehicle[3] and UVA irradiated and (j) 14 μg/cm^2 topical AP and UVA irradiated. Cytokeratin-10 stained tissues are evaluated by visual comparison for presence of stain relative to the basal layer (example stain indicated by bracket). UVA irradiated tissues showed delayed differentiation. Both medium and topical AP partially prevented this delay. Representative images are shown. *n=2, otherwise n=4.

[1]Medium AP treatment consisted of glucuronidated quercetin (a predominant polyphenol found in almond skin) to better mimic dietary delivery.

[2]Medium AP vehicle consists of a blank quercetin glucuronidation reaction reconstituted in PBS (1.25% of medium volume).

[3]Topical AP vehicle consists of 45 μL of 40% acetone/PBS.

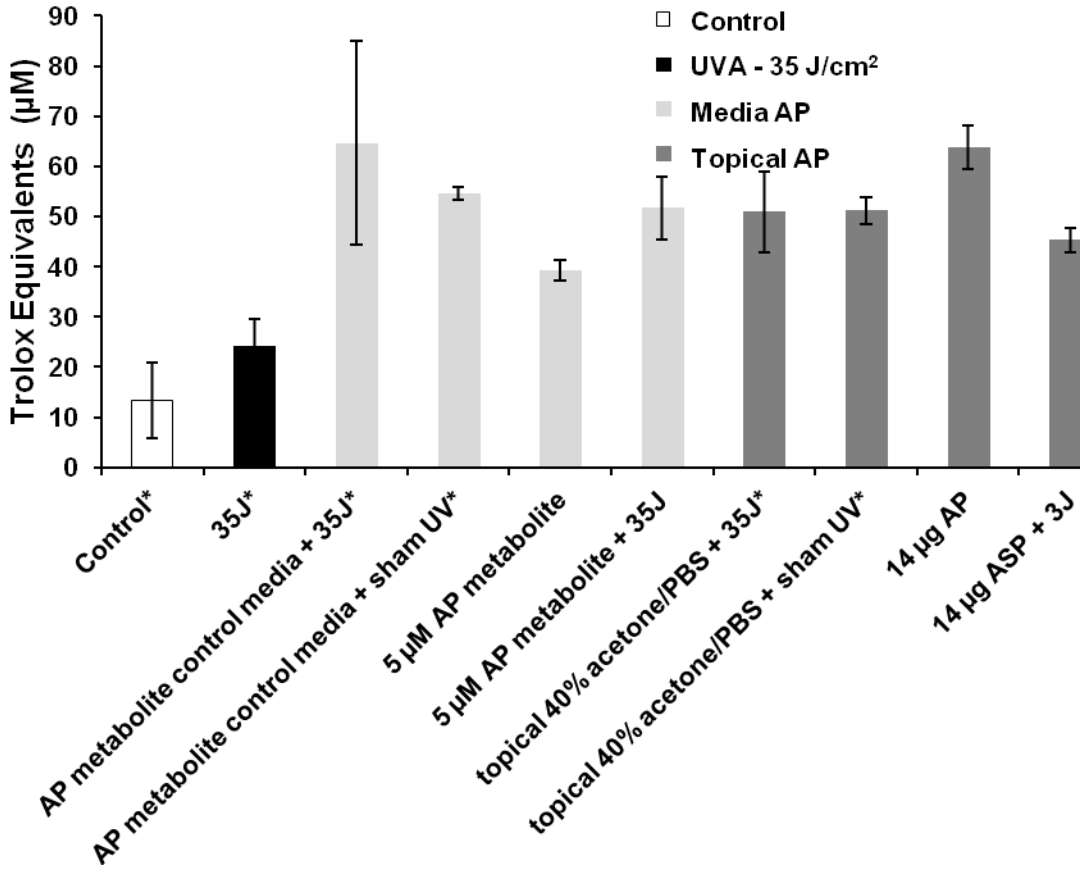

Figure 5. **UVA irradiation, AP treatment and vehicles increased antioxidant capacity in 3D tissues.** Antioxidant capacity (mean ± SEM) as assessed by FRAP assay 96 h after irradiation in medium of 3D tissues with the following conditions: untreated control (white); UVA irradiated (35 J/cm^2; black); medium AP[1] (vehicle[2] + UVA/sham irradiated and 5 µM quercetin metabolites + UVA/sham irradiated (light gray)); and topical AP (vehicle[3] + UVA/sham irradiated and 14 µg/cm^2 AP + UVA/sham irradiated (dark gray)). *n=2, otherwise n=4

[1]Medium AP treatment consisted of glucuronidated quercetin (a predominant polyphenol found in almond skin) to better mimic dietary delivery.

[2]Medium AP vehicle consists of a blank quercetin glucuronidation reaction reconstituted in PBS (1.25% of medium volume).

[3]Topical AP vehicle consists of 45 μL of 40% acetone/PBS.

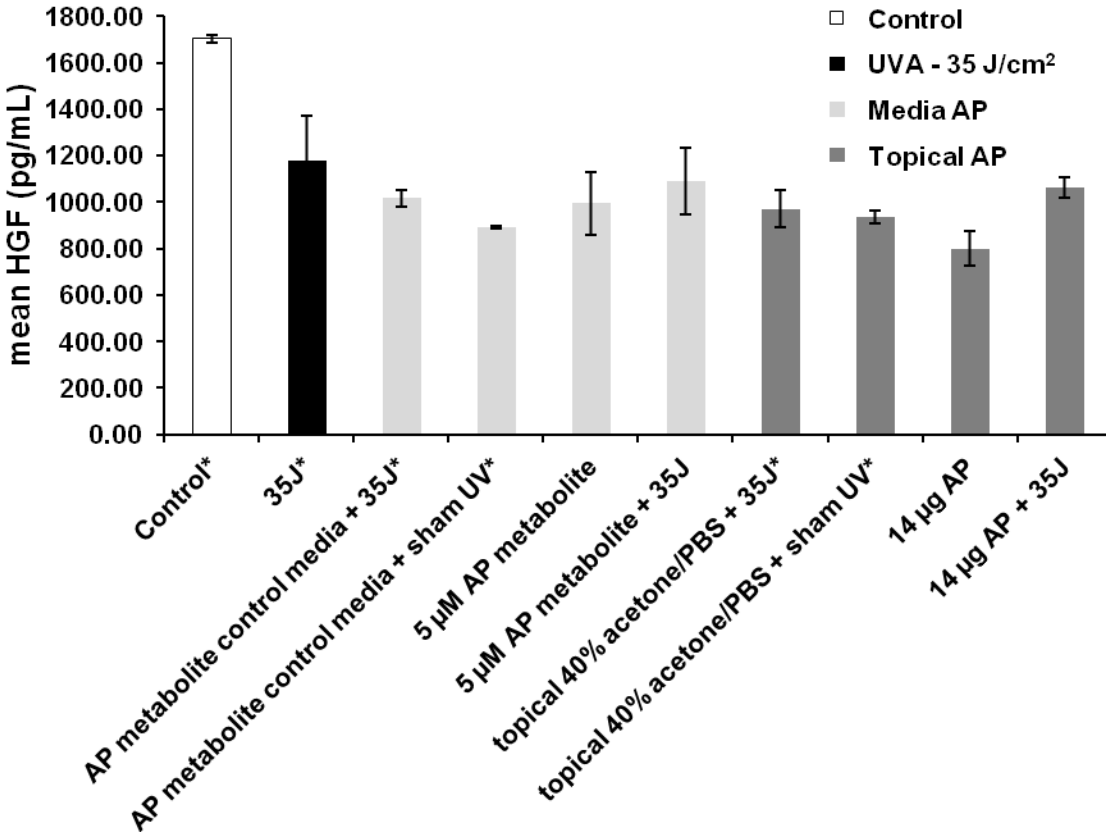

Figure 6. **UVA suppresses HGF secretion in 3D tissues.** HGF concentration (mean ± SEM) as assessed by ELISA 96 h after irradiation in medium of 3D tissues with the following conditions: untreated control (white); UVA irradiated (35 J/cm^2; black); medium AP[1] (vehicle[2] + UVA/sham irradiated and 5 µM quercetin metabolites + UVA/sham irradiated (light gray)); and topical AP (vehicle[3] + UVA/sham irradiated and 14 µg/cm^2 AP + UVA/sham irradiated (dark gray)). *n=2, otherwise n=4.

[1]Medium AP treatment consisted of glucuronidated quercetin (a predominant polyphenol found in almond skin) to better mimic dietary delivery.

[2]Medium AP vehicle consists of a blank quercetin glucuronidation reaction reconstituted in PBS (1.25% of medium volume).

[3]Topical AP vehicle consists of 45 µL of 40% acetone/PBS.

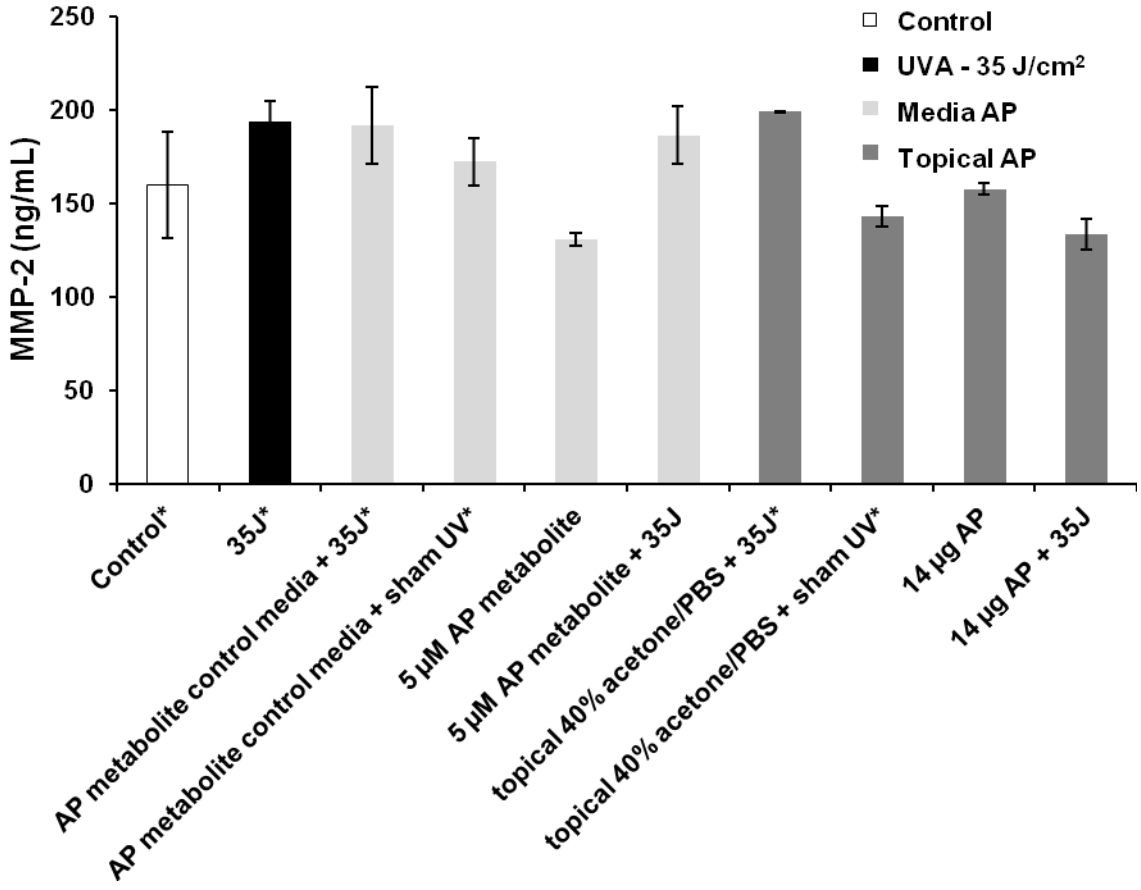

Figure 7. **Topical AP prevents UVA-induced MMP-2 secretion in 3D tissues.** MMP-2 concentration (mean ± SEM) as assessed by ELISA 96 h after irradiation in medium of 3D tissues with the following conditions: untreated control (white); UVA irradiated (35 J/cm^2; black); medium AP[1] (vehicle[2] + UVA/sham irradiated and 5 µM quercetin metabolites + UVA/sham irradiated (light gray)); and topical AP (vehicle[3] + UVA/sham irradiated and 14 µg/cm^2 AP + UVA/sham irradiated (dark gray)). MMP-2 secretion was greater in UVA irradiated 3D tissues but topical AP pretreatment attenuated this response compared to vehicle control. *n=2, otherwise n=4.

[1]Medium AP treatment consisted of glucuronidated quercetin (a predominant polyphenol found in almond skin) to better mimic dietary delivery.

[2]Medium AP vehicle consists of a blank quercetin glucuronidation reaction reconstituted in PBS (1.25% of medium volume).

[3]Topical AP vehicle consists of 45 μL of 40% acetone/PBS.

CHAPTER 7: SUMMARY AND FUTURE DIRECTIONS

7.1 Summary

The aims of this research were 1) assess the feasibility of nutrient studies in a 3-dimensinal (3D) human skin tissue model and 2) determine the photoprotection of AT and AP from ultraviolet-A (UVA) irradiation using this model.

Research Findings. First, we tested the safety of our nutrient treatments (AT and AP) and their vehicles in the model system. Second, we established incubation periods necessary for nutrient absorption. Third, we developed a protocol for reproducible UVA damage and identified a damaging but nontoxic UVA dose for subsequent studies. Finally, we pretreated skin tissue with AT or AP either topically or to the media (to mimic external application and dietary delivery, respectively) before UVA exposure to evaluate protection from morphologic changes; cell proliferation, apoptosis and differentiation; total antioxidant capacity; protein secretion (HGF, KGF, IL-1α and MMP-2). Morphology is the most important outcome measure because it provides a global view of tissue health. Proliferation, apoptosis and differentiation were measured because they are important processes that contribute to the overall tissue health. Growth factors (HGF and KGF) as well as IL-1α are important signaling molecules that facilitate communication between skin compartments. They help to maintain tissue homeostasis and regulate proliferation and apoptosis. MMPs are responsible for breakdown of the extracellular matrix. MMP-2 expression is responsive to UVA irradiation in humans (Oh *et al.*, 2004) and is able to degrade elastin and basement membrane components. The major findings of this research are summarized below.

(1) Safe doses of media and topical AT and AP and their respective vehicles for a 3D human skin model were established based on morphology, apoptosis and proliferation

outcome measures. The safe vehicles and doses are summarized in **Table 1**, as well as incubation times based on absorption studies or physiologic relevance.

Table 1. Safe AT and AP doses, vehicles and incubation times.

	Topical			**Media**		
	vehicle	*dose*	*incubation time (h)*	*vehicle*	*dose*	*incubation time (h)*
AT	45 μL acetone	1-5 mg/cm^2	2	0.1% DMSO	0-50 μM	2
AP	45 μL 40% acetone/PBS	1-14 μg/cm^2	48	1.25% PBS	0-100 μM*	2

* quercetin alone tested; glucuronides are thought to be less toxic (Terao *et al.*)

(2) AT is absorbed into the 3D human skin models from both media and topical application in time- and dose-dependent manners. Concentrations similar to that measured in human skin were achieved in the 3D skin model (30 ng/cm^2 epidermis, 3 ng/cm^2 dermis) after 48 h of 25 μM media application.

(3) A UVA dose of 35 J/cm^2 induced nontoxic damage to the 3D skin model, including negative morphologic changes, increased dermal apoptosis, decreased basal cell proliferation, delayed keratinocyte differentiation, decreased HGF secretion and increased MMP-2 secretion (**Table 2**). These results are consistent with the literature (Bernerd and Asselineau, 1998, 2008; de Laat *et al.*, 1997; de Laat *et al.*, 1996; Oh *et al.*, 2004). This is a physiologic UVA dose and can be achieved with less than five hours of midday summer sun exposure in a Mediterranean country (Fourtanier *et al.*, 2008). Because of its wavelength, UVA penetrates into the dermal layer. Its damage is thought to be induced indirectly by generation of reactive chemical species as it lacks the energy to directly break chemical bonds (McMillan *et al.*, 2008). Because the dermal compartment has a lower concentration of endogenous antioxidant

enzymes, such as catalase and SOD (Halliday, 2005), it is likely more susceptible to oxidative damage than the epidermis. UVA effects included apoptosis and loss of dermal fibroblasts, the primary source of many growth factors which are important for maintaining tissue homeostasis via communication with keratinocytes in the epidermal compartment in a paracrine fashion. We observe UVA-induced effects in the epidermis which may be secondary to the dermal effects. Specifically, we suspect that the decrease in HGF secretion reflects fibroblast loss and the UVA epidermal effects partially result from the decreased HGF secretion. HGF is a growth factor which is known to be secreted by fibroblasts and to support epithelial development and repair (Shirakata). In a similar 3D skin model, HGF suppression was linked to a significant decrease in epithelial proliferation (Shamis *et al.*). This could be investigated by comparison of epithelial outcome measures between tissues exposed to UVA alone and with HGF stimulation.

Table 2. Summary of Nutrient Photoprotection Study Results. Arrows indicate directional change compared to respective controls (--- indicates no change). Red indicates movement away from untreated controls while green indicates movement toward respective controls and homeostasis. ND indicated not detected

	UVA	Medium AT	Topical AT	Medium AP	Topical AP
Morphology	↓	↑	↑	↑ Vehicle effect	↑
Proliferation	↓	↑	---	---	↑
Apoptosis	↑	↓	↓	---	↓
Differentiation	↓	↑	↑	↑	↑
HGF	↓	↑	↑	---	---
KGF	---	ND	↑	ND	ND
IL-1α	ND	ND	↑	ND	ND
MMP-2	↑	↑	↑	---	↓
FRAP	↑	↑	↑	---	---

↑↓ indicates directional change compared to respective control (--- indicates no change)

ND = Not Detected

indicates movement away from untreated controls

indicates movement toward respective controls (homeostasis)

(4) All four treatments (AT and AP applied topically or to the media) provided some degree of UVA photoprotection. However, since chemicals used in the generation of

quercetin metabolites displayed a photoprotective effect, the photoproective action of quercetin metabolites at the current concentration of 5 μM was inconclusive. Because AT does not directly absorb UVA waves, we believe its mechanism of action to be indirect (Masaki *et al.*, 2002; Wu *et al.*, 2008). We hypothesize that AT protected fibroblasts from UVA-induced oxidative stress, enabling their survival and continued support of tissue homeostasis through cellular crosstalk. Specifically, both medium and topical AT pretreated tissues had fewer apoptotic fibroblasts and greater HGF secretions after UVA irradiation as compared to respective vehicle treated tissues. HGF's paracrine role was described previously but HGF has also been shown to act in an autocrine manner to prevent UVA-induced apoptosis in human dermal fibroblasts (Mildner *et al.*, 2007). The possible photoprotective effect of polyphenols might be attributed to several plausible mechanisms, e.g., UVA absorbance (Fahlman and Krol, 2009), radical scavenging and modulation of cellular signaling and endogenous antioxidant defenses (Fahlman and Krol, 2009; Kang *et al.*, 2008).

More research is warranted to investigate the mechanism of photoprotection of AT and polyphenols.

There are strengths and limitations to using the 3D skin model for these studies.

Strengths. Compared to the more conventionally used monolayer cell models, the 3D skin model provides better comparability to the *in vivo* condition and can be adapted to study needs (e.g. incorporation of embryonic stem cells to investigate their functional properties and potential for therapeutic transplantation). Our finding that nutrients were absorbed into this model at concentrations comparable to the *in vivo* situation further supports the feasibility of

using this research tool. Another strength of this model is that it can be used as a screening tool to rapidly assess many variables for safety and efficacy which can save both time, money and resources. For more longitudinal studies, 3D skin models can be grafted onto mice (Alt-Holland *et al.*). This would allow study of chronic nutrient and UV exposure, but the differences in murine nutrient bioavailability and metabolism may limit comparability of dietary studies.

Limitations. The model used in our study included the predominant skin cell types (fibroblasts and keratinocytes) while melanocytes and langerhan cells are present in human skin as well. These cells are responsive to UVA exposure (Poon *et al.*, 2003a; Poon *et al.*, 2003b) and their inclusion into a model allows for a more comprehensive evaluation of UVA damage and nutrient photoprotective effects. Other skin models have been developed that include these cells. Our study was conducted in a 3D skin model composed of cells derived from newborn foreskin, mimicking very young skin. 3D skin models can also be adapted to mimic skin of different aged subjects by incorporation of primary cells from subjects from a range of ages. However, these cells are less viable which creates a challenge for use in the model. It should be noted that the barrier function of 3D skin models is thought to be lesser than in humans (Van Gele *et al.*) and AT is delivered primarily to the skin's surface via sebum secretions by the sebaceous glands (Thiele *et al.*, 1999). While the barrier function varies and these glands are not present in our model, we are able to obtain physiologically relevant concentrations of AT.

Significance. This research is significant because it is the first comprehensive assessment of nutrients effects and their photoprotection in a 3D skin model. Our study was the first to study nutrient absorption in terms of time and dose dependence. This is important because the skin absorption and metabolism of many nutrients (e.g. polyphenols) are unknown. Our results indicate the 3D skin model to be an ideal platform for assessment of nutrient absorption,

localization and metabolism. Our study is comprehensive, evaluating nutrient safety, absorption and photoprotection and establishes both the feasibility of using this model for nutrient studies as well as the photoprotective effects of almond phytonutrient treatments.

7.2 Future directions

Long term AT/AP application effects on UVA damage prevention

The current study tested the effects of a single application of each AT/AP treatment on the prevention of acute UVA damage. Our results demonstrated some degree of UVA protection from each pretreatment, but it remains unknown whether long term pretreatment could provide greater protection. It is also unknown whether AT/AP pretreatment could prevent effects of chronic UVA exposure.

Mechanism of UVA photoprotection

This model is ideal for investigating mechanism of action because it better mimics *in vivo* skin conditions and signaling than monolayer cell models without need of scar-inducing punch biopsies from humans. While quercetin, a component of the AP treatment, is a weak direct absorber of UVA, the primary mode of protection of all 4 treatments is thought to be indirect via antioxidant activity and/or interaction with cellular signaling. While we did find evidence of increased total antioxidant status (assessed by FRAP) after UVA exposure with AP pretreatment, further investigation into antioxidant enzyme (SOD, glutathione peroxidase and catalase) expression and activity would be of great interest.

UV irradiation is known to activate several MAP kinase pathways, including the ERK, JNK and p38 pathways (Rittie and Fisher, 2002). Additionally, stress-activated p38 and JNK are

known to activate p53, which is associated with UV-induced apoptosis (Wu, 2004). AP, including quercetin and kaempferol, have inhibited 12-O-tetradecanoylphorbol 13-acetate-stimulated activation of ERK, JNK and/or p38 in human dermal fibroblasts (Lim and Kim, 2007). Because the tested AP and AT treatments partially prevented dermal apoptosis in our experiments, the MAPK pathways would be appropriate for further investigation of their mechanism of action.

Effect of nutrient combinations

Of interest would be the evaluation of other fat- and water-soluble nutrients such as carotenoids and polyphenols that have been suggested as photoprotectants (Sies and Stahl, 2004). Given the synergistic biologic activity combinations of these nutrients can have (Chen *et al.*, 2005; Fuhrman *et al.*, 2000), of further interest would be the study of combinations of nutrients on photoprotection using this skin tissue model.

Effect on UVA damage repair

We investigated the preventative effect of AT & AP on UVA damage, but there is evidence that suggests these nutrients are involved in the repair of UV damage as well. For instance topical AT application after UV exposure improved erythema response to UVR, but overall results appear to be mixed regarding AT photoprotection from post-UV exposure (Montenegro *et al.*, 1995). Results appear more consistent among polyphenols. For instance, quercetin improved gene expression of DNA repair enzymes after oxidative insult in Caco-2 cells (Min and Ebeler, 2009). Also, GTP have increased DNA repair of CPDs in UVB exposed skin (Nichols and Katiyar).

UVR photoprotection

As the importance of UVA exposure is coming to light, identifying compounds photoprotective of damage from this UV range is also important. But it cannot be forgotten that for most geographical regions and seasons, UVA is accompanied by UVB. Investigation of UVR (a combination of UVA and UVB to mimic sun exposure) photoprotection by AT and AP is warranted based on the positive results presented in this study.

References

Alt-Holland A, Sowalsky AG, Szwec-Levin Y, Shamis Y, Hatch H, Feig LA*, et al.* Suppression of E-Cadherin Function Drives the Early Stages of Ras-Induced Squamous Cell Carcinoma through Upregulation of FAK and Src. *J Invest Dermatol*.

Bernerd F, Asselineau D (1998) UVA exposure of human skin reconstructed in vitro induces apoptosis of dermal fibroblasts: subsequent connective tissue repair and implications in photoaging. *Cell Death Differ* 5:792-802.

Bernerd F, Asselineau D (2008) An organotypic model of skin to study photodamage and photoprotection in vitro. *J Am Acad Dermatol* 58:S155-9.

Chen CY, Milbury PE, Lapsley K, Blumberg JB (2005) Flavonoids from almond skins are bioavailable and act synergistically with vitamins C and E to enhance hamster and human LDL resistance to oxidation. *J Nutr* 135:1366-73.

de Laat A, Kroon ED, de Gruijl FR (1997) Cell cycle effects and concomitant p53 expression in hairless murine skin after longwave UVA (365 nm) irradiation: a comparison with UVB irradiation. *Photochem Photobiol* 65:730-5.

de Laat A, van Tilburg M, van der Leun JC, van Vloten WA, de Gruijl FR (1996) Cell cycle kinetics following UVA irradiation in comparison to UVB and UVC irradiation. *Photochem Photobiol* 63:492-7.

Fahlman BM, Krol ES (2009) Inhibition of UVA and UVB radiation-induced lipid oxidation by quercetin. *J Agric Food Chem* 57:5301-5.

Fourtanier A, Moyal D, Seite S (2008) Sunscreens containing the broad-spectrum UVA absorber, Mexoryl SX, prevent the cutaneous detrimental effects of UV exposure: a review of clinical study results. *Photodermatol Photoimmunol Photomed* 24:164-74.

Fuhrman B, Volkova N, Rosenblat M, Aviram M (2000) Lycopene synergistically inhibits LDL oxidation in combination with vitamin E, glabridin, rosmarinic acid, carnosic acid, or garlic. *Antioxid Redox Signal* 2:491-506.

Halliday GM (2005) Inflammation, gene mutation and photoimmunosuppression in response to UVR-induced oxidative damage contributes to photocarcinogenesis. *Mutat Res* 571:107-20.

Kang BY, Kim S, Lee KH, Lee YS, Hong I, Lee MO*, et al.* (2008) Transcriptional profiling in human HaCaT keratinocytes in response to kaempferol and identification of potential transcription factors for regulating differential gene expression. *Exp Mol Med* 40:208-19.

Lim H, Kim HP (2007) Inhibition of mammalian collagenase, matrix metalloproteinase-1, by naturally-occurring flavonoids. *Planta Med* 73:1267-74.

Masaki H, Okano Y, Ochiai Y, Obayashi K, Akamatsu H, Sakurai H (2002) alpha-tocopherol increases the intracellular glutathione level in HaCaT keratinocytes. *Free Radic Res* 36:705-9.

McMillan TJ, Leatherman E, Ridley A, Shorrocks J, Tobi SE, Whiteside JR (2008) Cellular effects of long wavelength UV light (UVA) in mammalian cells. *J Pharm Pharmacol* 60:969-76.

Mildner M, Mlitz V, Gruber F, Wojta J, Tschachler E (2007) Hepatocyte growth factor establishes autocrine and paracrine feedback loops for the protection of skin cells after UV irradiation. *J Invest Dermatol* 127:2637-44.

Min K, Ebeler SE (2009) Quercetin inhibits hydrogen peroxide-induced DNA damage and enhances DNA repair in Caco-2 cells. *Food Chem Toxicol* 47:2716-22.

Montenegro L, Bonina F, Rigano L, Giogilli S, Sirigu S (1995) Protective effect evaluation of free radical scavengers on UVB induced human cutaneous erythema by skin reflectance spectrophotometry. *Int J Cosmet Sci* 17:91-103.

Nichols JA, Katiyar SK Skin photoprotection by natural polyphenols: anti-inflammatory, antioxidant and DNA repair mechanisms. *Arch Dermatol Res* 302:71-83.

Oh JH, Chung AS, Steinbrenner H, Sies H, Brenneisen P (2004) Thioredoxin secreted upon ultraviolet A irradiation modulates activities of matrix metalloproteinase-2 and tissue inhibitor of metalloproteinase-2 in human dermal fibroblasts. *Arch Biochem Biophys* 423:218-26.

Poon TS, Barnetson RS, Halliday GM (2003a) Prevention of immunosuppression by sunscreens in humans is unrelated to protection from erythema and dependent on protection from ultraviolet a in the face of constant ultraviolet B protection. *J Invest Dermatol* 121:184-90.

Poon TS, Kuchel JM, Badruddin A, Halliday GM, Barnetson RS, Iwaki H*, et al.* (2003b) Objective measurement of minimal erythema and melanogenic doses using natural and solar-simulated light. *Photochem Photobiol* 78:331-6.

Rittie L, Fisher GJ (2002) UV-light-induced signal cascades and skin aging. *Ageing Res Rev* 1:705-20.

Shamis Y, Hewitt KJ, Carlson MW, Margvelashvilli M, Dong S, Kuo CK*, et al.* Fibroblasts derived from human embryonic stem cells direct development and repair of 3D human skin equivalents. *Stem Cell Res Ther* 2:10.

Shirakata Y Regulation of epidermal keratinocytes by growth factors. *J Dermatol Sci* 59:73-80.

Sies H, Stahl W (2004) Nutritional protection against skin damage from sunlight. *Annu Rev Nutr* 24:173-200.

Terao J, Murota K, Kawai Y Conjugated quercetin glucuronides as bioactive metabolites and precursors of aglycone in vivo. *Food Funct* 2:11-7.

Thiele JJ, Weber SU, Packer L (1999) Sebaceous gland secretion is a major physiologic route of vitamin E delivery to skin. *J Invest Dermatol* 113:1006-10.

Van Gele M, Geusens B, Brochez L, Speeckaert R, Lambert J Three-dimensional skin models as tools for transdermal drug delivery: challenges and limitations. *Expert Opin Drug Deliv* 8:705-20.

Wu GS (2004) The functional interactions between the p53 and MAPK signaling pathways. *Cancer Biol Ther* 3:156-61.

Wu S, Gao J, Dinh QT, Chen C, Fimmel S (2008) IL-8 production and AP-1 transactivation induced by UVA in human keratinocytes: roles of D-alpha-tocopherol. *Mol Immunol* 45:2288-96.